https://theses.gla.ac.uk/

Theses Digitisation:

https://www.gla.ac.uk/myglasgow/research/enlighten/theses/digitisation/

This is a digitised version of the original print thesis.

Copyright and moral rights for this work are retained by the author

A copy can be downloaded for personal non-commercial research or study, without prior permission or charge

This work cannot be reproduced or quoted extensively from without first obtaining permission in writing from the author

The content must not be changed in any way or sold commercially in any format or medium without the formal permission of the author

When referring to this work, full bibliographic details including the author, title, awarding institution and date of the thesis must be given

Enlighten: Theses
https://theses.gla.ac.uk/
research-enlighten@glasgow.ac.uk

Cloning and biochemical characterisation of two novel PDE4A cAMP phosphodiesterases

Fiona A Begg

Submitted to the faculty of IBLS, Glasgow University for the degree of Doctor of Philosophy September 2000

Supervisor Professor Miles Houslay

ProQuest Number: 10647526

All rights reserved

INFORMATION TO ALL USERS
The quality of this reproduction is dependent upon the quality of the copy submitted.

In the unlikely event that the author did not send a complete manuscript
and there are missing pages, these will be noted. Also, if material had to be removed,
a note will indicate the deletion.

ProQuest 10647526

Published by ProQuest LLC (2017). Copyright of the Dissertation is held by the Author.

All rights reserved.
This work is protected against unauthorized copying under Title 17, United States Code
Microform Edition © ProQuest LLC.

ProQuest LLC.
789 East Eisenhower Parkway
P.O. Box 1346
Ann Arbor, MI 48106 – 1346

Acknowledgements

Special thanks to my supervisors Professor Miles Houslay and Dr Michael Sullivan for their support and advice in helping me to complete this thesis.

Thanks also to everyone in the Houslay lab and the Molecular Biology team at Astra Charnwood for their friendship and advice.

More extra special thanks to Alison, Gordon and my family, for their immeasurable patience and support and to whom I am dedicating this work.

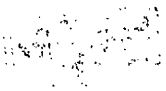

CONTENTS

CHAPTER 3

CHAPTER 4

Index of figures

Abstract

A large multi-gene family encodes many different phosphodiesterase (PDE) enzymes with alternative mRNA splicing generating additional complexity. This thesis details the discovery and cloning of two new PDE4A cyclic AMP specific phosphodiesterases. These two enzymes have been named hRD1 (HSPDE4A1) and PDE4A10. hRD1 is a PDE4A short-form and PDE4A10 is a PDE4A long-form. Previous to this study only a single active PDE4A short-form from rat RD1 (RNPDE4A1A) had been cloned and two active PDE4A long-forms, namely PDE4A5 (mammalian and rat) and PDE4A8 (rat).

Reverse transcriptase PCR analysis carried out in a previous study had indicated that RD1 homologues were conserved across species and sequencing of the HSPDE4A gene revealed the existence of the human homologue. The sequencing study located the 5' exon encoding the unique N-terminal region of the human homologue of the rodent isoform RD1 and also the splice junction used to produce this short-form. The work carried out in this thesis details how this information was used to clone the human short-form hRD1 as both the sequence encoding the unique N-terminal and the position of the splice junction had both been revealed.

The open reading frame encoding hRD1 (HSPDE4A1A, GenBank U97583) was engineered for expression in the plasmid pcDNA3 (Invitrogen) and this was transiently expressed in COS-1 cells. The mature hRD1 protein was detected as an 83kDa species, the majority of which was associated with the high-speed membrane fraction. The kinetic properties of this enzyme were also investigated and hRD1 displayed a K_m for cAMP of around 3 μM, an IC_{50} value for inhibition by the PDE4-selective inhibitor rolipram of

around 0.3 μM and the thermostability of the enzyme was found to be considerably more thermostable than rat RD1. The membrane binding capability of the enzyme was also investigated. This was done by generating human RD1 as a mature 80kDa species in an *in vitro* transcription-translation system which displayed the ability to bind to COS-1 cell membranes.

The data from these experiments showed that the rat and human homologues displayed very similar properties, particularly their intracellular location, K_m for cAMP and sensitivity to rolipram inhibition. They displayed marked differences in their thermostability which may be a result of conformational differences between the proteins in regions outside of their active sites.

The human PDE4A long-form PDE4A10 was cloned initially by Graham Rena in this laboratory. The sequence for the unique N-terminus of this isoform was based on a rat cDNA containing sequence which indicated a novel N-terminus. Existence of the human homologue was confirmed by reverse transcriptase analysis which detected PDE4A10 in human cell lines. Further sequencing of human cosmid clones containing HSPDE4A sequence confirmed the sequence and also revealed the position of the PDE4A10 splice junction.

This thesis details how PDE4A10 was engineered for expression studies. The construct which was originally engineered apparently contained three potential in-frame initiating methionines (ATG). This study defined the native ATG of PDE4A10 and a construct was engineered in the plasmid pSV-SPORT for expression in COS-1 cells. The mature PDE4A10 protein was detected as a species of around 125kDa on traditional 8% cross-linked SDS-polyacrylamide gels. This was very similar to the other PDE long-form

PDE4A4B (PDE46) and the difference in molecular weight between these two proteins could only be resolved on a pre-cast Tris-Acetate 3-8% polyacrylamide gel system (Novex). Using this system the calculated molecular weight of PDE4A10 was now around 120kDa compared to 125kDa for PDE4A4B calculated using the same system.

The majority of PDE4A10 expressed in COS-1 cells was detected in the cytosolic fraction and the majority of PDE4A10 activity was also found in the cytosolic fraction. Kinetic studies revealed that the enzyme displayed a K_m for cAMP of around 4 μM and an IC_{50} value for inhibition by the PDE4-selective inhibitor rolipram of around 0.3-1 μM in the membrane fractions and around 0.02 μM in the cytosolic fraction.

CHAPTER 1

1.1 Brief introduction to PDEs

Cyclic nucleotide phosphodiesterases (PDEs) play a key pivotal role in intracellular signalling as they provide the sole route for hydrolysis and thus inactivation of the ubiquitous second cell messenger cAMP and cGMP. Certain PDEs can hydrolyse both cAMP and cGMP while others are specific for one or the other.

PDEs are encoded by 19 different genes in mammals (Conti and Jin 1999; Conti et al., 1995; Beavo 1995; Fisher et al., 1998a, Fisher et al., 1998b; Soderling et al., 1998). However, further complexity arises from the rearrangement of the transcriptional units within each gene - so-called alternative mRNA splicing - giving the number of PDEs produced around 50 (Conti and Jin 1999; Muller et al., 1996). This gives rise to a vast range of similar proteins with subtle but crucial differences in their structural and functional properties (Beavo et al., 1994; Bentley et al., 1992; Butt et al., 1994).

Individual PDEs can be categorised according to their properties such as their apparent molecular mass, substrate specificity (K_m), immunological reactivity, sensitivity to synthetic inhibitors (IC_{50}) and mode of regulation (Barnett et al., 1995; Bolger, 1994; Charbonneau et al., 1986; Yan et al., 1996; Yan et al., 19950). But their basic function in each different cell type remains the same and that is to regulate the level of cAMP or cGMP available in the cell which is able to activate cyclic nucleotide-dependent protein kinases (PKA). These, in turn, initiate multiple cellular events, (Kemp et al., 1975; Walsh et al, 1994) by phosphorylation of target substrates.

The diagram below in figure 1 shows an overall scheme of where PDEs fit into the general signal transduction pathway within mammalian cells. The generation of the first

signal (cAMP) in response to extracellular stimuli at the cell surface in the form of neurotransmitters, hormones, phospholipids, photons, odorants, certain taste ligands and growth factors (Gutkind, 1998; Ji et al., 1998) will be discussed in the next section.

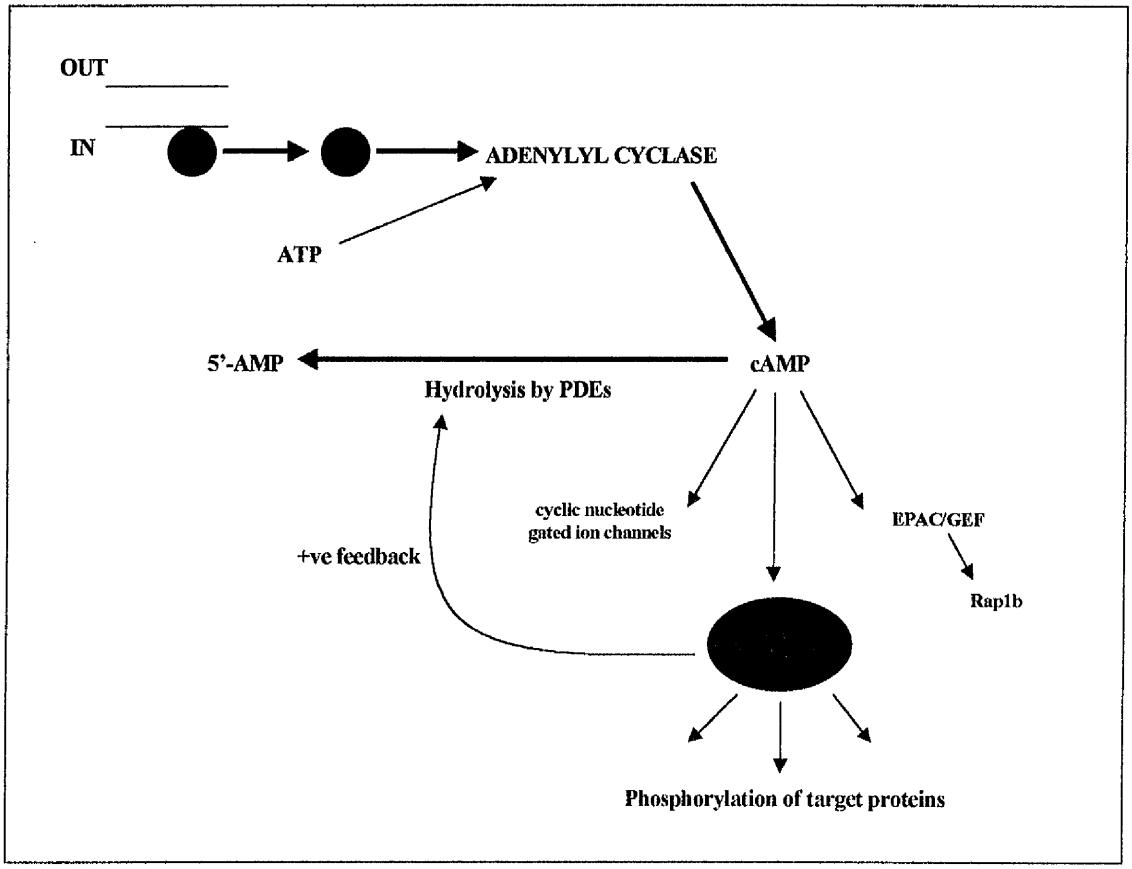

Figure 1. *Intracellular regulation of cAMP by phosphodiesterases. This figure outlines the way in which PDEs interact with intracellular signalling once a signal has been detected at the cell surface and transduced via G-protein-coupled receptors resulting in the formation of cyclic AMP. cAMP is able to exert its effect on cAMP-dependent protein kinase A, as well as EPAC, cAMP-GEF and cyclic nucleotide gated*

ion channels, which then triggers many events within the cell. The hydrolysis of cAMP by PDEs is the mechanism by which these events are regulated and the cAMP signal is attenuated or switched off.

1.2 Generation of the second messenger cyclic nucleotide (cAMP)

The molecule 3', 5'-cyclic monophosphate (cAMP) was discovered in the 1950s by Sutherland and his co-workers (Sutherland and Rall 1957). Generation of cAMP is the ubiquitous intracellular response to many stimuli at the cell surface. These stimuli are detected by a vast range of receptor molecules which span the cellular membrane. These receptors generally consist of seven transmembrane domains and are referred to as 7TM receptors or GPCRs, G-protein coupled receptors (Houslay and Milligan 1997; Mitzobe et al. 1996).

Stimuli in the form of certain neurotransmitters or hormones are able to activate specific members of the 7TM receptor family and this triggers an interaction between the receptor and the G-protein linked to it on the intracellular surface of the membrane (Gutkind 1998). In the case of ligands that increase cAMP levels their occupied receptors specifically interact with the guanine nucleotide regulatory protein G_s and allow this G-protein to exchange GDP with GTP. This causes a conformational change in the G-protein that results in the dissociation of the GTP-bound α-G_s subunit and also release of the $\beta\gamma$ complexes. The GTP-bound form of α-G_s then stimulates the transmembrane enzyme adenylyl cyclase. It is adenylyl cyclase that generates cAMP from ATP (Cooper

1998; Hanoune et al., 1997; Sunahara et al., 1996; Tang and Hurley 1998; Xia and Storm 1997) .

The formation of cAMP requires various changes in the molecule ATP. Specifically the 3'-hydroxyl group on ATP must be deprotonated in order to be activated. This makes it susceptible to nucleophilic attack which stabilises the transition state at the α-phosphate. This also confers stabilisation of increased negative charge on the leaving group pyrophosphate (Hurley 1999).

The structure and function of the ATP binding site of adenylyl cyclase has been revealed by P-site (phosphorylation site) inhibitor complex studies. These showed that a single Mg^{2+} ion was capable of interacting with both phosphate moieties of pyrophosphate and the ATP binding site was found to be made up of two Asp residues which are mutationally sensitive (Liu et al. 1997; Tang et al. 1995; Tesmer et al. 1997; Yan et al. 1997). This provides evidence for a two ion mechanism (Pieroni et al. 1995; Zimmermann et al. 1998) whereby one ion acts kinetically as free Mg^{2+} and the other binds in a complex with ATP.

There is a model for this interaction based on a similar situation in the DNA polymerase family. In this case two ions bind to DNA polymerase-primer-template-nucleotide complexes (Kiefer et al. 1998; Steitz 1998) showing how the two ions may be coordinated in the adenylyl cyclase active site. The ion observed in the adenylyl cyclase active site corresponds to the "B" metal ion in the polymerase and it binds all three nucleotide phosphates with tight interactions (Sawaya et al. 1997) which strongly suggests that this ion acts as the kinetically active ATP complex.

The metal ion A is less tightly bound in the adenylyl cyclase structure (Doublie et al.

1998) and interacts with the 3'-hydroxyl group and the nucleotide α-phosphate and both ions share in transition state stabilisation. Both of these metal ions are coordinated by Asps in the Mg^{2+} binding site and it is possible that the Asp-354 in the adenylyl cyclase or its equivalent in DNA polymerase may in these reactions act as a general base.

1.3 G-protein coupled receptors (GPCRs)

GPCRs are membrane-spanning proteins consisting of seven transmembrane domains. They have also been referred to as 7TM receptors (Baldwin et al. 1997; Unger et al. 1997). A vast array of these receptors exist, with more than 2000 GPCRs documented since 1986 (Dixon et al. 1986). They can be broadly classified by the type of molecule which they are able to bind and detect. They are also classified into more than 100 subfamilies based on their receptor function, ligand structure and sequence homology.

As mentioned above, GPCRs bind and detect the presence of many different molecules. These include biogenic amines, nucleosides, eicosanoids, and moieties of lipids (lysophosphatidic acid and sphingosine 1-phosphate), glycoprotein hormones, LSH, FSH, human CG, and TSH plus small neurotransmitters like Ca^{2+}, glutamate and GABA (Ji et al. 1998), as well as protease ligands such as thrombin.

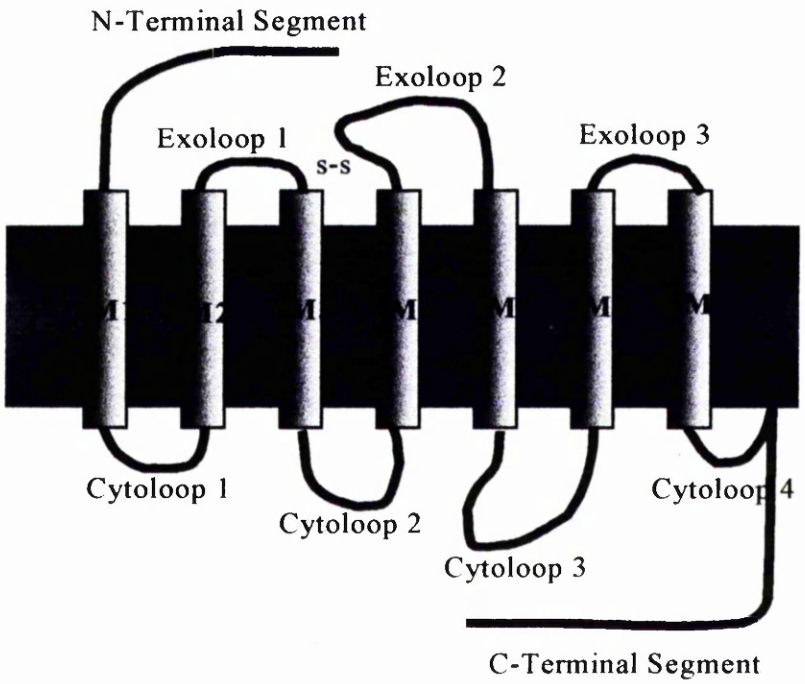

Figure 2. *Basic structure of GPCRs showing the N-terminal segment, seven TM domains, which form the TM core, three exoloops, four cytoloops and a C-terminal segment. Signals can be generated by cleavage of the N-terminal segment, the remainder of which then interacts with exoloops to generate a signal. Other molecules bind to the N-terminal segment and the liganded N-terminal segment interacts with exoloops to generate a signal. Smaller molecules bind to the N-terminal segment and the liganded N-terminal segment interacts with the membrane-associated domain, generating a signal. A fourth cytoloop is formed when the C-terminal segment is palmitoylated at Cys. Adapted from Ji et al. 1998.*

Figure 2 shows the basic structure of GPCRs. This consists of an extracellular N-terminal segment, seven transmembrane domains forming the TM core, three exoloops, four cytoloops and a C-terminal segment. The seven transmembrane sections are each made up of around 20-27 amino acids. However, the various loop and N- and C-terminal sections of the receptors vary widely in their size. It has been proposed that the length of the N-terminal segment correlates to the size of ligand which it can bind (Ji et al. 1995).

All GPCRs adopt the same basic seven TM structure, with N- and C-terminal segments on opposite sides of the membrane, allowing glycosylation and ligand binding at the N-terminal segment and phosphorylation and palmitoylation at the C-terminal segment, which allows for desensitisation and internalisation of the receptor (Lefkowitz 1998).

GPCR agonists are capable of conformational changes which are part of the mechanism by which signals are transduced and are able to be relayed to the G-proteins which are coupled to the receptors. Recently GPCRs have been shown to be capable of activating G-proteins in the absence of agonist and this capability is enhanced by mutations in structural domains of the receptor, presumably acting in the same way as but instead of conformational changes normally triggered by agonist binding (Altenbach et al. 1996; Chidiac 1994; Farrens et al. 1996; Samama et al. 1993; Wess 1997).

The seven TM domains are able to orientate themselves in different ways in the membrane so as to offer maximal diversity for ligand binding. This also provides different mechanisms for binding. One example concerns the binding of lysophosphatidic acid which has a fatty chain associates with it. If TM domain 7, which is normally apposed to TMs 1 and 2 (Sealfon et al. 1997), is orientated more closely to TM 2 than

TM 1 then this opens up a long crevice between TMs 1 and 7 which creates a binding site for such a molecule.

Other types of agonists bind to the receptor in a similar way, using various regions of the different TM domains. Receptor activation can be thought of a three step process. The first step is signal generation, then TM signal transduction and finally signal transfer to signalling molecules (G-proteins) at the cytosol surface of the plasma membrane (Ji et al. 1995). TM domain hydrogen bonds play the major part in this process. In this way the ligand binds and generates a signal which is transduced through the TM core (Ji et al. 1998).

One example of this involvement of hydrogen bonds in the TM domains is the way in which photoactivation of retinal affects configuration of the receptor. This causes the kinked conformation to straighten which in turn changes the packing of TMs 3 and 5-7 through rearrangement of the hydrogen bonds. In the case of some receptors it has been fairly easy to establish that ligand binding and signal generation are separate occurrences taking place at different TM domains. For example in biogenic amine receptors TM3 is thought to be the primary site for ligand binding with signal generation occurring primarily at a different locations on TMs 5 and 6, although these processes in other receptors can be difficult to distinguish (Ji et al. 1998).

Another group of agonists which trigger signalling in a different way using different parts of the GPCR structure are the glycoprotein hormones, LH, FSH, CG and TSH which are the largest and most complex of the GPCR agonists. They bind firstly only to the N-terminal domain with high affinity which then undergoes a conformational change (Ji et al. 1995) and a signal is generated through secondary interactions with the membrane-

associated domain. The first high affinity interaction involves both the common α-subunit and the hormone-specific β-subunit of the glycoprotein coming into contact with the N-terminal segment of the receptor (Dias et al. 1998; Grossmann et al. 1997). Signal generation, however, takes place at the exoloops as secondary binding occurs between the liganded N-terminal segment and exoloops 1-3 (Remy et al. 1996; Ryu et al. 1998). Interestingly it has been shown that mutations occurring in these exoloops can actually lead to constitutive activation of the receptor confirming their role in receptor activation (Parma et al. 1995).

There is a basic model for GPCR agonist activation which is called the ternary complex model (Gether and Kobilka 1998). This helps to explain why so many different classes of agonists (full, partial, neutral and inverse) are able to have an effect on the receptor signalling through GPCR interactions with the G-protein. The model proposes that the receptor exists in a state of equilibrium between the inactive (R) and active (R*) state and the agonist effect depends on its ability to alter this state (Kenakin 1997). The active state R* is also the conformational state in which the receptor is capable of activating G-proteins.

The ways in which conformational changes can be induced are various. For several non-GPCR receptor families, including receptor tyrosine kinases and the growth hormone receptor family, agonist-induced receptor dimerisation is required for signal transduction (Wells, 1996). In the case of GPCRs recent evidence has suggested that they can also form dimers which indicates that dimerisation may also be a part of the activation process (Cvejic and Devi 1997; Herbert et al. 1996; Romano et al. 1996). Protonation also plays a role in receptor activation. In the case of the rhodopsin GPCR family they have a highly

conserved DRY motif at the cytoplasmic side of TM3 (Probst et al. 1992). The arginine in this motif (ArgIII:26) is usually conserved and is held in a hydrophilic pocket by polar residues conserved in TMs 1, 2 and 7. Receptor activation may occur through protonation of AspIII:25 which causes ArgIII:26 to become exposed to the cytoplasm as it moves out of the polar pocket.

Previously hidden sequences in the second and third intracellular loops are now exposed.

The mechanisms above lend support to the theory of the active (R*) state of the enzyme, in which its conformation has changed causing activation. This also implies that the GPCRs must have stable intramolecular interactions in order to remain in an inactive (R) state. Indeed small mutations such as one in the C-terminal region of the third intracellular loop can lead to a large increase in agonist-independent receptor activity (Lefkowitz et al. 1993).

A startling array of complexity and adaptation is displayed by the GPCRs and this is only the first level of cellular signalling, the detection stage. The next section will discuss the second stage in signal transduction where signals received by the GPCRs are relayed onto the G-protein, the first stage of signalling within the cell.

1.4 G-proteins

As seen in the previous section, signals arriving at the exterior of the cell are detected by receptors coupled to G-proteins. These proteins are heterotrimeric and they relay signals from the receptors and transform them into intracellular responses.

G-proteins are made up of several subunits, α, β and γ and many gene products are known to encode each subunit. The G-proteins fall into three distinct classes based on their activities within the cell and these are; G_s, which activates adenylyl cyclase, G_i, which inhibits adenylyl cyclase and G_q, which activates phospholipase C. Two other G-protein groups are known to exist (G_{12} and G_{13}) but their functions are not known (Hamm 1998).

When G-proteins are in their inactive heterotrimeric state they bind GDP. They become activated when the receptor catalyses a reaction involving guanine nucleotide exchange which leads to GTP binding to the α subunit. GTP binding causes the dissociation of the α subunit (with the GTP bound to it) from the rest of the G-protein molecule, the β and γ subunits (Lambright et al. 1994; Lambright et al. 1996). These two separate units, the GαGTP and the Gβγ, are now both able to exert downstream effects. The Gα has intrinsic GTPase activity and hydrolyses the GTP back to GDP causing desensitisation. The speed of this reaction becomes the rate limiting step in attenuating cellular responses to G-proteins.

Gα subunits consist of two domains. The G domain is structurally identical to the superfamily of GTPases including small G-proteins, and is involved in binding and hydrolysing GTP and the unique helical domain buries the GTP in the core of the protein (Hamm et al. 1998). The core of the α subunit contains the catalytic core that contains the gaunine nucleotide-binding site which is able to bind and hydrolyse GTP to GDP. It consists of 5 α helices surrounding a 6-stranded β-sheet and contains the consensus sequences involved in GTP binding that bind the phosphate group and guanine ring of GTP. The core also contains a binding consensus site for Mg^{2+} which is essential for

catalysis (Sprang 1997).

The β-subunit of G-proteins has an N-terminal helix followed by a repeating 7-membered β-propeller structure based on its 7 WD repeats (Lambright et al. 1996; Sondek et al. 1996). Each of the seven similar β-sheets consist of four antiparallel strands which make up one propeller. The γ-subunit is made up of two α helical structures with no inherent tertiary structure. Interaction with the β-subunit occurs through the N-terminal helix of the γ-subunit which forms a coiled-coil with the N-terminal helix of the β-subunit. The remainder of the γ-subunit makes extensive contacts all along the base of the β-subunit (Lambright et al. 1996; Sondek et al. 1996).

The β- and γ-subunits together form a functional unit that only becomes dissociated by denaturation. When the G-protein is activated by receptors this causes GTP binding on the Gα-subunit to occur. There is a GTP-mediated switch on the Gα-subunit whose structural nature causes a conformational change of three flexible regions, referred to as Switches I, II and III to a well ordered, GTP-bound activated conformation. This has a lower affinity for the Gβγ-subunit (Lambright et al. 1994). The GαGTP now has increased affinity for effectors and subunit dissociation which leads to the generation of free Gβγ which is now able to activate effectors.

Many studies have focussed on determining which parts of the G-protein interact with the receptor. Two possible sites of membrane interaction have been discovered in the N-terminal region of the α-subunit and the C-terminal region of the γ-subunit. These regions are lipidated (Resh 1996) and relatively close together in the heterotrimer and evidence exists that all three subunits possess good receptor contact areas.

The C-terminal region of the Gα-subunit has been particularly well studied and

mutagenic analyses have shown that the C-terminus of the third extracellular loop of receptors is capable of binding to the C-terminus of the Gα-subunits (Martin et al. 1996; Sprang, 1997).

Mutational analysis of the β-subunit has shown that mutations in residues that make contact with the α-subunit causes a block in receptor-mediated GDP-GTP exchange. This provides evidence that the βγ-subunits of the heterotrimeric G-protein are required to enhance receptor interaction with the α-subunit and suggests that the γ-subunit must be holding the α-subunit in place for GDP release to occur. Indeed one particular region of the G-protein, the C-terminal region of the γ-subunit has been shown to be involved in receptor coupling and specificity (Kiesselev et al. 1995; Yasuda et al. 1996).

When the three subunits, the α-subunit (1) and the βγ-subunit (2 and 3), of the heterotrimeric G-protein dissociate upon GTP binding to the α-subunit the G-protein is now in its active state and a new surface becomes available on the Gα-subunit (Skiba et al. 1996). These subunits are now able to interact with effectors with a greatly increased affinity (20-100 fold higher) through these particular surfaces than in their GDP-bound state. These surfaces on the Gα-subunits also display remarkable specificity for effector interaction (Skiba et al. 1996).

The Gβγ once separated from the GαGTP is capable of activating many proteins (Clapham and Neer 1997). These include some isoforms of second messenger enzymes such as PLCβ2 and -β3 (Morris and Scarlata 1997) and adenylyl cyclase, certain G-protein-responsive K^+, Ca^{2+} and some Na^+ channels (Schneider et al. 1997), more than one phosphatidylinositol 3-kinase isoform (Tang and Downes, 1997) and has also been reported to bind to members of the Rho family of GTPases, Rho and Rac (Harhammer et

al. 1996).

There is evidence that Gβγ interactions with effectors may occur through the Gα binding site as the Gβγ conformation when free is the same as it is in the G-protein heterodimer (Sondek et al. 1996). This also implies that Gα is able to inhibit the action of free Gβγ through binding to the Gα binding site on Gβ (Chen et al. 1995; Chen et al. 1997). Other regions that may be involved in effector interactions include the N-terminal coiled coil (Pellegrino et al. 1997) and blades 1 and 7 of the β-propeller of Gβ (Bluml et al. 1997).

1.5 Adenylyl cyclase

Adenylyl cyclase is the molecule which is able to generate cAMP from ATP. There are nine isoforms of adenylyl cyclase, two of these have splice variants. The various adenylyl cyclase families and the effects of various regulators on them can be seen in figure 3.

Adenylyl cyclase	Splice Variants	Chromosomal location
AC-I		7p12-7p13
AC-II		5p15.3
AC-III		2p22-2p24
AC-IV		14q11.2
AC-V	2	3q13.2-3q21
AC-VI	2	12q12-12q13
AC-VII		16q12-16q13
AC-VIII		8q24.2
AC-IX		unknown

Figure 3. *The different isoforms of adenylyl cyclase and the two splice variants which belong to families V and VI. Also shown are the chromosomal locations of each adenylyl cyclase isoform.*

All adenylyl cyclase molecules share a basic primary structure. This consists of two transmembrane regions named M_1 and M_2 and there are two cytoplasmic regions C_1 and C_2 (Hurley 1999; Krupinski et al. 1989; Taussig and Gilman 1995). Figure 4 below, shows a diagrammatic representation of these subunits which make up adenylyl cyclase and their position within the cell membrane.

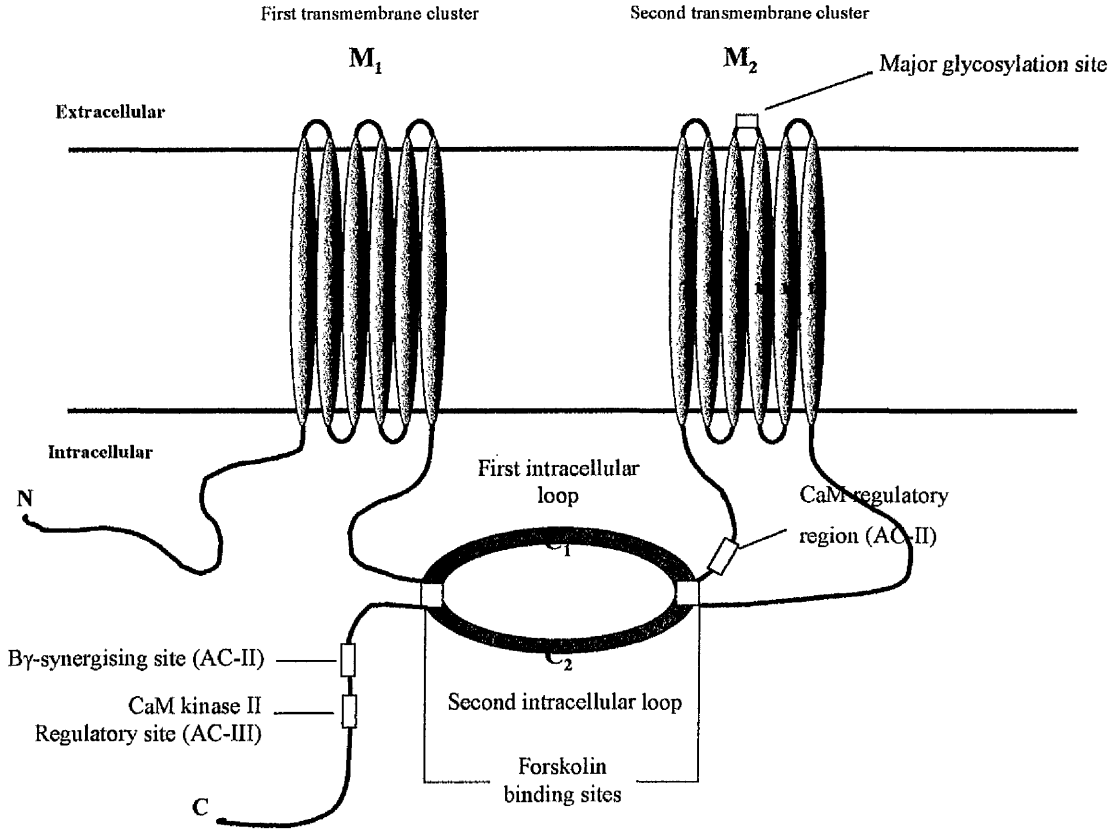

Figure 4. *Relative positions of the subunits making up the basic structure of adenylyl cyclase. There are two transmembrane subunits, M_1 and M_2 which are each made up of six helices, and two cytoplasmic regions C_1 and C_2. The active site is contained within the cytoplasmic regions. The regulatory elements are also situated in this region including the CaM (Calmodulin) regulatory region which is situated next to the cytoplasmic domains. Diagram adapted from Houslay and Milligan 1997.*

The transmembrane regions are each made up of six membrane-spanning helices and

their function, other than to locate the molecule in the membrane, is unknown. They do, however, show similar topology to some membrane transporters although none of the mammalian isoforms of adenylyl cyclase have been shown to display this type of activity (Sunahara et al. 1996).

There is a high degree of homology shown in the cytoplasmic regions between the family members and more variation is seen in the transmembrane helices between families (Houslay and Milligan 1997). The active sites of the enzyme are contained within the cytoplasmic domains. These two regions C_1 and C_2 are both subdivided into two units, a and b (C_{1a}, C_{1b} and C_{2a}, C_{2b}). The subunits C_{1a} and C_{2a} are highly homologous to each other, contain all of the catalytic domain and are able to heterodimerise with each other in solution (Tang and Gilman 1995; Whisnaut et al. 1996; Yan et al. 1996) leading to reconstitution of the enzyme activity.

The region C_{1b} is fairly large, around 15kDa, and is thought to contain several regulatory domains, whereas the C_{2b} region is extremely small and has no identified function to date.

Structural analysis of adenylyl cyclase type II has revealed that the C_2 region is formed of two C_2 monomers making a homodimer of a circular shape with ventral groove between the two monomers. There are two forskolin binding sites within this ventral groove of the homodimer (Zhang et al. 1997). Forskolin can bind to and activate all forms of adenylyl cyclase except type IX. Many mutagenesis studies have shown that the adenylyl cyclase active site, i.e. the ATP binding site, must be located within this ventral groove and two particular residues (Asn1025 and Asn 1029) have been shown to be critical for enzyme activity (Tang et al. 1995; Yan et al. 1997; Tucker et al. 1998).

Another region of the adenylyl cyclase molecule which has been implicated as playing a

role in ATP binding is the carboxyl terminal. It may be that this region has a regulatory influence on the binding. It was not possible to deduce the crystal structure of this region at the same time as the C_2 structure was resolved but this suggested that the C-terminal region was disordered and became more ordered upon ATP binding to the catalytic site (Zhang et al. 1997). It has been proposed that the C-terminal region forms a flap or a lid when it is bound in the catalytic site and in this position it is able to exert a regulatory influence on catalysis.

Other molecules are known to play a role in regulation of mammalian adenylyl cyclase activity. They are strongly activated by Mn^{2+} and inhibited by very low (millimolar) concentrations of Ca^{2+}. The activation of many enzymes is dependent on Mg^{2+} and this can often be replaced with Mn^{2+} resulting in the same effect. In the case of adenylyl cyclase the effects of the Mn^{2+} and Ca^{2+} ions are unlikely to have distinct physiological significance or reflect particular binding sites for these ions. A possible physiological inhibition of type V and VI adenylyl cyclase has been reported when Ca^{2+} is present at higher concentrations. In this case the free Ca^{2+} is binding competitively to the Mg^{2+} sites on the enzyme but does not activate it catalytically in the same way (Yoshimura and Cooper 1992).

Forskolin has also been shown to be a very strong activator of adenylyl cyclase. It binds to the catalytic core of the enzyme in the ventral cleft that also contains the active site but at the opposite end. It acts as glue using hydrophobic and hydrogen bonding to bind these two regions in the core together and activating the enzyme. Particular residues have been implicated in this binding as type IX adenylyl cyclase is unresponsive to forskolin. It was found to have a Ser to Ala and a Leu to Tyr change in the binding pocket. When these

sites were reversed by site-directed mutagenesis the resulting mutant of type IX is now activated by forskolin (Yan et al. 1998). It is also possible that an equivalent endogenous activator to forskolin exists but has so far not been discovered.

The GTP-bound G-protein α-subunit $G_s\alpha$ is able to potently activate all of the adenylyl cyclases and acts in the same way as forskolin does to bind the two regions C1 and C2 together. This subunit must also have another function and studies have shown that it must be capable of inducing a conformational change stimulating catalysis (Yan et al. 1997; Zimmermann 1998).

Ca^{2+}/calmoduin is also capable of activating type I adenylyl cyclase and is thought to bind to a helical region on the C_{1b} region. The specific mechanism is unknown but it may be interfering with an autoinhibitory interaction in the catalytic core between the C_{1a} and C_2 domains (Vorherr et al. 1993; Wu et al. 1993).

Adenylyl cyclase can also be regulated by protein phosphorylation and protein kinase C has been shown to activate type II by phosphorylation at Thr-1057. This particular region is known to contain a site which is required for protein kinase C activation. This phosphorylation site is at the edge of the carboxyl terminal tail which upon ATP binding to the active site folds over it. It is though that phosphorylation may help this region to adopt the correct conformation for this action (Bol et al. 1997; Levin and Reed 1995).

A region on the outer edge of the active site is phosphorylated by CaM kinase II at Ser-1076 and inhibits type III adenylyl cyclase by interfering directly with catalysis (Wei et al. 1996). Protein kinase A phosphorylates Ser-674 in the C1b region of type VI and may be regulating a low affinity secondary binding site for $G_s\alpha$ (Chen et al. 1997). Type I adenylyl cyclase is phosphorylated by CaM kinase IV in the C_{1b} domain which interferes

with calmodulin binding sites therefore disabling the Ca^{2+}/calmodulin activation of the enzyme (Wayman et al. 1996). Figure 5 summarises the information above concerning which elements regulate which isoforms of adenylyl cyclase and the effects they have on them, whether they are positively or negatively influential on activation.

Adenylyl Cyclase	Regulators	**Ca2+**	**G-prot βγ**	**G-prot αG_i**	**PKC**	**PKA**
AC-I		+	-	-	+	?
AC-II		nc	+(+αG_s)	nc	+	?
AC-III		+(+αG_s)	Nc	?	+	?
AC-IV		nc	+(+αG_s)	nc	nc/-	?
AC-V		-	Nc	-	nc/+	-
AC-VI		-	Nc	-	nc/+	-
AC-VII		nc	+	?	+(?)	?
AC-VIII		+	-	-	?	?
AC-IX		-	Nc	?	?	?

Figure 5. *The effects of various regulators on the activity of different adenylyl cyclase isoforms. +, signifies increase in activity; - signifies decrease in activity; nc signifies no change and (+αG_s) signifies synergy seen with αG_s. Table adapted from Houslay and Milligan 1997.*

The resolution of the precise structure of the other adenylyl cyclase subunits will enable

further mutational experiments to determine the exact nature of the various regulatory elements in the context of various stimulatory pathways.

The last few sections have looked at the many different elements which are influential in the production of cyclic AMP by adenylyl cyclase. There are many ways in which its activity can be regulated either directly or indirectly as a result of agonist binding to the GPCR and the effects of this on the G-protein which brings the ATP molecule into contact with the adenylyl cyclase. The next section will focus on the effects that the molecule cAMP has within the cell, the molecule which it is able to activate, and the resulting effects of signal transduction from the exterior cell surface.

1.6 Protein kinase A

Nearly all of the effects within the cell in response to extracellular signals which lead to the generation of cAMP are mediated through protein kinase A (PKA). Indeed the primary action of cAMP in eukaryotic cells is to activate PKA which is often described as being cAMP dependent. These proteins are the mediators of the actions of hormones and neurotransmitters which are detected at the cell surface by the GPCRs (Beebe and Corbin 1986; Edelman et al. 1987; Francis and Corbin 1994; Taylor et al. 1990). Fundamentally important physiological processes in cells which are regulated by PKA include synaptic transmission, ion channel and transporter activities, carbohydrate and lipid metabolism, cell growth and differentiation and gene transcription (Rubin 1994).

More than 300 protein kinases are now known to play crucial roles in various aspects of

cellular control (Walsh et al. 1994). Diversity within the protein kinase A group is created by the existence of three C subunit isoforms, α, β and γ. The PKA holoenzymes containing the predominant Cα and Cγ isoforms show very slight differences in their kinetic profile with regards to cAMP sensitivity and very little difference in their substrate specificities and interactions with the cAMP binding R subunits of which there are two forms, RI and RII (Gamm et al. 1996; Scott et al. 1991; Taylor et al. 1990). It is the homodimeric R subunits which display greater variation with regards to cAMP binding affinity and localisation within cells (Corbin et al. 1975).

PKAs, once activated, are able to phosphorylate a wide range of cellular substrates which display serine or threonine residues in a particular context. These residues either have to be presented in the sequence context of Arg-Arg-Xaa-Ser/Thr or Lys-Arg-Xaa-Xaa-Ser/Thr (Dell'Acqua and Scott 1997; Kemp et al. 1977; Kemp and Pearson 1990). Many proteins display these particular sequence motifs so several regulatory mechanisms are in place to prevent indiscriminate phosphorylation and to ensure that both cAMP levels and kinase activity are tightly controlled (Adams et al. 1991; Bacskai et al. 1993; Barsony and Marks 1990; Pawson and Scott 1997). Intracellular cAMP levels are controlled by a balance of adenylyl cyclases and degradation by cAMP phosphodiesterases. The cAMP concentration is further regulated in localised areas by signal-terminating mechanisms such as desensitisation of adenylyl cyclase and compartmentalised activation of cAMP phosphodiesterases (Dell'Acqua and Scott 1997).

PKA isoforms are heterotetramers composed of two regulatory subunits (R) and two catalytic subunits (C). The regulatory subunits maintain the catalytic units in an inactive state and it is also the regulatory subunits which bind cAMP (Corbin et al. 1973; Corbin

and Keeley 1977; Potter et al. 1978; Potter and Taylor 1979).

When the cAMP levels rise in response to extracellular stimuli from hormones and neurotransmitters each R subunit binds two cAMP molecules. The previously inactive PKA holoenzyme dissociates upon cAMP binding (Su et al 1993, 1995) into an R_2-$cAMP_4$ complex and active C monomers. The C subunits become active as dissociation from the R subunits alleviates an autoinhibitory contact (Gibbs et al. 1992; Wang et al. 1991). Once the C subunit are activated the kinase is free to phosphorylate any residues which are presented in the protein sequence context mentioned earlier. When substrates are phosphorylated either their functional and / or structural properties are altered.

The active C subunits phosphorylate target proteins in the plasma membrane, cytoplasm, nucleus and other specialised areas within the cell. From previous studies it has been shown that these kinases were cytosolic enzymes as the majority of PKA activity is usually found to be associated with the soluble (cytosolic) fraction of cell and tissue homogenates. However, one particular protein, the *trans*-acting, nuclear protein CREB is also dependent on phosphorylation by PKA C-subunits in order to elicit gene transcription (Gonzalez and Montminy 1984), but the PKA holoenzyme is not found in the nucleus. A mechanism involving rapid diffusion of activated C-subunits of PKA into intracellular compartments demonstrated how it was able to gain access to the nucleus (Gonzalez and Montminy 1984).

Both the active and inactive forms of CREB are bound constitutively to DNA in chromatin so translocation of active C-subunits of PKA from the cytoplasm to the nucleus is an essential step in cAMP-controlled transcriptional activation (Hagiwara et al. 1993). This was demonstrated by injecting C and R subunits, which had been coupled to

fluorophores, into the cytoplasm of intact fibroblasts or neurons. Accumulation of the dissociated C subunits was observed in the nucleus whereas R subunits and holoenzyme remained in the cytoplasm (Adams et al. 1991; Backscai et al. 1993; Fantozzi et al. 1992; Meinkoth et al. 1990).

There are several ways in which the activity of PKAs is controlled. It is necessary to limit their activity as the motifs which they phosphorylate occur relatively frequently in many proteins within the cell and inappropriate and unlimited responses would occur if no control mechanisms were in place. Control of PKA action starts with factors relating to the level of second messenger available in the cell which is able to activate PKA in the first place. Adenylyl cyclase activity is controlled, for example through desensitisation, and the action of cAMP phosphodiesterases generates concentration gradients of cAMP within cells (Beavo et al. 1994; Tang and Gilman 1992). Other ways in which cAMP gradients are determined in cells are due to localisation of both phosphodiesterases (PDEs) and the PKAs themselves. PDEs are found to be localised to discrete areas of the cell and so are able to establish localised cAMP gradients within the cell (Cooper et al. 1995; Mons et al. 1995; Shakur et al. 1993; Smith et al. 1996).

The idea that PKAs may be localised and able to sample cAMP gradients at distinct points was first shown when Lohman and co-workers discovered a novel protein from neurons which binds RII isoforms with high affinity in the early 1980s (Lohmann et al. 1984). The binding proteins copurified with RII after affinity chromatography on cAMP sepharose and were thought to be contaminating proteins until many of them were shown to retain their ability to bind RII after immobilisation on nitrocellulose filters (Lohmann et al. 1984). A slight variation of this technique became the standard method for

identifying PKA binding proteins using RII subunit as the probe (Hausken et al. 1997). The diagram in figure 6 below shows a schematic representation of the RII dimer binding to the anchoring protein. Studies mapping the sites on RII which are required for interactions with AKAPs (A kinase anchoring proteins) firstly concluded that RII dimerisation is a prerequisite for anchoring and then found that the first 45 residues of RII were involved in AKAP binding (Hausken et al. 1994; Luo et al. 1990; Scott et al. 1990). Site-directed mutagenesis analyses defined isoleucines at positions 3 and 5 within this region of RII as essential determinants for association of RII with AKAPs (Hausken et al. 1994, 1996). It has also been discovered that leucines and iosleucines are crucial factors on the reciprocal binding surface of the AKAP (Glantz et al. 1993) although additional AKAP-binding determinants have been mapped between residues 11 to 25 of each RII molecule (Li and Rubin 1995).

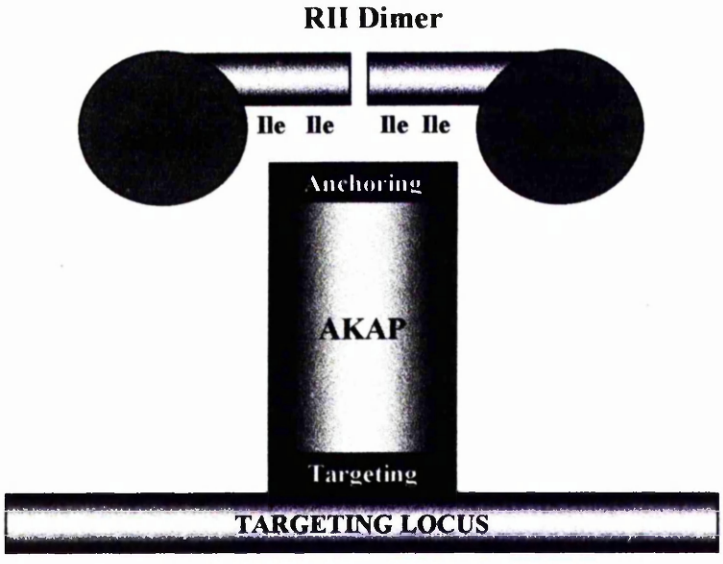

Figure 6. *This diagram represents how the RII dimer binds to the A Kinase Anchoring protein (AKAP) anchoring it in place. The regions where the PKA associates with the binding protein (Anchoring) and the area interacting with subcellular organelles or structures (Targeting) are both indicated. The anchoring domain highlights the isoleucines (Ile) at positions 3 and 5 within the first 45 residues of the RII binding domain which are essential determinants for association with AKAPs. Adapted from Dell'Acqua and Scott 1997.*

It was then proposed that the co-purified protein and other related RII binding proteins are able to bind PKAII at specific intracellular locations (Bregman et al. 1989; Bregman et al. 1991; Leiser et al. 1986; Sarkar et al. 1984) . This would place kinases in close

proximity with certain substrate proteins leading to rapid reception and propagation of the original signal carried by the second messenger cAMP. These RII binding proteins were named A Kinase Anchor Proteins and abbreviated to AKAPs (Glantz et al. 1992; Hirsch et al. 1992). Following the discovery of RII binding proteins further investigation revealed other proteins capable of binding RII in Golgi membranes, the nucleus, centrosomes and the cortical actin cytoskeleton and which therefore may be involved in the functional modification or localisation of PKAII isoenzymes. Subsequent studies have identified many other AKAPs that are associated with particular organelles (Scott et al. 2000). Most of these have been discovered using a combination of subcellular fractionation and immunochemical techniques such as the RII overlay assay. The diagram in figure 7 gives an idea of where these different AKAPs are located and indicates just how PKA activity can be directed to very specific areas of the cell through binding to AKAPs.

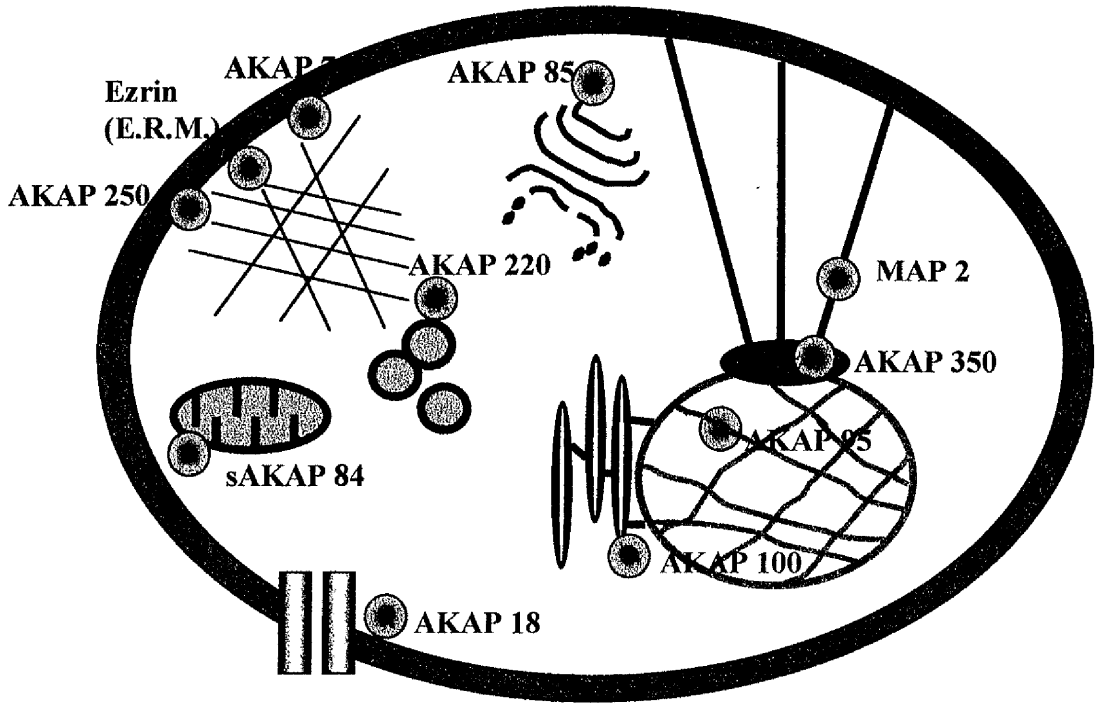

Figure 7. *Approximate location of various known AKAPs indicating how they bring about targeting of various PKAs within the cell. Adapted from Scott et al. 2000.*

1.7 Phosphodiesterases

Phosphodiesterases make up a multi-gene family to supply the activity to convert 3', 5' cAMP to 5'-AMP (Beavo et al. 1994; Conti and Jin 1999, Manganiello 1995b; Torphy et al. 1993). PDEs were discovered around the same time as cAMP in the 1960's and very shortly afterwards the level of diversity within this group of enzymes became apparent as distinct types, or isoforms as we now know, of PDE were separated and partially purified

from various different tissues (Manganiello et al. 1995). To begin with PDEs could only be identified using basic biochemical criteria and were classified according to fractionation using ion-exchange chromatography (Beavo et al. 1971; Thompson et al. 1992; Thompson and Appleman 1971). The first PDEs to be discovered were the calmodulin regulated PDEs and were classed as type I simply because they were usually the first PDE activity to be eluted from a standard diethylaminoethyl (DEAE) ion-exchange column. Only since the advent of molecular biology techniques has it been possible to classify the PDEs more fully and relate their DNA sequence to their structure and possible function (Beavo and Reifsnyder 1990).

1.7.1 Structural organisation of PDEs

Most PDEs characterised so far fall into two main categories based on their specificity for and sensitivity to substrate. Some are able to hydrolyse cAMP or cGMP and some are able to hydrolyse both. Some are inhibited by cGMP (Beltman, et al. 1995). Despite these functional differences many studies have shown that most PDEs characterised so far share a structurally conserved region of around 300 amino acids (see figure 8.).

This conservation was revealed after it had been noticed that segments of the protein kinases which bind and are regulated by cyclic nucleotides appear to be homologous with each other (Takio et al. 1984) and with the *Escherichia coli* catabolite gene activator protein (CAP), a protein which allows regulation of gene expression by cAMP in *E. coli* (Weber et al. 1982). It was also noted that there is a 7-residue segment of identity

between the *dnc*+ -encoded PDEs and a cAMP binding site from the regulatory subunit of the cAMP-dependent protein kinase (Chen et al. 1986).

One particular study had revealed partial amino acid sequences from a Ca^{2+}/calmodulin-stimulated PDE from bovine brain and a cGMP-stimulated PDE from bovine heart (Charbonneau et al. 1986). These sequences were compared with the nucleotide sequences of two distantly related PDEs, one a yeast PDE2 gene and the other the *Drosophila* dunce+ gene (Chen et al. 1986; Sass et al. 1986). This comparison showed a region of homology consisting of between 200 to 270 amino acids which was shared between all of these PDEs. Even though the molecular weights of these proteins varied from 40 to 150 kDa the region of homology seemed to be restricted to one specific segment of each protein. These related segments were proposed to represent the catalytic site of the enzymes and the lack of total homology between the sequences showed that they must be unique gene products (Charbonneau et al. 1986).

Further studies have supported this hypothesis by using controlled proteolysis of PDE1 (Kincaid et al. 1985; Tucker et al. 1981) and PDE2 (Stroop et al. 1989) or deletion mutagenesis of PDE3 (Pillai et al. 1994; Cheung et al. 1996) and PDE4 (Jin et al. 1992; Pillai et al. 1993; Jacobwitz et al. 1996; Kovala et al. 1997; Owens et al. 1997). These experiments showed the direct link between the conserved amino acid regions in these PDE sequences and the domain in the proteins which were involved in substrate recognition and catalysis (Conti and Jin 1999).

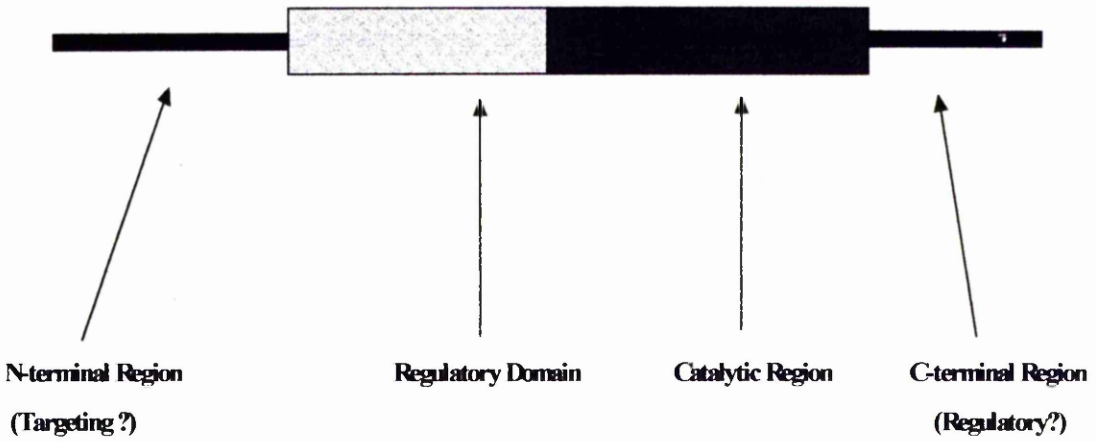

Figure 8. *The general structural domain organisation of PDEs. The particular function of each domain is derived from either sequence similarities, deletion and site-directed mutagenesis and controlled proteolysis (in the case of the catalytic domain) or biochemically and from mutagenesis in the case of the regulatory domains specific for each PDE. The properties of the targeting domains are inferred from the behaviour of native or recombinant proteins and from deletion mutagenesis.*

1.7.2 PDE families

There are currently 19 genes which have been identified as encoding PDEs. These enzymes share a certain amount of sequence homology in the core catalytic domain but they vary widely outside of this, reflecting different properties. They differ with regard to molecular mass, chromatographic qualities, substrate specificity, immunological

reactivity, sensitivity to inhibitors, modes of regulation and their distribution within different areas of the cell and tissue types. Multiple PDE forms can be found in the same tissue and even within the same cell (Beavo et al. 1982; Strada et al. 1984; Wells and Hardman 1977), however, distinct cell-type specific expression patterns are evident.

The different PDE are now classified numerically on the basis of sequence as this determines their distinct functional properties. The naming of these various PDEs is, however, dependent upon their substrate specificity and regulatory properties (Beavo 1988). They can be broadly classified based upon their substrate specificity into the following groups; i) the PDE1, Ca^{2+}/calmodulin-dependent PDEs, ii) the PDE2 cGMP-stimulated PDEs, iii) the PDE3 cGMP-inhibited PDEs, iv) the PDE4, PDE7 and PDE8 cAMP-specific PDEs, and v) the PDE5, PDE6, PDE9 and PDE10 cGMP-specific PDEs (Conti et al. 1991; Torphy et al. 1993). PDE10 and PDE11 are, however, thought to hydrolyse both cAMP and cGMP.

1.8 PDE1

PDE1 enzymes were among the first PDEs discovered and are encoded for by three separate genes PDE1A, PDE1B and PDE1C. Added complexity is provided by alternative mRNA splicing (Bentley et al. 1992; Borisy et al. 1992; Charbonneau et al. 1991; Rossi et al. 1988; Shenolikar et al. 1985). They are known as the Ca^{2+}/calmodulin-dependent PDEs (CaM-PDEs) as they are all activated by calmodulin in the presence of calcium. They also serve to hydrolyse both cAMP and cGMP.

Particularly high levels of PDE1C mRNAs have been found in olfactory epithelium, testis, and regions of mouse brain.

The various PDE1 splice variants all tend to exhibit a higher affinity for cGMP than for cAMP (Butt et al. 1994) but respond differently to Ca^{2+} stimulation and respond differently to inhibitors. A study using substrate competition assays interestingly revealed that there appeared to be only one catalytic site for both the substrates cAMP and cGMP (Yan et al. 1996).

The Ca^{2+}/calmodulin binding region of these enzymes is found on the N-terminal side of the catalytic unit, as seen in figure 9, (Charbonneau et al. 1991) and splice variants with similar Ca^{2+} sensitivities share similar N termini. The CaM-binding is also found in a region which displays similarities to the cGMP-binding regions in PDE2 and the UCR domains in PDE4.

Where N-terminal sequence divergence occurs between isoenzymes, differences in affinities for CaM are also observed. This implies that a role for alternative splicing at the N-terminus of PDE1A is to generate isoforms with different affinities for CaM. This will have a direct effect on PDE activity as binding of CaM to the CaM-binding domain is able to stimulate PDE activity (Charbonneau et al. 1991). To support this theory it has been proposed that in the absence of Ca^{2+}/CaM, the CaM-binding domain binds the catalytic domain and is able to suppress activity. Once Ca^{2+}/CaM binding to the CaM-binding site occurs this results in a conformational change which exposes the active site in the catalytic domain (Charbonneau et al. 1991).

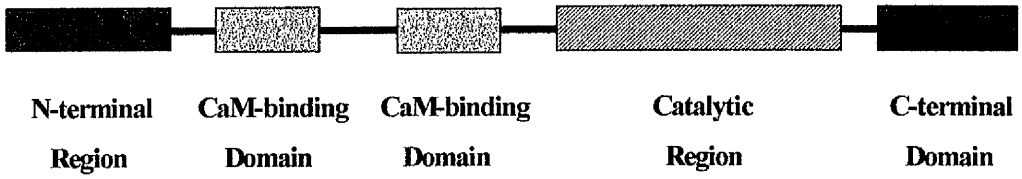

Figure 9. *Schematic representation of the organisation of the various domains (with function attributed if known) within type PDE1 isoforms.*

1.9 PDE2

PDE type 2 enzymes are similar to PDE1 in that they too are able to bind and hydrolyse both cAMP and cGMP. They are stimulated by cGMP and appear to have a lower K_m for cGMP than for cAMP. In the case of PDE2 there are two allosteric cGMP binding sites known as GAF domains (Fawcett et al. 2000; Soderling et al. 1999) found on the N-terminal side of the catalytic unit. Thus when cGMP binds to this site the enzyme is stimulated to hydrolyse cAMP. This occurs due to positive cooperative kinetics and the effect of the cGMP binding is to increase the affinity of the enzyme for cAMP (Beavo 1988). In the case of both PDE1 and PDE2 families the N-terminal regions are able to act

as regulatory domains capable of exerting an influence over the catalytic activity presumably by triggering a conformational change in the catalytic domain.

So far the PDE2 enzymes have all been shown to derive from a single gene. Alternative mRNA splicing results in three known isoforms; PDE2A1, PDE2A2 and PDE2A3. Once again within this group of enzymes sequence analysis has shown that the different isoforms shared the same C-terminal sequences but they have different N-terminal sequences which could determine their localisation within the cell as some of these N-terminal sequences have been shown to associate with membranes (Yang et al. 1994).

Comparison of sequences from PDE2A1 and two other PDE types, PDE5 which is cGMP-specific, and the photoreceptor PDE6 has shown a second region of homology shared by all of these isoforms. This region is distinct from the conserved catalytic domain and is located near the middle of PDE2A1. Experiments have shown that this region binds cGMP with high affinity and is also involved in allosteric regulation of the PDE2 enzymes (Stroop et al. 1989; Stroop and Beavo 1991). Multiple-sequence alignment of these regions has shown two internally-homologous repeat sequences within the cGMP binding or GAF domains (see figure 10) of all three of these PDEs (Trong et al. 1990; McAllister-Lucas 1993) although the significance of this is unclear.

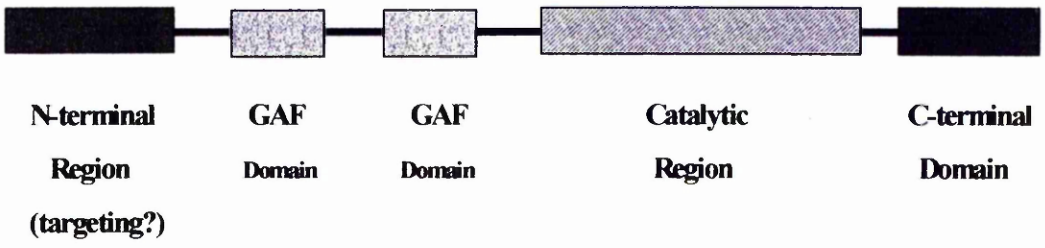

Figure 10. *Schematic representation of the organisation of the various domains which make up PDE2 isoforms and the function of the domain where known.*

1.10 PDE3

There are two genes, A and B, which encode for the two known PDE3 family members. In contrast to PDE2, these are all potently inhibited by low concentrations of cGMP. They are also different from members the PDE2 family in that they specifically hydrolyse cAMP and not cGMP. In fact cGMP acts as a very potent competitive inhibitor binding to the catalytic site of these isoforms rather than binding to a regulatory region. Interestingly PDE3 enzymes contain a unique insert found within the catalytic domain of this enzyme family that has been suggested to explain the high cGMP binding of this enzyme.

Early research using biochemical methods identified two distinct PDE3 enzymes, one found in both platelets and heart (McPhee et al. 1986; Harrison et al. 1986) and the other in adipose tissue (Degerman et al. 1988). These initial findings were later confirmed

using cDNA cloning techniques. This showed that there are two PDE3 genes which allow distinct expression patterns. PDE3A is expressed in heart and platelets (Meacci et al. 1992) while PDE3B is expressed in adipocytes (Taira et al. 1993).

Additional data suggests that multiple promoters in the PDE3A gene are responsible for producing at least two different mRNAs that encode proteins which differ at their N termini (Kayusa et al. 1995).

1.11 PDE4

This PDE family is encoded for by four genes, PDE4A, PDE4B, PDE4C and PDE4D. Their sequences show the highest degree of homology to the *Drosophila melanogaster dunc* PDE. This particular PDE was discovered due to several mutants of *D. melanogaster* which were defective in learning and memory processes and showed lesions at the dunce (*dnc*) locus (Aceves-Pina et al. 1984; Dudai et al. 1976; Gailey et al. 1982; Tempel et al. 1983). These *dnc* flies were shown to have a deficiency in the activity of one form of cAMP PDE compared to normal (Byers et al. 1981; Davis and Kauvar 1984). The *dnc* locus generates numerous alternatively spliced mRNAs and many of these are produced from independent transcriptional start sites (Engels et al. 1994; Obernotle et al. 1993).

Based on this information and the fact that most of the PDE4 isoforms can be inhibited by rolipram (interestingly the *dnc* PDE4 is rolipram insensitive), a compound with anti-

depressant effects in humans (Nemoz et al. 1985), linkage studies have tried to reveal their involvement in psychiatric and behavioural disorders (Milatovich et al. 1994).

Enzymes of this family are characterised by their high affinity for cAMP and a low affinity for cGMP which it neither hydrolyses nor is inhibited by. PDE4s are able to hydrolyse 3',5' cyclic AMP to the inactive form 5'-AMP (Bentley and Beavo 1992; Chen et al., 1986). The products of each particular PDE4 gene share a region in their C-terminal domains that are identical and this can be exploited to produce antisera which distinguish between isoforms generated from other PDE4 genes (Huston et al. 1996; Lobban 1994; Shakur 1995).

PDE4 enzymes are also insensitive to inhibition by cGMP and unaffected by the presence of Ca^{2+}/calmodulin. This very large family of enzymes comprised of many different isoforms all of which are uniquely sensitive to inhibition by rolipram. They have been particularly well studied due to the fact that selective inhibitors for these enzymes have proved to be particularly useful as anti-inflammatory agents.

1.11.1 Discovery of PDE4

This cAMP-specific and rolipram-inhibited PDE was first described in heart extracts (Reeves et al. 1987) and separated out from other PDEs by ion exchange chromatography. The next leap in understanding type 4 PDEs came when a rolipram inhibited, cAMP-specific PDE, named RD1, was cloned from rat brain (Davis et al. 1989). Although the *dunc* PDE is not sensitive to rolipram it was used as a probe to

screen a rat brain cDNA library (Henkel-Tigges and Davies 1990). This was underlined by the cloning of other rodent forms and the idea that PDE4s were the products of four different genes with extra diversity created through alternative mRNA splicing became accepted. This idea was supported by the existence of many human PDE4 isoforms and the mapping of the genes encoding them to separate chromosomes (Bolger et al. 1993; Horton et al. 1995; Swinnen et al. 1989; Szpirer et al. 1995). The notion that diversity within each subtype is generated by alternative mRNA splicing is supported by comparisons of human and rat PDE4D isoforms (for which 5 splicing variants have been reported) which all show a similar splicing pattern indicating that this is a conserved feature (Bolger et al. 1997; Sette et al. 1994; Nemoz et al. 1996). In the case of PDE4 enzymes all of the genes encoding the various isoforms in this family have been mapped to particular chromosomes. These can be seen in figure 11.

Subtype	Chromosomal location
PDE4 A	**19 (p13.2)**
PDE4 B	**1 p31**
PDE4 C	**19 (p13.1)**
PDE4 D	**5 q12**

Figure 11. *The chromosomes to which the various genes encoding the type 4 family isoforms A, B, C and D have been assigned through mapping. Localisation is usually accomplished using fluorescence in-situ hybridisation (FISH) (Gordon et al. 1995). Fine mapping in the case of PDE4A and PDE4C has been accomplished through sequencing.*

1.11.2 PDE4 domain organisation

1.11.2.1 The catalytic domain

It has long been established that PDEs contain a core domain which contains the catalytic activity (Charbonneau et al. 1986). Indeed, proteolysis experiments have confirmed the link between this conserved region and the domain involved in substrate recognition and

catalysis. However, the homology is not uniform and this is one feature that can help distinguish between various PDE families and subtypes. The identification of these regions of homology was established using alignment of sequences from various PDE isoforms. This highlighted a common region of 30-40% similarity that appeared to be around 300 residues in length and provided the catalytic domain of these enzymes (Charbonneau 1990). The catalytic region (see figure 12) of the PDE4 isoenzymes forms a unit of around 357 residues (332 to 689 in PDE4A) and this region shows around 84% homology between the four PDE4 family members as well as the *dunce* PDE. The active isoenzymes from each particular PDE class all have identical sequence at their extreme C-termini.

In the case of PDE4 enzymes the region of catalytic activity has also been defined using mutational studies. These studies have identified individual residues, within this central region, that once mutated lead to either complete or substantial loss of catalytic activity (Jacobitz et al. 1997; Jin et al. 1992; Shabb and Corbin 1992; Woodford et al. 1989).

Several regions in the conserved region are invariant but they are interspersed with regions of considerable diversity. These regions are likely to be major determinants of the structure of the catalytic core, directly effecting the substrate recognition or being involved in maintaining the tertiary structure of the region. The regions of diversity are likely to confer sub-family specific properties on the function of the enzyme.

Several studies have attempted to define the minimum catalytic core. The discovery of a catalytically inactive PDE4A species called 2EL (Horton et al. 1995) containing 278 residues from within the catalytic core demonstrated that the sequences outwith this segment are essential to maintain catalytic activity. It is possible to restore the catalytic

activity of this enzyme by constructing a chimera which replaces the C-terminal region but replacing the N-terminal portion has no effect. This shows that the functional catalytic unit extends beyond residue 643 in PDE4A4B and others studies have shown that C-terminal truncations from residue 772 are active, placing the functional core between 643 and 722.

These studies, however, can become difficult to interpret because of the influence of other regulatory domains and the N-terminal on catalytic activity. Deletions within the N-terminal regions produce confusing results reflecting the influence of different sub-regions on the catalytic domain (Jacobitz et al. 1996; Owens et al. 1997).

1.11.2.2 UCR1 and UCR2, Upstream Conserved Regions

These regions are shown in the diagram in figure 12. They were identified as regions of particular homology by sequence alignment of PDE4s and are not present in any other form of PDE (Bolger et al. 1994). The 60-residue UCR1 region is found N-terminal to the 80-residue UCR2 region and is separated from UCR2 by a linker region named LR1. Similarly, UCR2 is joined to the catalytic unit by another linker region named LR2. LR1 and LR2 are distinct for each of the various PDE4 classes and are respectively around 33 and 10 to 28 residues in length. The linker regions may confer a regulatory role on the UCRs giving them more isoform specific properties. These two regions are quite different in structure, LR1 has both hydrophilic and hydrophobic domains whereas LR2 regions are all hydrophobic. LR1 sequences in particular display a large degree of

heterogeneity between the various long-form PDE4 isoforms. This could give rise to structural differences between isoforms produced by the various PDE4 genes.

It is possible that the LR2 regions may be acting to hold UCR1 and UCR2 in particular positions relative to one another and also relative to the catalytic region of the enzyme. The orientation of the extreme N-terminal regions unique to each splice variant would also be controlled by the position of these sections. In this way UCR1 and UCR2 are likely to play a pivotal role in determining the effects of each unique N-terminal region on the catalytic unit. The regulatory effects of these regions on the catalytic activity may be isoform specific due to the linker regions LR1 and 2. This may be resolved through further structural studies.

Structural analysis has shown the first half of UCR1 is very polar and that this region is likely to be highly flexible. The C-terminal half of UCR1 in contrast is very hydrophobic and helical wheel analysis suggests that this region forms an amphipathic helix with some charged groups to one side. There is evidence to suggest that changes in the conformation of UCR1 can cause major functional changes. A serine in the motif RRESW (Ser^{54}) of PDE4D3 has been shown to be phosphorylated by PKA (Alvarez et al. 1995; Hoffman et al. 1998; Sette and Conti 1996). This action is believed to alter the conformation of this region and leads to an increase in catalytic activity of the enzyme (Alvarez et al. 1995; Sette and Conti 1996; Sette et al. 1994). Interestingly, this motif (RRESW) is conserved in all the long-form PDEs and also the *Drosophila melanogaster dunc* PDE, indicating its functional significance.

It has been suggested that the phosphorylation of Ser^{54} causes a change in overall charge (from positive to neutral) in this region which may disrupt of modify the putative

interaction between the UCR1 and UCR2 regions. This may in turn transmit a conformational change to the catalytic unit altering catalytic activity. There is already evidence (for PDE4A) that the structure of N-terminal splice regions or their interaction with membrane and cytoskeletal components can lead to altered enzyme activity (Houslay 1996; Houslay et al. 1995).

UCR2 has a markedly different primary structure to UCR1. It is extremely hydrophilic and secondary structure plots suggest that it forms a series of three helical regions (Houslay et al. 1998). These regions may form amphipathic helices as the first and last helical regions are anionic whereas the central region appears to be cationic overall.

1.11.2.3 Alternative mRNA splicing

PDE4 genes generate a family of active isoenzymes through alternative mRNA splicing. Three 5' splice junctions have been identified, giving rise to isoenzymes with different N-terminal regions. The first splicing junction produces RNAs which encode the long-form PDE isoforms and the second and third splice junctions produce the short-form PDE4 isoforms. A catalytically inactive form is also generated from the 4A gene through both 5' and 3' splicing. These splice junctions can be seen in the diagram in figure 12.

The alternative splicing seen in PDEs is very similar to that seen in the *dunc* gene of *D. melanogaster* and the same pattern of transcripts being created from alternative transcriptional start sites within the genes (Qui and Davis 1993). The gene structure enabling production of a large number of mRNA transcripts is likely to be complex.

Genomic studies have already revealed the full genomic sequences for PDE4A and PDE4C and partial genomic sequences for rat PDEB and D genes but these have so far only described the short-form PDEs (Monaco et al. 1994). The upstream 5' sequence in which any additional transcriptional start sites and promoters are likely to be located but these were not included in the study.

However, recently the gene locus encoding PDE4A was cloned and this was investigated for the presence of both short and long-forms and the cDNAs encoding them. This study was also able to determine the number of separate exons in each cDNA. The existence of a number of PDEs including PDE46, TM3 and 2EL was also confirmed and the exons encoding both the initiating codon for the PDE46 ORF and its unique N-terminal were identified. The exons encoding UCRs, 1 and 2 were also identified and found to each be encoded by three whereas the catalytic domain is encoded for by six exons (Sullivan et al. 1998).

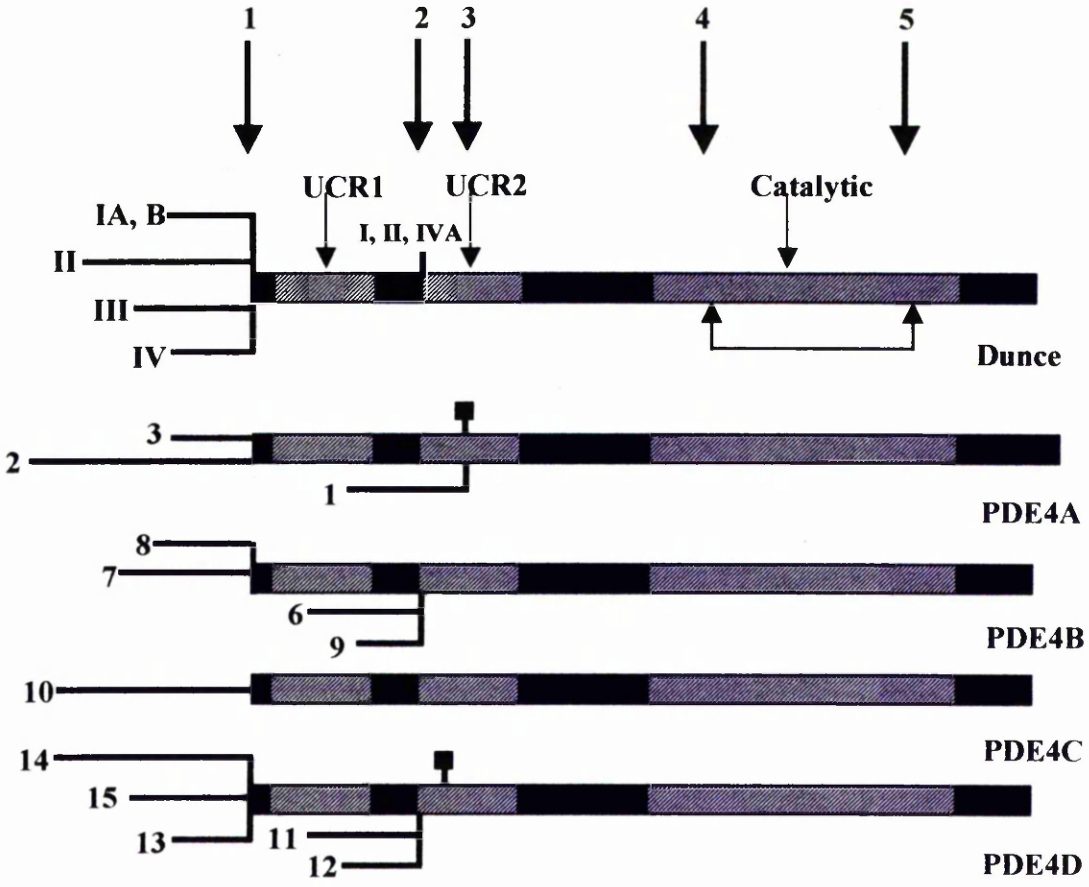

Figure 12. *mRNAs encoded by the mammalian cAMP-specific PDE genes PDE4A, PDE4B, PDE4C and PDE4D. Also shown are the transcripts of the* dunc *gene from* Drosophila melanogaster. *The hatched areas show the sequences with the highest level of homology (UCR1, UCR2 and catalytic). The individual splice variants are shown by the thinner solid lines and the arrows marked 1, 2 or 3 showing where the three splice junctions exist. Splice junction 1 creates long-form PDE4s; splice junction 2 creates short-forms in PDE4B (4B2) and PDE4D (4D1), and splice junction 3 creates short-*

forms in PDE4A (PDE4A1) and PDE4D (4D2) which both have a truncated UCR2. Adapted from Houslay et al. 1998.

1.11.2.4 Unique N-terminal domains created by alternative mRNA splicing

Alternative mRNA splicing generates unique regions of N-terminal sequence which confer distinct functional properties on specific isoforms. There are two major splice junctions that give rise to alternative splicing in both human and *Drosophila dunce* PDE genes. A third has been described in the genes for PDE4A and PDE4D. The location of these splice junction can be seen in figure 12. Characterisation of the HSPDE4A gene locus revealed an explanation for the difference in between the point of divergence used to create either the PDE4A and one PDE4D (4D2) short-forms or the PDE4B and other PDE4D short-form cDNAs. The "short" isoforms from the PDE4B and PDE4D genes (except 4D2) encode proteins that possess a complete UCR2 whereas the active PDE4A and PDE4D2 "super" short-form cDNAs only possess 2 of the three exons that encode UCR2. These PDEs lack the N-terminal part of UCR2.

Analyses of the HSPDE4A gene also revealed a sequence of 55bp that encodes the unique N-terminal of RD1. This region is situated in the intron that separates two of the three exons that encode UCR2. The location of this 5' exon explains why the PDE4A short-form RD1 has a disrupted UCR2. The short-forms PDE4B and PDE4D (except

4D2) have intact UCR2 regions as their unique 5' exons are located between exons 5 and 6 (Sullivan et al. 1998).

The presence of these unique N-terminal regions appear to confer particular functional properties on the various PDE4 isoforms. These properties include susceptibility for membrane association and intracellular targeting, regulation of the V_{max} of the enzyme activity, influencing the thermostability, conferring susceptibility to regulation by phosphorylation and the ability to bind SH3 domains.

The ability of unique N-terminal regions to confer susceptibility for membrane association and intracellular targeting has been particularly well studied. PDE4 activity is found not only in the cell cytosol but also in the particulate fractions that contain the cell membranes and cytoskeleton. It was first proposed PDE4 might have a particular ability to associate with membranes by binding to an anchor protein for the PPM-PDE4 enzyme from hepatocytes (Houslay and Marchmont 1981).

Studies carried out on the rodent short-form PDE4A, RD1, provided the first definitive evidence that alternative splicing could yield a membrane targeted isoform (Scotland and Houslay 1995; Shakur et al. 1993). This isoform is found to be associated with the (high-speed) membrane fraction when expressed in COS cells and the first 25 residues of the unique extreme N-terminal splice region of RD1 were shown to determine the membrane targeting of this splice variant. This was demonstrated by the generation of an in-frame chimera formed between this region of RD1 and the normally soluble bacterial protein chloramphenicol acetyl transferase (CAT). Plasmids encoding either 1-25 RD1-CAT or 1-100 RD1-CAT were transfected into COS cells and these chimeras showed subcellular

distribution identical to that seen with RD1. However, the truncated chimera species 26-100 RD1-CAT was found to be located exclusively in the cytosol.

Structural analyses of the N-terminal splice region of RD1 revealed that it is formed of two folding helical regions separated by a mobile hinge region. One region in particular forms a polar helical region and it is unlikely that the overall structure of the RD1 N-terminal domain would be able to insert into biological membranes. It has therefore been suggested that RD1 becomes membrane-associated through protein-protein interactions, either directly with an integral membrane protein or indirectly through an adaptor protein. This interaction would appear to be hydrophobic, involving the tryptophan-rich Pro^{14}-Trp^{20} domain, as RD1 membrane association is disrupted by very low concentrations of the non-ionic detergent Triton X-100 but not by high ionic strength.

The unique N-terminal domain of RPDE6 (RNPDE4A5) and its human homologue PDE46 (HSPDE4A4B) while found in the cell cytosol are also found to be associated with the membrane fractions. In contrast to RD1, RPDE6 is not readily solubilised by the non-ionic detergent Triton X-100 or by repeated washing with high ionic strength solutions. This implies RPDE6 forms strong associations with cytoskeletal components (McPhee et al. 1995). The same observations were made for the human homologue PDE4A4B (Huston et al. 1996). Laser scanning confocal microscopy studies showed that both PDE4A4B and RPDE6 immunoreactivity in transfected COS cells was localised to the margins of the cell where specialised cytoskeletal structures such as cortactin and fodrin associate with actin. Cortactin and fodrin both exhibit Src Homology 3 (SH3) domains. They are found in many proteins that have important signalling structures and

allow them to recruit interacting proteins to specific locations within the cell (Sparks et al. 1996; Wu and Parsons 1993).

SH3 domains interact with binding proteins through proline (and arginine)-rich motifs in the form of PXXPXXR found in the binding protein. Both RPDE6 and PDE4A4B possess such motifs in their unique N-terminal splice regions. Indeed RPDE6 was shown to interact with certain SH3 domains expressed as a GST fusion protein indicating specificity (O'Connell et al. 1996). RPDE6 interacted strongly with SH3 domains of the tyrosyl kinases fyn, lyn and src and also those from the cytoskeletal proteins fodrin and cortactin. Neither the long-form PDEA isoform RPDE39 or the core rodent PDE4A species met^{26}RD1 displayed any interaction with SH3 domains. This indicates that motifs within the unique extreme N-terminal 110 residue splice region of RPDE6 confer this ability.

1.11.2.5 Distribution of PDE4 subfamilies

1.11.2.5.1 Distribution of PDE4A

The human PDE4A gene encodes for at least four long-form isoenzymes (PDE4A4B, PDE4A4A (truncated), PDE4A4C (truncated), PDE4A5 and PDE4A8A) and two short-forms (PDE4A1A and PDE4A10) as shown in figure 12. The rat PDE4A gene has so far been shown to encode six long-forms and one short-form.

The molecular weights of the human isoforms range from around 76 to 125 kDa and their K_m for cAMP varies from 2-6 μM. They all have an IC_{50} value for the inhibitor rolipram in the μM range.

The intracellular localisation of the rodent short-form PDE4A RD1 and the rodent long-from PDE4A RPDE6 were discussed in the previous section. Another rodent long-form PDE4A, RNPDE39 (RNPDE4A8) has a unique N-terminal splice region of 21 residues (compared to 112 unique to RPDE6) which is followed by the "common" long-form splice region of around 154 residues that is also seen in RPDE6. RPDE39, like RPDE6, is found to be associated with both membrane and cytosolic fractions but has very different expression patterns to RPDE6.

RPDE39 appears to have a restricted distribution, being found in testis and hepatocytes. This suggests that RPDE39 may have a functional role distinct to that of RPDE6.

The targeting of RD1 may also suggest a distinct functional role for the rodent short-form RD1, as it is found to be expressed in the CNS, in particular synaptosomes especially those enriched in postsynaptic densities. When these cells were examined at the subcellular level the distribution of RD1 showed a similar pattern to that observed in transfected COS cells. RD1 was predominantly associated with plasma membrane and Golgi bodies. It has been suggested that RD1 may play a role in the control of neurotransmitter release and the expression of PDE4A species in the CNS which is consistent with the PDE4 inhibitor rolipram having anti-depressant effects (Wachtel 1983).

1.11.2.5.2 Distribution of PDE4B

The human PDE4B gene encodes two long-forms (PDE4B1, PDE4B3) and one short-form isoenzymes (PDE4B2) as shown in the diagram in figure 12. Four rodent PDE4B isoforms have also been cloned. The human long-form PDE4B isoenzymes both have molecular weights of around 104 kDa whereas the human short-form is around 80 kDa.

All of these isoenzymes are found in both the cytosolic and membrane fractions of COS cells and an IC_{50} value for the inhibitor rolipram which is generally one tenth to one hundredth lower than that of the PDE4A isoenzymes (around 0.05 to 0.2 μM).

The subcellular localisation of PDE4B isoforms has not been studied in great detail. Data obtained for the distribution of two long and one short human PDE4B isoforms expressed in COS cells indicated that they all displayed similar distribution between particulate (around 20%) and cytosolic fractions.

1.11.2.5.3 Distribution of PDE4C

Only one human PDEC "long" isoform has been studied in detail (see figure 12) although eight human PDEC isoforms have been cloned, and two rodent isoforms. So far no human short-form PDE4C has been cloned. HSPDE4C2 has a molecular weight of around 80 kDa and an IC_{50} value for the inhibitor rolipram in a concentration range similar to that of PDE4B isoforms (around 0.08 μM).

Relatively little analysis of the subcellular localisation of PDE4C isoforms has been carried out and distribution studies have so far shown PDE4C to have restricted expression. RT-PCR analysis have detected PDE4C transcripts in brain, lung and kidney whereas all the other PDE4 sub-families have so far been shown to have a fairly wide distribution in tissues. Studies investigating the involvement of PDE4 isoenzymes in inflammatory diseases have also suggested that PDE4C isoforms may play a role in regulating the functioning of immune cells.

1.11.2.5.4 Distribution of PDE4D

The PDE4D gene encodes three long isoforms (PDE4D3, PDE4D4 and PDE4D5) and two short-forms (PDE4D1 and PDE4D2) also shown in figure 12. Five rodent forms have also been cloned. Characterisation of the human PDE4D isoenzymes has shown that the short-forms have a molecular weight of around 68 kDa while the long-forms range from 95-119 kDa. They all have a K_m for cAMP of around 1μM. The short-form PDE4D isoforms are found to be cytosolic and have an IC_{50} value for inhibition by rolipram at concentrations of around 0.05μM.

The long-form PDE4Ds are found both in the cytosol (IC_{50} value for inhibition by rolipram also around 0.05μM) and to be associated with the membrane fraction. The membrane associated PDE4Ds have a higher IC_{50} value for inhibition by rolipram of up to 0.59μM although PDE4D4 has an IC_{50} value equal to that of the isoforms located in

the cytosol. RT-PCR analysis has detected PDE4D transcripts in a wide range of tissues and their expression does not appear to be restricted.

Studies have shown that the long-form PDE4D isoforms have the potential for targeting to distinct intracellular compartments and these associations may be cell-specific depending on the means through which they are anchored. The expression of the short PDE4D isoforms in COS cells has so far shown them to be cytosolic although this does not exclude the possibility of their being targeted to intracellular sites when they are expressed natively.

Interestingly all three of the long-form PDE4D isoforms were solubilised by detergent and high NaCl concentrations although treatment with detergent alone only partially solubilised PDE4D3 and PDE4D5 but not PDE4D4. Treatment with high NaCl concentrations alone to release isoforms binding via electrostatic interactions only partially solubilised PDE4D5 and had little effect on either PDE4D3 or PDE4D4. These findings highlight differences in modes of anchorage between these isoforms which are likely to be distinct properties of their unique extreme N-terminal regions.

1.12 PDE5

This family of PDEs have a high specificity for cGMP. Sequence analysis showed that they contain a region homologous to that found in all of the other PDEs which is the conserved catalytic domain but also a second region of homology. They contain two high-affinity binding sites for cGMP which are non-catalytic. These were discovered by

comparing this region of PDE5A1 sequence to the same region of sequence in PDE2 and PDE6 which had been previously described as a putative cGMP-binding domain. This region from residues 142-526 contains two homologous repeat sequences. These have been named repeat 'a' which runs from residues 228-311 and repeat 'b' which runs from residues 410-500 (McAllister-Lucas et al. 1993; Thomas et al. 1990). Evidence from analyses of the cGMP binding and dissociation kinetics has shown that there are two functionally and structurally distinct cGMP binding sites on PDE5A1 which appear to have different affinities for cGMP (McAllister-Lucas et al. 1995).

There is another site on PDE5A1, distinct from the two cGMP binding sites in the homologous repeat sequences, which contains a serine residue (Ser92) that can be phosphorylated by cGMP-dependent protein kinase. Phosphorylation in this case requires binding of cGMP to the allosteric site on the enzyme and is thought to effect the enzyme by causing an increase in catalytic activity (Lochhead et al. 1997; Thomas et al. 1990; Wyatt et al. 1998).

Protein kinase A has also been shown to activate PDE5 (Burns et al. 1992) and in this case does not require prior binding of cGMP to the PDE (Burns and Pyne 1992). In addition, the phosphorylation of PDE5 by protein kinase A that triggers an increase in phosphodiesterase activity, also severely decreases inhibition of the enzyme by Zaprinast (Burns et al. 1992). This suggests that protein kinase A can alter the inhibitory effect of Zaprinast through alterations to a non-catalytic binding site (Burns and Pyne 1992).

Activation by protein kinase A can be blocked by recombinant PDE6 γ-subunit and a peptide corresponding to amino acids 24-46 in this protein (Lochead et al. 1997). Further investigations using a specific antibody against amino acids 24-46 of the PDE6 γ-subunit

revealed two small proteins (p14 and p18) which appeared to form a complex with PDE5. It has been suggested that these proteins may interact with PDE5 to prevent its activation by PKA (Lochead et al. 1997).

1.13 PDE6

PDE6 enzymes are known as photoreceptor PDEs as they are effector enzymes in photoreceptor signal transduction. They are found in the mammalian rod and cone photoreceptor cells. PDE6 is activated by the retinal G-protein transducin which in turn is activated by rhodopsin. The activation of PDE6 leads to a decrease in intracellular cGMP concentrations and results in closure of the cGMP-gated cationic channels of the photoreceptor plasma membrane (Beavo et al. 1994).

Like PDE5 and PDE2 enzymes PDE6 family members are cGMP specific. They also possess a high-affinity non-catalytic cGMP-binding region. Distinct isoforms of PDE6 are found in the two types of photoreceptor cells. Structural details of these isoforms have come from studies carried out on bovine forms of these PDEs. The PDE holoenzyme in bovine rods is composed of three basic subunits α, β, and γ. The two subunits α and β are similar in size (around 88kDa and 84kDa respectively) and contain the catalytic activity (Li et al. 1990; Lipkin et al. 1990; Ovchinnikov et al. 1987). They associate with two smaller γ subunits (of around 13kDa) which act as internal enzyme inhibitors (Deterre et al. 1988). PDE6 found in bovine rod cells consists of two α' subunits, which are identical, and these are associated with three smaller subunits of 15, 13 and 11 kDa. Each type of

subunit is encoded for by a different gene. α subunits are encoded by the gene PDE6A, β subunits by PDE6B and the α' subunits by PDE6C (Gillespie and Beavo 1988). Sequence analyses of the subunits have revealed 72% identity between the rod α and β subunits and 63% identity between the rod PDE α or β subunit and the cone-PDE α' subunit equivalents.

The α and β subunits also possess the high-affinity noncatalytic cGMP-binding site which is located in the N-terminal half of the subunit. When compared to the cGMP-binding regions in the PDE2 and PDE5 enzymes the sequence for this region in PDE6 was also found to contain the two internal homologous repeats 'a' and 'b' seen in 2 and 5 (Baehr et al. 1991; Khramtsov et al. 1993).

1.14 PDE7

PDE7 enzymes were discovered several years ago. PDE7 was recognised as a distinct PDE isoform when an IBMX-insensitive species was found in hepatocyte and liver tissue preparations (Lavan et al. 1989) although it has now been shown to be IBMX sensitive.

A novel PDE with such properties was first cloned from human T cells. PDE7 enzymes hydrolyse and have a high affinity for cAMP but the first clone encoding this isoform was derived from complementation in yeast which were deficient in PDE activity (Ichimura and Kase 1993; Michaeli et al. (1993). This clone was expressed in yeast and displayed a high affinity for cAMP and as well as an insensitivity to IBMX it was also insensitive to type 3 and type 4 PDE inhibitors. Since then at least two splice variants

have been shown to exist, PDE7A1 and PDE7A2 which are encoded for by the same gene (Bloom and Beavo 1996; Han et al. 1997).

The main differences between the two isoforms are that PDE7A1 has a N-terminal region that is rich in proline, serine and positively charged amino acids whereas the N-terminus of PDE7A2 is mostly hydrophobic with possible palmitoylation and myristolylation sites (Bloom and Beavo 1996; Han et al. 1997). PDE7A2 may also possess a targeting motif in its N-terminus as a species with similar electrophoretic mobility is found to be associated with the membrane fraction of human foetal skeletal muscle and heart extracts. PDE7A1, however, is usually found in the cytosolic fraction or distributed between the membrane and cytosolic fractions (Bloom and Beavo 1996; Han et al. 1997). One interesting feature of PDE7A1 is that it was found to contain a cAMP-dependent protein kinase pseudosubstrate motif (RRGAIS) but a functional significance has yet to be established although it could mean that the PDE is regulated in some way by PKA (Han et al. 1997).

1.15 The discovery of new PDE enzymes (PDE8, 9,10 and 11)

After the discovery of the involvement of a cAMP PDE in the *dnc* locus of *D. melanogaster* this gene was cloned and used as a probe to find novel human and rat PDEs in cDNA libraries. This was complemented by another approach which used a strain of yeast (*S. cerevisiae*) which had elevated cAMP levels resulting from mutations which lead to constitutive activation of adenylyl cyclase. This strain of yeast is also

particularly sensitive to heat shock, a phenotype which is rescued by overexpression of proteins which interfere with cAMP signalling (Colicelli et al. 1991). Other mammalian PDEs have been discovered through the use of PDE1 and 2 which are both more sensitive to heat shock and by disruption of the yeast PDE4 gene which lowers yeast protease activity and resulted in increased expression of human recombinant PDE4 (McHale et al. 1991; Michaeli et al. 1993; Sullivan et al. 1994).

Other approaches focus on more molecular techniques such as using known genetic sequences (already known clones) as probes in low-stringency hybridisation experiments, using RACE technology (Huston et al. 1997) or PCR using known conserved sequence to design primers which then act as probes for new PDEs in cDNA libraries (Engels et al. 1995; Livi et al. 1990; McLaughlin et al. 1993).

With the advent of Bioinformatics and developments in the Human Genome Project which have resulted in an acceleration in genetic information becoming available it is now possible to probe databases to look for new genes. This has occurred through the technique of cloning short expressed sequences (ESTs) of unknown function, a scatter-gun approach which never-the-less cuts out intronic sequence and therefore saves time and generates many novel sequences. The EST databases can be searched using known sequence from a similar gene and the level of homology required can be controlled in a BLAST (Basic Local Alignment Search Tool) search (Altschul et al. 1990) which is available at the National Centre for Biotechnology Information (NCBI). If a positive hit is found and the EST sequence does not represent part of a sequence which is already deposited in GenBank then a clone containing the EST sequence can be ordered. This approach has recently been used to clone several new PDEs including four new PDE

families 8, 9, 10 and 11. One major difference with the cloning of PDE11 was that the research group were able to search the commercial EST database, the Incyte LifeSeq database, which contains many sequences not yet publicly available.

So far any search for ESTs containing novel PDE4 sequence have only found parts of clones which have already been isolated and documented. Indeed I recently carried out a search using parts of conserved PDE4A sequence flanking more variable regions to probe for new PDE4A sequence in the database but did not generate any hits.

PDEs 8, 9, 10 and 11 have only been discovered very recently and have rapidly expanded the list of known PDE families. PDE8 is encoded for by two genes, A and B, and shows specificity for cAMP and PDE8B. It is not inhibited by most PDE inhibitors, including IBMX, with the exception of dipyridamole for which it has a fairly high IC_{50} value (Hayashi et al. 1998).

PDE9 is highly specific for cGMP with the lowest Km reported for a cGMP specific PDE. It is also not inhibited by the nonselective PDE inhibitor IBMX or the PDE5 inhibitor sildenafil but is inhibited by a PDE1/5 inhibitor compound known as SCH51866 (Soderling et al. 1998). This PDE also shows higher homology to the PDE recently found in *Dictyostelium discoideum* than to any of the other known mammalian PDEs (Shaulsky et al. 1996).

PDE10 and PDE11 are different in that they appear to hydrolyse both cAMP and cGMP. In the case of PDE10 a full-length clone was identified and named PDE10A1 but another incomplete cDNA was also found (PDE10A2) and identified as such due to a divergent N-terminal sequence (Loughney et al. 1999). The carboxy terminal of these two PDEs showed homology to the catalytic regions of other mammalian PDEs and the N-terminal

domain contained sequence that shared partial homology with the cGMP-binding domains of PDE2, 5 and 6. PDE10 was insensitive to all PDE inhibitors tested except the nonselective inhibitor IBMX.

PDE11 is most closely related to PDE5 and shows 50% homology to PDE5 in the sequence encoding the catalytic domain. PDE11 is similar to PDE10 in that it is able to hydrolyse both cGMP and cAMP and is inhibited by the nonselective PDE inhibitor IBMX. It diverges in the fact that it has a different sequence encoding the region of the tandem repeat in the cGMP-binding domain which is also found in PDE2, 5 and 6 (Fawcett et al. 2000). This enzyme also differs from PDE10 in that it is inhibited by several PDE inhibitors which are normally selective for the cGMP-specific PDEs. These inhibitors include zaprinast and dipyridamole.

1.16 PDE4 inhibitors: Potential therapeutic roles

PDE4 isoenzymes have a very wide distribution in tissues and their inhibitors have therefore been suggested as having potential therapeutic use in many disease states. The discovery that multiple PDE4 isoforms exist, some with tissue-specific patters of expression, indicated that inhibitors specifically targeted to one particular isoform could be developed. Two main therapeutic areas have been the focus of PDE4 inhibitor development. These include disorders of the central nervous system and also immune system disorders, particularly asthma. The use of PDE4 inhibitors in the treatment of vascular disorders such as pulmonary hypertension has also recently been investigated.

Rolipram was identified as an antidepressant even before its mode of action had been identified (Canizzaro et al. 1989). At therapeutic doses it inhibits all known PDE4 isoenzymes to a more or less equal extent (Muller et al. 1996). This lack of selectivity may account for some of the side-effects such as nausea and somnolence which were major side-effects seen in some Phase I and Phase II clinical trials (Krause et al. 1990; Scott et al. 1991). These are common side-effects seen in clinical trials of PDE4 inhibitors and therefore few are currently available for general clinical use. Nevertheless PDE4 inhibitor studies provide valuable insights into the modulation of disease states and improved specificity may reduce side-effects.

The use of PDE4 inhibitors may be of therapeutic use in the treatment of pulmonary arterial hypertension. Proliferation of smooth muscle cells is just one of the elements of the pathophysiology of this disease. PDE4 inhibitors have been shown not only to alter PDE4 function in vascular smooth muscle but also to inhibit injury-induced proliferation of smooth muscle cells in rats (Pan et al. 1994; Polson and Strada 1996).

The majority of PDE4 inhibitor studies have focussed on their use as anti-inflammatory or immunomodulatory agents. The presence of PDE4 enzyme activity, protein and or mRNA has been detected in many immune cells including monocytes, basophils, neutrophils, eosinophils, lymphocytes and polymorphonuclear leukocytes (Obernotle et al. 1993). However, the precise isoform present in a particular cell type has not been defined. Raising levels of cAMP in immune cells can have effects such as inhibiting chemotaxis, cytotoxicity and cell aggregation (Torphy and Undem 1991).

Asthma is characterised by both acute and chronic inflammatory processes and also increased tone of airways smooth muscle cells. PDE4 inhibitors may therefore be useful

in the treatment of asthma due to their anti-inflammatory effects and their ability to reduce airway smooth muscle tone (Banner and Page, 1995; Giembycz 1996; Torphy et al. 1994).

Rolipram has been shown to stereospecifically suppress the production of TNFα, lymphotoxin α and to a lesser extent IFN-γ in human autoreactive T cells (Sommer et al. 1995; Genain et al. 1995). These mediators are of central pathogenic importance in experimental autoimmune encephalomyelitis (EAE) which is an animal model of multiple sclerosis(MS) (Sommer et al. 1995). Rolipram has been shown to be an effective treatment for EAE which suggests that PDE inhibitors may have a role to play in the therapy of MS (Raine, 1995).

Recent studies have also shown PDE4 inhibitors to have the potential to suppress the actions of inflammatory cells such as neutrophils, macrophages and $CD8^+$ T cells that are associated with the progression of chronic obstructive pulmonary disease (COPD) (Torphy and Page 2000). The novel PDE4 inhibitor compound Ariflo™ (SB207499) has produced encouraging data in Phase II clinical trials into its use in the treatment of COPD.

Another novel PDE4 inhibitor, piclamilast (RP73401), has also been used in the treatment of rheumatoid arthritis (RA) with patients reporting improved symptom relief but higher dosage levels could not be increased due to nausea and vomiting in trial patients. Recent studies to develop PDE4 inhibitors with improved therapeutic ratios and fewer side-effects have revealed a novel PDE4 inhibitor PD189659. This inhibitor produces a broad-spectrum of anti-inflammatory effects and so far does not induce vomiting in dogs or ferrets (Torphy and Page 2000).

1.17 Conclusion

PDEs play a central and crucial role in controlling the effects of signals received at the cell surface. Their complex gene structure means that many different type of PDEs exist with distinct functional differences between families and very subtle changes from isoform to isoform. This means that their expression is tailored to a particular cell and a particular area of the cell and their rates of catalysis may be different.

The implications for this are that signals disseminated in the cell through cAMP may be localised due to the position of the PDE. If they are positioned nearer to adenylyl cyclase then they are able to lower the concentration of cAMP nearer the cell membrane so effects of cAMP will be less in other areas of the cell. Perhaps the most interesting development in the story of cell signalling is the discovery of the AKAPs anchoring PKAs to distinct locations in the cell. If PDEs are also located in this manner, through various anchoring methods, then they can effect the PKA activity in very specific areas of the cell. In this way all of the different PDEs expressed in one cell are able to create both local and general differences in cAMP concentration and this has implications for both the sensitivity of PKA to cAMP and the timing of various cellular events due to signals from outside of the cell.

The very specific nature of the characteristics of each PDE means that they must each have very discrete roles within the cell. cAMP is a ubiquitous second messenger therefore without a very sophisticated method of controlling and attenuating its effects on particular effectors, cellular events would happen in a random and inappropriate manner.

Of course the vast range of PDEs and the subtle differences between isoforms makes it very difficult to produce inhibitors which are specific enough not to have effects on more than one PDE. This situation is made more complicated by the fact that interactions with other proteins in the cell or modifications due to phosphorylation change the conformation of the PDE and can effect inhibitor binding. New approaches, however, may be able to focus on disrupting protein-protein interactions therefore removing a particular PDE from its functional locus. Further studies into the structural conformation of PDEs and the interactions between domains within the enzyme will aid the design of new inhibitors. For example the effects of the Linker Regions on UCR1 and UCR2 will aid the understanding of how conformational changes in these regions effect the catalytic activity.

The last few years has seen a sudden surge in the discovery of new PDEs. The availability of new ESTs along with the completion of the Human Genome Project will add to this trend and we can expect further isoforms and perhaps new PDE families to be discovered which were previously very hard to detect using standard techniques.

PDE4 enzymes are therapeutically of considerable importance. Their selective inhibitors have been of use in the treatment of central nervous system (CNS) disorders such as depression, immune and inflammatory system diseases, particularly asthma and also in the treatment of vascular disorders including pulmonary hypertension. However, to achieve more highly specific inhibition with minimal side-effects it is crucial to identify the full range of PDE4 enzymes. In this thesis I describe the cloning and characterisation of two new PDE4 isoforms. These may provide novel therapeutic targets in the future.

CHAPTER 2

Methods

2.1 Advantage-GC cDNA PCR Kit (including GC-Melt) Clontech

For each sample of cDNA four different GC-Melt concentrations must be used in order to optimise the reaction. PCR mixtures are as follows:

Final GC-Melt Conc. (M)	0	0.5	1.0	1.5
PCR grade H_2O	35	30	25	20
5X Klen Taq GC reaction buffer	10	10	10	10
GC-Melt (5M)	0	5	10	15
DNA Template	1	1	1	1
Primer Mix (10mM each)	2	2	2	2
50X dNTP mix (10mM each)	1	1	1	1
Advantage Klen Taq polymerase mix (50X)	1	1	1	1
Total Volume (µl)	50	50	50	50

Cycling parameters: One cycle of 94°C for 1 minute then 25 cycles of 94°C for 30seconds, 55°C for 3 minutes, 68°C for 3 minutes and then the reaction should be cooled to 4°C.

Advantage Genomic PCR Kit using the Advantage Tth polymerase Kit (Clontech).

PCR reaction mix.

Component	Volume required (µl)
PCR grade H_2O	33.8
10X Tth PCR reaction buffer	5
25mM $Mg(Oac)_2$ 1.1mM final	2.2
DNA template	5
Primer mix	2
50X dNTP mix	1
Advantage Tth polymerase mix (50X)	1
Total reaction volume	50

If the target size is under 5Kb then the following cycling parameters should be used:

One cycle at 94°C for 1 minute and then 25 cycles of 94°C for 30 seconds then 68°C for 3 minutes. Finally one cycle at 68°C for 3 minutes then the reaction should be cooled to 4°C.

2.2 Agarose Gels

Analytical grade Agarose was melted in 1X TAE buffer (to 1 litre H_20 add 4.84g Tris Base, 1.142ml Glacial Acetic Acid, 2ml 0.5M EDTA at pH8.0) depending on the percentage of Agarose gel and volume required. The percentage of gel required depends on the size of DNA fragments to be visualised later using Ethidium Bromide. The smaller the fragments the higher the percentage of Agarose in the gel. Usually a 0.8-1% gel would be required for DNA fragments of around 1-2Kb in size or larger.

The molten gel is cooled to around hand heat and 1µl of Ethidium bromide is added before being poured into the mould. When the gel is solid, samples (suspended in DNA loading dye: 30% Glycerol, 0.25% Bromophenol Blue and 0.25% Xylene Cylanol FF in H_20) are loaded into the wells and the gel is also run suspended in 1X TAE buffer at 50-100 Volts.

2.3 Bradford Assay

1. Make a stock solution of BSA at 1mg/ml.
2. A range of standard protein concentrations are required to construct a standard curve. A reasonable range is 0, 1, 2, 5, 10, 15, 20µg.

3. Pipette the BSA into Eppendorfs (e.g. 1µl for 1µg) and make up to 800µl with water. Note it is easier to add the water first.
4. Add 200µl of Bradford reagent and vortex.
5. Measure the absorbance at 595nm, blanked against 0µg BSA.
6. Perform identically for samples. Note these will usually have to be diluted to give a reading within range of the assay. Try to keep the volume of the sample added low i.e. less than 10µl.
7. Read the protein concentration from the standard plot which should be a straight line.

2.4 Competent Cells (Electrocompetent *E.coli*)

1. Inoculate 50ml L-Broth in a 250ml conical flask with a single colony of *E. coli* cells. Grow with shaking (200 rpm) at 37°C overnight.
2. At the same time pre-aerate 1L L-Broth at 37°C overnight.
3. Inoculate the pre-aerated 1L L-Broth with 50ml of the overnight culture.
4. Incubate with shaking at 37°C for 2-3 hours until it reaches an optical density of A600nm=0.6-0.7.
5. Divide the 1L culture equally into 4 pre-chilled (on ice) centrifuge bottles (250ml capacity) and incubate on ice for 20 minutes.
6. Centrifuge at 3500rpm for 15 minutes at 4°C.
7. Resuspend the cell pellets with 250ml cold sterile water per centrifuge bottle.
8. Centrifuge as above.

9. Resuspend the cell pellets with 125ml cold sterile water per centrifuge bottle. Pool the contents of two bottles.
10. Centrifuge as above.
11. Resuspend the cell pellets with 20ml cold 100% glycerol per bottle or (7% DMSO).
12. Transfer to pre-chilled small centrifuge tubes and centrifuge as above.
13. Resuspend the cell pellets with 2ml cold 10% glycerol.
14. Dispense into 50ml aliquots and snap-freeze on dry-ice. Store at -80°C.
15. NB: It is vital that all washing steps are performed ON ICE.

2.5 Ethanol Precipitation of DNA

A general guide to precipitating DNA to rid the solution of excess salt or other contamination is to add $1/10^{th}$ volume of 3M Sodium Acetate and then 2.5X volume of 75% Ethanol. Vortex to mix and then incubate at -80°C for at least 20 minutes. DNA can also be stored this way. Centrifuge the sample at maximum speed in a bench top microcentrifuge and carefully remove the liquid and leave the DNA to air dry.

2.6 ELISA

1. Dilute the bait protein in TBS or carbonate over a range of concentrations in a final volume of 100µl.
2. Plate out in triplicate and leave for one hour at room temp.
3. Wash 3 times with 1% Tween TBS (200µl per well).
4. Block with 5% marvel, 100µl per well and leave for 1hr at room temp.
5. Wash 3 times with 1% tween TBS as before.
6. Dilute the Py Ab 1 in 10,000 in 1% marvel and add 100µl per well. Leave at room temperature for 1hr.
7. Wash as before.
8. Dilute the alkaline phosphatase conjugated 2nd Ab in 1% marvel as before and add 100µl per well. Leave for 1hr at room temp.
9. Wash 3X as before.
10. Detect with Blue-phos (mix 50:50). Add 100µl per well and develop for 10 minutes. Stop with 100µl 2% EDTA.
11. Read at 590nm in plate reader.

2.7 First Strand cDNA Synthesis

Using the Pharmacia Kit

To a sterile 0.5ml microcentrifuge tube add:

5μg (1-5μg) of total RNA

DEPC H_2O to total of 20μl

Heat to 65°C in PCR machine for 10 mins then chill on ice.

Gently pipette the "Bulk 1st strand cDNA mix" up and down to mix and give a brief spin.

To a second sterile 0.5ml microcentrifuge tube add:

11μl of "Bulk 1st strand cDNA mix"

1μl "DTT" solution

1μl of "Not1-d(T)18" (0.2μg/μl) primer

20μl heat-denatured RNA from 1st tube

Pipette up and down to mix and Incubate at 37°C for 1 hour.

This can be stored at -70°C.

2.8 Glycerol stocks

Pipette 800µl of culture to be frozen into a sterile cryotube and add 200µl sterile glycerol. Mix well and store at -80°C.

2.9 LDH Assay

Pyruvate + NADH gives LDH plus Lactate + NAD

Rate of decrease of OD @340nm is proportional to the LDH activity.

96 well plate format, note: reaction starts very quickly so do 1 row at a time and do not set up on ice.

Free LDH	186µl	0.15M Tris pH7.4
(Cytosolic)	7µl	10mM Na pyruvate
	7µl	sample

Mix by pipetting. **To start** add 10µl 2mM beta NADH and **READ IMMEDIATELY.**

TOTAL LDH	172µl	0.15M Tris pH 7.4
	7µl	10mM Na pyruvate
	7µl	sample

ADD 14µl 30% Triton X-100

Mix by pipetting. **To start** add 10µl 2mM beta NADH and **READ IMMEDIATELY.**

%age contamination

% lysis of P1 fraction or whole cell lysate (lysis is normally around 98%)

FREE LDH / total LDH X 100 = %age lysis

To calculate cytosol contamination of P1

FREE LDH P1 / total free LDH P1+P2+S2 X 100

Slope of the curve in the linear range = rate so the higher the rate the more LDH there is.

14µg sample per well should be adequate.

2.10 Ligation of DNA fragments

As a general guide a 10:1 molar insert to vector ratio should be used and no more than 5µl of a PCR reaction if being used.

The following reaction mix should be set up:

1µl	Linearised Vector (25ng)
1 to 5µl	PCR product with appropriate 3' and 5' overhangs
1µl	10X ligation buffer
9µl	Sterile water to a total volume of 9µl
1µl	T4 DNA Ligase (4U/µl)
10µl	Total volume

Incubate at 16°C for at least 1 hour or overnight. Place the reaction on ice for transformation or store at -20°C until ready to transform cells.

2.11 Lysis of COS Cells

1. Wash 100mm confluent plate of cells with 10ml ice-cold PBS.
2. Remove all PBS and add 500ml of lysis buffer (55mM Tris/HCl, pH7.4, 132mM NaCl, 22mM sodium fluoride, 11mM sodium pyrophosphate, 1.1 mM EDTA, 5.5 mM EGTA) containing protease inhibitor cocktail.
3. Scrape cells, transfer to 1.5ml eppendorf and lyse with 8 strokes of 261/2G needle.
4. A post-nuclear supernatant was prepared by centrifuging the cell homogenate for 5min at 2000 rev./min (350 gav) at 4°C in a refrigerated Biofuge bench top centrifuge. Retain pellet and supernatant. Wash pellet twice with lysis buffer.
5. This produced the P1 pellet and the resulting supernatant was centrifuged for 30 minutes at 100,000 gav at 4°C which produced the P2 fraction and the resulting high speed supernatant the S2 fraction. Wash pellet twice with lysis buffer.
6. All fractions were resuspended to the same final volume in complete KHEM.
7. Assay P1, P2 and S/N fractions for protein content (Bradford assay) and subject 50mg of each fraction to gel electrophoresis and Western blot with 4A common antisera.

A more detailed protocol for COS cell fractionation is described below

1. COS-7 cells were transfected as above and incubates for up to 72 before being prepared for homogenisation as follows:

2. the growth medium was removed and the cells incubated in cold complete KHEM buffer (50mM KCl, 10mM EGTA, 50mM Hepes pH 7.2, 1.92 mM MgCl2, 1mM DTT and protease inhibitor cocktail (used in tablet form, 1 per 50ml solution, from Boehringer Mannheim).
3. This was carried out at 4°C and the plates were rocked every few minutes.
4. The complete KHEM was then removed and the cells were washed with 10mM triethanolamine/0.15M KCl (pH 7.2) for 10 minutes at 4°C.
5. This was removed after 10 minutes and the cells were washed with KHEM (no additions).
6. After aspirating the KHEM the cells were then washed in complete KHEM for 2 minutes before the buffer was drained off.
7. The cells were then scraped from the culture plate and a final volume of approx. 100µl per 100cm^2 was transferred to a glass/glass Dounce homogeniser and subjected to 20 passes of the pestle.
8. Mock transfected cells were prepared in exactly the same way.

2.12 Maxiprep/Miniprep DNA

This was carried out according to the manufacturers instructions depending on the amount of DNA required. For sequencing the DNA would be prepared using a Miniprep kit as the DNA tends to contain less contamination and will provide better data after sequencing. Both Promega and Qiagen DNA preparation kits were used.

2.13 Multiple Choice cDNA Screening

This was carried out using Multiple Choice™ cDNAs from OriGene Technologies Inc. according to the manufacturers instruction manual. Each kit included First Strand cDNA from six tissues from either human, rat or mouse (human in two different kits in this case) and control primers for β-Actin and a tissue specific gene (Cyclophilin in this case).

2.14 Membrane Association Assay

1. The Promega T7-coupled cell free transcription translation system (TNT) was used in order to produce mature cell free hRD1 protein.
2. 1μg hRD1 DNA was added to the reaction mix to a final volume of 50μl using rabbit reticulocyte lysate and other components from Promega according to the manufacturer's instructions.
3. [35S] methionine was included to a final concentration of 0.8 mCi/ml. The reaction mix was incubated at 30°C for 1-2 h and a post-translational aliquot (5μl) was taken for analysis.
4. All samples were adjusted to give equal volumes prior to SDS/PAGE analysis and the mature protein was visualised using a PhosphoImager.
5. [14C] labelled molecular weight standard markers (Amersham) were used in order to assess the molecular weight of the protein produced in this system.

6. 5µl volumes of this protein were incubated with 27µg of untransfected COS-7 P1 or P2 fraction (resuspended in complete KHEM buffer) for 30 minutes on ice at 4°C.

7. This was to determine whether or not post-translational modifications were required in order to facilitate binding of hRD1 to components in the P1 or P2 fractions.

8. Samples were subject to centrifugation as described previously and the supernatant collected.

9. To investigate the nature of the binding one set of samples were then washed once with complete KHEM containing 0.1% Triton X-100 before centrifugation and the supernatant resulting from this wash step was added to the first.

10. Both P1 and P2 pellet and supernatant fractions were analysed by SDS/PAGE and visualised using a PhosphoImager.

11. Similarly hRD1 transfected COS-7 cytosolic fraction (S2) was incubated with 27µg of untransfected COS-7 P1 and P2 fractions for 30 minutes at 4°C on ice.

12. These samples were subject centrifugation as above and resulting pellet and supernatant fractions were analysed by SDS/PAGE and Western blotting.

2.15 NaCl Treatment of Membranes

1. Aliquots of P1 and P2 fractions were diluted in 150µl complete KHEM buffer so that a 50µl volume would give around 14,000 CPM when subject to a PDE assay.
2. The complete KHEM buffer contained increasing concentrations of NaCl (from 0.001M to 2M) and the P1 and P2 fractions were incubated in this buffer on ice at 4°C for 30 minutes.
3. The P1 fraction was then centrifuged at 2000 rev./min (350 gav) for 5 minutes at 4°c and the P2 fraction at 100,000 gav for 30m minutes at 4°C.
4. In both cases the resulting pellet was resuspended in 150µl complete KHEM containing the appropriate NaCl concentration.
5. Aliquots of 50µl were taken in duplicate from both the P1 and P2 supernatant and pellet fractions and analysed in a PDE assay (at a substrate concentration of 1µM).

2.16 Phophatase Treatment

Alkaline Phosphatase treatment of cells.

10X Alkaline Phosphatase reaction mix (Promega)

0.5M Tris pH 9.3 (HCl)

10mM $MgCl_2$

1mM $ZnCl_2$

10mM Spermidine

Method. Cells grown in 100mm plates in serum free medium overnight to confluency. Scrape cells into 500µl calf intestinal Alkaline Phosphatase buffer.

The Alkaline phosphatase (20 Units) is added after lysis of the cells which is carried out using a 27G needle and centrifuged at 2500rpm at 4°C for 5 mins. The Supernatant is taken and 20µl Alkaline Phosphatase is added. This is mixed gently and incubated for 1 hour at 37°C. After incubation the sample is boiled for 5 mins in 100µl of sample buffer. As a control another set of cells grown in exactly the same way should be subject to the same treatment but without the Alkaline Phosphatase enzyme added to the mix.

2.17 Phosphodiesterase Assay

1. Cyclic nucleotide phosphodiesterase activity was assayed by a modification of the two-step procedure of Thompson and Appleman and Rutten et al. as described previously by Marchmont and Houslay (1980).
2. All assays were carried out at 30°C and in all experiments a freshly prepared slurry of Dowex:H20:ethanol (1:1:1) was used for determinations of activities.
3. Initial rates were taken from linear time courses of activity.
4. For the determination of K_m values PDE assays were conducted using cAMP concentrations over a range from 0.1µM to 100µM.

5. The PDE4 inhibitor Rolipram was used in order to determine the IC_{50} value of hRD1, h46 and PDE4A10 for this particular inhibitor.
6. Rolipram was dissolved in 100% DMSO as a 10mM stock and diluted in PDE assay buffer (20mM Tris/HCl/10mM MgC_{l2} at a final pH of 7.4) to provide a range of concentrations from 0.0001µmol to 100µmol.
7. IC_{50} values were determined using a substrate concentration (cAMP) equal to the Km value of each fraction.
8. The PDE activity found in mock transfected cell fractions was also analysed, and although always below background or up to 1% of the activity found in hRD1 transfected COS-7 cells, was subtracted from those activities found in hRD1 transfected cells.

2.18 Protein Sequencing

1. Choose a gel system which gives good separation of the desired protein bands; a band running in the lower half of the gel will blot better than if it is in the top half so adjust the acrylamide concentration accordingly.
2. Avoid Urea in the gel if possible - it can cause N-blocks at alkaline pH.
3. Pre-run with separating gel buffer containing 0.1mM (6.977µl/L) Thioglycollic acid (in the upper electrode buffer), before pouring the stacking gel. The mobile Thiol will run ahead of the protein and scavenge for N-blocking free-radicals.
4. Use this gels and ensure acrylamide is of high quality and deionise before use.

5. Where possible, cast gels a day before use to allow the polymerisation to go to completion - free acrylamide can N-block proteins.
6. Using 100-200pmol of each protein in one or two tracks of the gel, run the gel and then soak it, with shaking, in transfer buffer for 10 min. If poor transfer or over-transfer is experienced, increasing the equilibration time to 30 min can be beneficial. Transfer buffers commonly used are 25mM Trizma, 190mM glycine, 10% MeOH; 10mM CAPS, 5mM DTT, 10%MeOH, pH 11; 50mM N-ethylmorpholine pH8.3, 10% MeOH, 5mM DTT. The Trizma buffer is suitable for most applications where the proteins of interest are below 50-60kDa. The inclusion of SDS is not usually necessary, but for difficult proteins (e.g. pI>7) the presence of no more than 0.02% SDS can be helpful. Higher amounts of SDS can reduce the binding capacity of PVDF for protein. The CAPS buffer is generally preferable for high MW proteins (e.g. >50 000). For difficult membrane proteins, the inclusion of 0.05% Triton X-100 or Tween in the equilibration buffer only can help to keep the protein soluble; omit the detergent from the transfer buffer.
7. Where problems of N-blocking are encountered, the use of a lower pH gel system can be advantageous and may be worthwhile routinely.
8. NB All washing/equilibration steps must be done with gentle agitation or shaking. Wearing gloves at all times when handling PVDF, prepare the PVDF membrane by immersion in AR MeOH for 10 sec followed by equilibration in transfer buffer for 5 min. Prepare a gel/PVDF/blotting paper sandwich as for Western blotting, ensuring exclusion of all air bubbles. When blotting onto PVDF for the first time with a given protein whose behaviour on electroblotting is unknown, the inclusion of 2 membranes

on the anionic side of the gel and 1 membrane on the cathodic side will monitor excessive transfer or the presence of extremely electropositive proteins respectively.

9. Conduct the electroblotting using conditions similar to those used for Western blotting to nitrocellulose. In wet-blot, 300mA for 1-3h is generally sufficient although transfer time and current must be optimised for each protein studied. Excessive transfer time (i.e. overnight) can be detrimental and insufficient transfer leads to poor yield. In this respect, it is advisable to optimise the transfer of related proteins before submitting the protein under study should this be in short supply. In semi-dry blots, 0.8-1mA/cm^2 for 30min-1.5h is usually satisfactory.

10. When transfer is thought to be complete, remove the PVDF membrane and wash immediately in water for 10min with shaking. If the membrane is allowed to dry at any stage, even partially, it must be re-wet with MeOH before immersion in aqueous medium. Immobilon P - stain the membrane with 0.1% Coomassie Blue R in 50% MeOH for 5min and destain with several changes, 2-5min each, of 50% MeOH; 10% Acetic acid. Problott - Stain the membrane with 0.1% Coomassie Blue R in 50% MeOH, 1% acetic acid for 5min and destain with several changes, 2-5min each, of 50% MeOH. The membrane will remain a feint blue colour, do not try to make it white! Finally wash the membrane in water (5min) and air-dry thoroughly; damp membranes will not be accepted for sequence analysis. Place the membrane in a plastic bag and store dry at -20°C.

11. If your protein does not react with Coomassie, Amido Black and Ponceau S stains are compatible with sequence analysis.

2.19 Purification of DNA from Gels or Solution

In order to purify DNA fragments from Agarose gel slices it is necessary to melt the agarose with a suitable buffer so that the DNA is in solution. Various kits are available to purify DNA from gel slices and if the DNA is already in solution the kits can also be used instead of Ethanol precipitation. The most commonly used kit here was from Qiagen and employed beads to which the DNA bound in order to separate it from the solution. Another kit which was frequently used was the Advantage™ PCR-Pure Kit from Clontech. The protocol is described below:

A Purification of DNA from solution

1. Measure the volume of DNA solution and estimate the DNA concentration.
2. Add SALT solution (3X the volume of the DNA solution). Mix well.
3. Vigorously vortex the PCR-Pure BIND, and add the required amount of BIND to the DNA solution. Always use a minimum of 5μl of BIND per sample. For DNA samples less than 1μg use an extra 1μl of the BIND per μg of DNA.
4. Incubate at room temperature for 5min to allow DNA to bind to the PCR-Pure BIND. Keep the BIND in suspension by gently flicking the tube occasionally by hand.
5. Centrifuge the BIND/DNA complex at 14,000rpm for 5sec. Remove SALT supernatant and set aside. Although the DNA should remain with the pellet (BIND), save the supernatant until you have assessed the yield.

6. Add 1ml of WASH solution to the pellet. *For DNA >15Kb Resuspend the pellet in the WASH solution by gently pipetting up and down. For DNA smaller than or up to 15Kb do not Resuspend the pellet. Instead, soak the pellet for 5min in the WASH solution.
7. Centrifuge the BIND/DNA complex at 14,000rpm (10,000xg) for 5sec. Remove WASH supernatant.
8. Centrifuge the BIND/DNA complex at 14,000rpm for 5sec again. Remove any residual WASH solution with a narrow pipette tip. Dry the pellet.
9. Resuspend the pellet in H_2O or a low-salt buffer such as TE. Use 2X the volume of the PCR-Pure BIND used in step 3 above. Completely resuspend the pellet by gently pipetting up and down. Do not vortex.
10. Incubate at room temperature for 5min to elute the DNA from the BIND. Keep pellet in suspension by gently flicking the tube occasionally by hand.
11. Centrifuge the tube at 14,000rpm for 1min at room temperature.
12. As soon as the centrifuge stops, carefully remove the supernatant (containing the DNA) using a pipette tip. Avoid taking up the white pellet material with the DNA. Transfer the DNA to a fresh tube.
13. Assess the yield of the DNA. It is now ready to use.

B DNA Extraction from Gels

1. Excise the desired band(s) from the EtBr/agarose gel. Weigh the gel slice(s) to estimate the volume (1g = 1ml).

2. For TBE-buffered gels only: add MELT solution (0.5X the volume of the gel slices).
3. Add SALT solution. For TBE-buffered gels: use 4.5X the volume of the gel slices. For TAE-buffered gels: use 3X the volume of the gel slices.
4. Incubate at 55°C for 5-10min. Gently invert or flick the tube occasionally to mix contents and to promote melting. Do not vortex. Make sure that the gel is completely melted before proceeding to step 5.
5. Vigorously vortex the PCR-Pure BIND and add the required amount of BIND to the DNA solution. Always use a minimum of 5µl of BIND per sample. For DNA samples >µg use an extra 1µl of BIND per µg of DNA.
6. Incubate at room temperature for 5min to allow DNA to bind to the PCR-Pure BIND. Keep the BIND in suspension by gently flicking the tube occasionally by hand.
7. Centrifuge the BIND/DNA complex at 14,000rpm (10,000g) for 5sec. Remove SALT supernatant and set it aside. Although the DNA should remain with the pellet (BIND), save the supernatant until you have assessed the yield.
8. Add 1ml of WASH solution to the pellet. For *For DNA >15Kb resuspend the pellet in the WASH solution by gently pipetting up and down. For DNA smaller than or up to 15Kb do not resuspend the pellet. Instead, soak the pellet for 5min in the WASH solution.
9. Centrifuge the BIND/DNA complex at 14,000rpm (10,000xg) for 5sec. Remove WASH supernatant.
10. Centrifuge the BIND/DNA complex at 14,000rpm for 5sec again. Remove any residual WASH solution with a narrow pipette tip. Dry the pellet.

11. To recover the DNA, resuspend the pellet in H_2O or a low-salt buffer such as TE. Use 2X the volume of the PCR-Pure BIND used in step 5 above. Completely resuspend the pellet by gently pipetting up and down. Do not vortex.
12. Incubate at room temperature for 5min to elute the DNA from the BIND. Keep pellet in suspension by gently flicking the tube occasionally by hand.
13. Centrifuge the tube at 14,000rpm for 1min at room temperature.
14. As soon as the centrifuge stops, carefully remove the supernatant (containing the DNA) using a pipette tip. Avoid taking up the white pellet material with the DNA. Transfer the DNA to a fresh tube.
15. Assess the yield of the DNA. It is now ready to use.

2.20 QuickChange Mutagenesis

This was carried out according to instructions accompanying the Stratagene QuickChagne™ Site-Directed Mutagenesis Kit. There are very specific considerations regarding the design and synthesis of the QuickChange primers which must be adhered to.

2.21 RNA Isolation for RT-PCR

RNA Isolation

1. Remove medium from confluent cells (or spin down suspension cells).
2. Wash with PBS.
3. Add 1ml TRI-REAGENT per 10cm2 cells or 1ml suspension cells, and scrape cells.
4. Remove cells and place in a 1.5ml eppendorf.
5. Homogenise cells by pipetting up and down 10X with a 1ml syringe and needle.
6. Centrifuge at 12,000 g for 10 min @ 4°C, keeping the clear supernatant.
7. Allow samples to stand for 5 min @ room temp.
8. Cell lysate can be stored in TRI-REAGENT for up to 1 month @ -70°C
9. Add 0.2ml chloroform per ml TRI-REAGENT used. Cover sample and shake vigorously for 15 sec then stand for 2-15 min@ room temp.
10. Centrifuge the mix @ 12,000 g for 15 min @ 4°C
11. This produces 3 phases: red organic, protein: interphase, DNA: colourless upper aqueous, RNA. These phases can also be stored.

Preparation for RT-PCR

1. After transfer of aqueous phase to a fresh tube, mix with a tenth vol. isopropanol and store @ room temp for 5 min.

2. Centrifuge @ 12,000 g for 10 min @ 4°C.

3. Transfer supernatant to fresh tube and precipitate RNA by adding remaining amount of isopropanol.

4. Add 0.5ml isopropanol per ml of TRI-REAGENT used in sample preparation and mix. Stand for 5-10 min@ room temp and centrifuge@ 12,000 g for 10 min @ 4°C.

5. RNA will form a pellet on side and bottom of tube.

6. Remove s/n and wash RNA by adding 1ml 75% EtOH per ml TRI-REAGENT used.

7. Vortex then centrifuge @ 7,500 g for 5 min @ 4°C. If RNA floats, perform wash in 75% EtOH at 12,000 g. Samples can be stored in EtOH @ 4°C for 1 week or -20 for 1 year.

8. Briefly dry RNA pellet for 5-10 min by air-drying. DO NOT LET PELLET DRY COMPLETEY.

9. Add an appropriate vol. of Formamide, H2O or 0.5% SDS solution to the RNA pellet. To facilitate dissolution, mix by repeated pipetting with a micro-pipette @ 55-60°C for 10-15 min.

10. SPEC. The RNA should have a 260/280 ratio of equal or more than 1.7. Typical yields (microgRNA/1X10 6 cells): epithelial:8-15 μg, fibroblasts: 5-7μg.

2.22 Sequencing

Nearly all sequencing was carried out on an ABI Prism^{TM} 377 automated sequencer. The protocol for preparing the sequencing gel is detailed below.

1. Wash sequencing plates: warm water - Alconox - warm water - dH_2O - air dry (wash plates, spacers and combs in this way).
2. Prepare the reagents. Mix (for 36cm) : Urea 18g, 40% Acrylamide stock 5ml, dH_2O 25ml, mixed-bed, ion-exchange resin 0.5g. Stir until urea dissolves. While stirring mount plates in cassette.
3. To mount plates place cassette on level surface, lift beam stop and open cassette plate clamps. Clean inside of plates. Place lower plate - spacers (drops of dH_2O to hold) - upper plate. Make sure plates go between beam stop and bottom bracket, stops at bottom engage lower plate notches. Close plate clamps to hold plates in.
4. To mount the gel in the injection device, place assembly on raised LEVEL platform. Slide side pegs of clear brace under clamps, then slide top pegs over top edge of front glass plate. Attach bottom support and press down against top edge of rear glass plate. Hold bottom fixture at 45° angle against bottom of plates, then lay down on plates, rubber gasket making flat contact with glass. Turn side tensioning knobs to hold.
5. Inject the gel, filter solution - degas 2-5 min - transfer to 100ml graduated cylinder. Add 5ml 10X TBE buffer and adjust the volume to 50ml with dH_2O. Get a clean comb, clamps and a 50ml (60 cc) syringe. Gently add to the solution 250µl 10% APS and 35µl TEMED. Draw 30-50ml into the syringe. Screw tip of the syringe onto

bottom fixture. Inject solution slowly and steadily until it pools in a notch at the top of the plates. Remove the syringe and remove the bottom fixture. Insert gel casting comb and clamp down top fixtures with plate clamps. Wait 2 hours.

6. When the gel is set it can be placed in the frame inside the sequencer, then the running buffer (1X TBE) added to the top reservoir. After a pre-run (controlled by the ABI Prism software run on an Apple Mac) samples suspended in appropriate loading dye are then slowly injected into the wells.
7. The sequencer is run using ABI Prism software on Apple Mac.

2.23 Sequencing mixes

Dynamic Universal

Use 2µl of either the A, C, G or T label with 3µl of DNA template to be sequenced. Use the following sequencing cycle: 95°C for 30 seconds, 45°C for 15 seconds, 70°C for 45 seconds, for a total of 30 cycles.

After the sequencing cycle the products are spun down in a microcentrifuge and the A, C, G and T reactions pooled for each clone being sequenced.

Add 8µl of Formamide dye to each tube and load 2µl into a lane on the sequencing gel.

Mixed deaza ET Reverse Primers

	A	C	G	T
Mixes	2	2	4	4
ET Reverse primer	1	1	2	2
Template DNA	5	5	10	10
Total (μl)	8	8	16	16

The PCR cycling conditions are as above and then the reactions (A, C, G and T) for each clone are pooled.

The products are Ethanol precipitated using 3.6μl of 7.5M ammonium acetate and 120μl of Ethanol. After being spun in a microcentrifuge the products are washed with 70% Ethanol and resuspended in 4μl of Formamide dye. 2μl of this is loaded into a well on the sequencing gel.

BIG DYE

The sequencing reaction mix is made up as follows:

8μl	Terminator mix
200-500ng	Template DNA (ds)
3.2pmol	Primer

make up to a total volume of 20μl with dH_2O.

Cycling parameters are as follows: 25 cycles of 96°C for 30s, 45°C for 15s, 60°C 4min.

Samples are then precipitated using Isopropanol as follows:

1. Add 80µl 75% Isopropanol.
2. Vortex then incubate for 15min to precipitate.
3. Centrifuge at maximum speed in a bench-top microcentrifuge for 20min and then remove the supernatant.
4. Add 250µl 75% Isopropanol and vortex.
5. Centrifuge at maximum speed for 5min.
6. Remove supernatant and air dry for 10-15min or on a block at 90°C for 1min.

2.24 Synthesis of cDNA from Poly A+ RNA

Reverse Transcriptase reaction

1-5µg total RNA (stim)

10.5µl H_2O (treated to remove Rnases)

1µl oligo DT (or a specific primer)

This mixture was placed at 65°C for 10 minutes and then at room temperature for 2 minutes. The following was then added in order:

1.0µl Rnase inhibitor

4.0µl 5X RT buffer

1.0µl 100mM dNTPs

1.0µl Na Pyrophosphate

0.5µl AMV RT

Mix by tapping, spin in a microcentrifuge then incubate at 42°C for 1hr. Then raise the temperature to 95°C for 2 minutes. Dilute the product with 80µl of sterile H_2O and store in the -20°C freezer.

2.25 TA cloning

This is a particularly good way to clone small fragments of DNA which need to be sequenced. The fragments have generally been created by PCR and then gel-purified so they need to be treated with Taq before cloning can proceed in order to re-create the correct "A" over-hangs for TA cloning. This eliminates any enzymatic modifications of the PCR product. Taq polymerase has a nontemplate-dependent activity which adds a single deoxyadenosine (A) to the 3'ends of PCR products. The linearised vector supplied with the Invitrogen kit has a single 3' deoxythymidine (T) residues allowing PCR inserts to ligate efficiently with the vector.

The Invitrogen kit was used for TA cloning and used the vector PCR2.1 for ligation of the PCR inserts. The vector PCR2.1 was supplied with the kit and cloning was carried out according to the instructions in the Invitrogen manual supplied with the kit.

2.26 Thermostability assay

1. Aliquots of S2, P1 and P2 fractions from hRD1 transfected COS-7 cells were diluted in complete KHEM (in 50ml universals) so that 50µl volume would produce 14,000 CPM when subject to a PDE assay.
2. 50µl aliquots of each fraction were taken while the fractions were still on ice and then the universals containing the fractions were placed in a water bath at 50°C.
3. Once again 50µl aliquots of each fraction were taken in duplicate every two minutes and removed to ice-cold micro-fuge tubes every two minutes over a period of 40 minutes. This entire procedure was repeated at 55°C.
4. These samples were then assayed for cyclic AMP PDE activity at a substrate concentration of 1µM.

2.27 TNT reticulocyte lysate system

This cell-free transcription-translation system is available from Promega and the reaction should be carried out according to the instructions in the manual supplied with the kit. One consideration before ordering the kit is the type of promoter contained within the vector from which the insert is to be expressed in the TNT system. For example if the vector contains a T7 promoter upstream of the initiating ATG for the insert sequence then a TNT T7 Coupled Reticulocyte Lysate System kit will be required.

A general protocol for the reaction can be seen below:

1. To reduce the chance of Rnase contamination, gloves should be worn when setting up experiments and all microcentrifuge tubes and pipette tips should be Rnase-free. It is recommended that Rnasin Ribonuclease inhibitor is added to all TNT Lysate reactions to prevent degradation of RNA.
2. It is also recommended that a control reaction containing no added DNA is included. This reaction will allow measurement of any background incorporation of labelled amino acid.
3. Remove the reagents from storage at -70°C. Immediately place the TNT RNA polymerase on ice. Rapidly thaw the TNT Reticulocyte Lysate by hand warming and place on ice. The other components can be thawed at room temperature and then stored on ice.
4. Following the example below assemble the reaction components in a 0.5ml or 1.5ml microcentrifuge tube. After addition of all the components, gently mix the lysate by

pipetting the reaction up and down. If necessary, centrifuge briefly to return the reaction to the bottom of the tube.

5. Example of a TNT® Lysate reaction using ^{35}S-methionine:

TNT® Rabbit Reticulocyte Lysate	25µl
TNT® Reaction buffer	2µl
TNT® RNA Polymerase (SP6, T3 or T7 if appropriate)	1µl
Amino Acid Mixture Minus Methionine; 1mM	1µl
^{35}S-methionine (1000Ci/ml) at 10mCi/ml	4µl
RNasin® Ribonuclease Inhibitor, 40units/µl	1µl
DNA template(s)	1µg
Nuclease-free H_2O	to a final volume of 50µl

NB: Small scale reactions may be performed by reducing the volumes proportionally; reactions of 25µl are common.

Incubate the reaction at 30°C for 60-120min (depending on the promoter - see manual). Then analyse the results of the translation reaction using an appropriate gel system.

2.28 Transfection of COS cells

1. COS-7 cells were seeded at approx. 50% confluency 24 h prior to transfection on 600cm2 plates and grown in complete DMEM at 37°C.
2. 10μg hRD1 DNA was diluted to 250μl (for each 100cm2 of COS-7 cells) in TE buffer to which 200μl of DEAE Dextran was added.
3. This was left at room temperature for 15 minutes while the medium was aspirated from the cells and replaced with DMEM containing 10% Nu serum and 0.1% chloroquine.
4. The DNA/DEAE Dextran was dropped onto the cells and mixed by swirling.
5. These plates were incubated for 3-4 h before being shocked with 10% DMSO in PBS.
6. After shocking the cells were incubated in complete DMEM for 48 to 72 h before harvesting.

2.29 Transformation of DNA into Bacteria

This can be achieved in two ways, either chemically or using electricity. Both are described below and depends on the bacteria being used being either electro or chemically-competent.

Electrotransformation of E. coli

1. Chill the required number of 0.2cm electroporation cuvettes at -20°C.
2. Add 2 vol of sterile water to ligation mixture. Heat inactivate T4 DNA Ligase at 65°C for 10 minutes. NB: Ignore this step if transforming plasmid DNA that was resuspended in water.
3. Thaw the electrocompetent cells on ice.
4. Add 2µl of the ligation sample per 50 aliquot of cells. Mix gently using a pipette tip.
5. Incubate 1min before pulsing.
6. transfer to the chilled cuvette and electroporate with a single pulse of 600Ω, 25µF and 2kV (use Biorad electroporator at 2.5kV).
7. Immediately add 1ml L-Broth and incubate the cells with shaking at 37°C for half an hour before spreading onto plates containing a suitable medium (e.g. LB-agar).

Chemical transformation of E. coli cells

1. Centrifuge the vials containing the ligation reactions briefly and place on ice.
2. Thaw on ice one 50µl vial of E. coli cells for each ligation/transformation.
3. Add 2µl of 0.5M β-Mercaptoethanol to each vial of competent cells and mix by tapping gently. Do not mix the cells by pipetting.
4. Pipette 1 to 10µl of each ligation reaction directly into the competent cells and mix by tapping gently. The remaining ligation mixes can be stored at -20°C. 1µl of diluted supercoiled pUC18 plasmid (Invitrogen) can be used for the transformation control.

5. Incubate the vials on ice for 30min.
6. Incubate for exactly 30s in the 42°C water bath. Do not mix or shake.
7. Remove vials from the 42°C water bath and quickly place them on ice for 2min.
8. Add 250µl of pre-warmed *SOC medium to each vial. (SOC is a rich medium so good sterile technique must be employed to avoid contamination).
9. Place the vials in a microcentrifuge rack on its side and secure vials with tape. Shake the vials in the rack for 37°C for exactly 1h at 225rpm in a shaking incubator.
10. Place the vials with the transformed cells on ice.
11. Spread 20µl to 200µl from each transformation vial on separate labelled LB agar plates. Note: Plate 50µl from the transformation control. The remaining transformation mix may be stored at +4°C and plated out the next day if desired.
12. Invert the plates and incubate at 37°C overnight.
13. Select colonies for further analysis by plasmid isolation, PCR or sequencing.

*SOC medium is made in the following way:

1. To 950ml dH_2O 20g tryptone, 5g yeast extract and 0.5g NaCl.
2. Prepare 250mM KCl (0.86g KCl in 100ml dH_2O) and add 10ml of this to step 1.
3. Adjust the pH to 7 with 5M NaOH and adjust the volume to 980ml with dH_2O.
4. Make a 1M solution of $MgCl_2$ (20.33g $MgCl_2.dH_2O$) in 100ml dH_2O.
5. Autoclave both solutions.
6. Make a 2M solution of glucose (36g glucose in 100ml dH_2O) and filter sterilise.

7. Let the autoclaved solutions cool to around 55°C then add 10ml of the 2M glucose and 10ml of the 1M $MgCl_2$ to the solution prepared in step 3. Store at room temp or -4°C.

2.30 Triton X-100 Treatment of COS cell Membranes

1. Aliquots of P1 and P2 fractions were diluted in 150µl complete KHEM buffer containing a range of Triton X-100 concentrations (from 0.1% to 5%) so that a 50µl volume would give a reading of around 14,000 CPM when subject to a PDE assay.
2. The fractions were incubated in the above buffer for 30 minutes on ice at 4°C before centrifugation.
3. The P1 fraction and P2 fraction were centrifuged as described previously.
4. The resulting pellets were resuspended in 150µl complete KHEM containing the appropriate Triton X-100 concentration and 50µl aliquots were taken in duplicate from both the supernatant and the pellet fractions of both P1 and P2 for analysis by PDE assay (at a substrate concentration of 1µM).

2.31 Western Blotting (after SDS-PAGE)

1. Acrylamide (10%) or low Bis-Acrylamide gels or Novex minigels were used and the samples boiled for 2 minutes after being resuspended in Laemmli buffer (or reducing sample buffer in the case of Novex minigels and then the manufacturers protocol was followed for running of the gels).
2. Gels were run at 8 mA/gel overnight or 50 mA/gel for 4-5 h with cooling.
3. For detection of hRD1, h46 and PDE4A10 in Western blotting, 30-50 µg of protein samples were separated by SDS/PAGE and then transferred to nitro-cellulose before being immunoblotted using antiserum (antibody 97) to the catalytic core PDE4A region.
4. Labelled bands were identified using anti-rabbit peroxidase-linked IgG (Sigma) and the Amersham ECL Western blotting visualisation protocol.
5. Bio-rad prestained molecular weight standard markers were used (myosin, 203 kDa; ß-galactosidase, 116 kDa; bovine serum albumin, 83 kDa; ovalbumin, 48.7 kDa; carbonic anhydrase, 33.4; soybean trypsin inhibitor, 28.2 kDa; lysozyme, 20.7 kDa; aprotinin, 7.6 kDa) in order to determine the molecular weight of hRD1 and the results indicated a size of approx. 82.4 kDa on SDS/PAGE (predicted size 72 kDa).

General Protocol for Western blotting:

1. After running the gel, wet (with transfer buffer: 72g glycine plus 15g Tris made up in 4L then add 1L MeOH) 4 pieces of blotting paper and 1 piece of nitrocellulose, all cut slightly larger than the gel.
2. Make sandwich, with nitro-cellulose covering the gel, in between two layers of blotting paper (and then sponge), above and below the gel. Make sure there are no air bubbles between the nitro-cellulose and the gel.
3. Place in a transfer tank for 1h at 1Amp (with cooling) or 2h at 0.5Amps. Use the transfer buffer made earlier in the tank during transfer.
4. Take the nitro-cellulose blot out of the sandwich.
5. Wash the blot with, then stain with Ponceau red stain (optional). Then wash with TBS/PBS buffer (TBS: 0.5M NaCl, 20mM Tris HCl at pH 7.5 or PBS made using 1 PBS tablet per 100ml dH_2O which disolve upon sterilisation) .
6. Block for 1h or overnight with 5% Marvel (or 2% BSA).
7. Add 1^{st} Antibody (dilution usually 1 in 1000 to 1 in 10,000) in TBS/PBS with 2% Marvel for 1h or overnight.
8. Wash 3 times for 5min in 1% Tween 20 in TBS/PBS.
9. Add 2^{nd} Antibody-HRP conjugated (1 in 1000) in TBS/PBS with 2% Marvel and incubate for 0.5-1h.
10. Wash 3 times for 5min in TBS/PBS.
11. Put on ECL (5ml of each solution A and B using a different pipette for each) for 1 minute.

12. Quickly drip-dry the blot and put in film cassette between 2 pieces of sparkle film.

13. Expose from 1min to 30min depending on the intensity of the bands.

CHAPTER 3

3.1 Cloning of hRD1

3.1.1 Introduction to cloning of hRD1

RD1 is a rodent short-form PDE (Shakur et al. 1993). Short-form PDEs differ to long-forms in that they only contain UCR2 whereas the long-forms contain both UCR1 and UCR2. RD1 is unique in that the protein is found to be associated with the membrane. Detection using immunological methods revealed that RD1 was exclusively associated with the membrane fraction (McPhee et al. 1995). Further studies showed that ability to target this isoform to the membrane was contained within the first 23 residues of the unique N-terminal (Scotland and Houslay 1995).

Sequencing of the HSPDE4A gene revealed the existence of a human homologue to the rodent RD1 with an identical N-terminal sequence. It was decided to clone and express the sequence encoding this isoform and investigate whether or not the same targeting properties would be exhibited by the protein.

Fine mapping of the HSPDE4A gene on to chromosome 19 (Sullivan et al. 1998) authenticated the existence of the human RD1 by locating the exons encoding the unique N-terminal sequence. This work also demonstrated that the point of alternative mRNA splicing in short-form PDE4A is distinct from that used in the generation of PDEB and PDED short-forms. PDE4B and PDE4D sequences both encode a complete UCR2 whereas the active PDE4A short-form cDNA only possesses 2 of the 3 exons that encode UCR2.

In this chapter I have identified, cloned and characterised the short human homologue of rat RD1. I found that it is a catalytically active species and has the ability to associate with membranes.

3.1.2 PDE4A1 (hRD1) sequence

The schematic diagram in figure 13 shows the location of the hRD1 splice junction relative to the other structural components of this PDE enzyme. The diagram in figure 14 shows the entire coding sequence for the long-form PDE isoform PDE4A4B (h46) highlighting the sequence encoding the particular domains (N-terminal domain, UCR1, UCR2, position of the hRD1 splice junction site, the catalytic domain and the C-terminal region) of this isoform. The position of all primers used for sequencing hRD1 clones are also shown as the majority are located in the PDE4A common region which is sequence shared with PDE4A4B (h46).

Forwards primers used included: FB15a, FB2, FB3, FB4, 4AS1, 4AS3, 4AS5, 4AS7, 4AS8 and Universal primer to read in from the 5' vector sequence. The reverse primers which were used were as follows: FB7, FB6, FB5, FB9, 4AS2, 4AS4, 4AS6, 4AS9, 4AS10, 4A3' and Reverse primer to read in from the 3' vector sequence (see schematic in figure 15 and also figure 14 for specific location).

3.1.3 Primers designed to target regions of unique sequence encoding hRD1

In an attempt to clone the sequence encoding the human form of RD1 the first strategy was to PCR amplify the sequence from an endogenous source. Various human cDNAs were used as the template and it was hoped to amplify the region encoding both the unique N-terminal region as well as some common PDE4A sequence downstream of the splice junction. The sequence encoding the entire open reading frame for the gene could then be obtained either through direct PCR from human cDNA or else the unique N-terminal region could be spliced onto the common region already placed within an expression vector.

The following primer pairs were designed to attempt to amplify unique human RD1 sequence (including some common region in the fragment) from various cDNA sources (detailed below). The primer pair used for hRD1 used the 5' primer FB-RD1 (CCA TGT AAC CAG GGC T) and the 3' primer FB6 (CTG GAG AAC CTG AAC AAG) and the expected band size 407. The cycling conditions used were 94°C for 10 seconds, 55°C for 30 seconds and 72°C for 1 second.

3.1.4 Screening Clontech cDNAs for hRD1 plus RTPCR Using Poly A+ RNA (also from Clontech)

The cDNAs used as template for the target gene hRD1 were purchased from Clontech and Stratagene and the range included cDNA from the following tissues: Frontal Cortex, Liver A, Liver B, Lung (normal), Heart as well as a haematopoetic cell line (HL60) and T-cell DNA. The PCR conditions were optimised and changed several times but these investigations did not yield any positive results.

The major problem involved in attempting to amplify native hRD1 sequence was now becoming apparent. The sequence encoding the unique hRD1 N-terminal region is very GC-rich (this would include any sequence with more than 60% GC content) as is the sequence directly upstream of it. Any sequence with a majority of GC content is likely to be difficult to PCR due to the formation of secondary structure which prevents primers annealing to it. It was also possible that the cDNA may have not been of high enough quality so the first strategy was to order RNA from which to produce cDNA instead of using ready-made cDNA.

RNA was ordered from Clontech from which to make cDNA. This included human brain whole cerebellum Poly A+ RNA, human whole cerebral brain Poly A+ RNA and human skeletal muscle Poly A+ RNA. New primers were also designed to amplify hRD1 and figure 16 lists all of the primers used in this particular investigation.

3.1.5 Clontech Advantage-GC-Melt cDNA PCR Kit

None of the previous PCR reactions to amplify native hRD1 sequence from human cDNA had been working. A Clontech Advantage-GC-Melt cDNA PCR kit was used to overcome the problems involved in amplifying very GC-rich sequences. Such sequences possess strong secondary structure that resists denaturation and prevents primer annealing so the PCR fails to yield a product.

The GC-Melt kit included a buffer containing DMSO which disrupts base-pairing in GC-rich sequences and a GC-Melt reagent which further weakens the base-pairing. These PCR reactions were carried out with two different types of enzymes. TaqStart and TthStart are both designed to improve efficiency and specificity of PCR amplification and both have neutralising monoclonal antibodies directed against Taq and Tth polymerases respectively. The polymerase activity is restored at the onset of thermal cycling because the antibodies are rendered non-functional by temperatures greater than 70°C and the polymerase regains complete enzymatic activity for the PCR.

Despite the use of these reagents none of the PCR reactions designed to amplify unique human RD1 sequence from human cDNA templates produced any positive results.

3.1.6 hRD1 cloning strategy

None of the previously detailed methods designed to amplify the unique human RD1 N-terminal sequence from an endogenous source had yielded positive results. A new

approach was required and this was based on the fact that the sequence encoding the unique N-terminal region of human RD1 (the rodent short-form PDE4A) was already known (from sequencing of the HSPDE4A gene) and so too was the position of the splice junction, from the rodent RD1 sequence. This was particularly useful as we could now engineer a full length hRD1 sequence by synthesising the N-terminal sequence and splicing it onto the PDE4A common region at the same position as in the rodent form. This would remove any problems caused by the GC-rich nature of the N-terminal sequence.

The strategy to clone the full length hRD1 sequence included synthesising the unique 87 base pair-long N-terminal region which was 100% homologous to the rodent form. This was achieved by synthesising two long oligonucleotides containing the unique N-terminal sequence, one reverse and complimentary to the other, which could then by annealed together to form double stranded DNA. The sequence chosen would also include restriction enzyme sites suitable for cloning this DNA into an expression vector. This would create a stable situation for the newly created DNA as it would be more prone to dissociate if it were not contained within a larger piece of DNA. Sequencing of the 87 base pair N-terminal sequence is also easier when it is contained within an expression vector as sequencing primers annealing outside of the sequence can be used to give good quality sequencing data to verify the bases at the N- and C-terminal ends of the cloned fragment. Sequencing is necessary to check that the two long oligonucleotides have annealed as expected where they are reverse and complimentary to each other and not in any other way.

The core or common PDE4A region (the region downstream from the RD1 splice junction) containing the conserved catalytic domain, a region of 1.8Kb, was PCR amplified separately. The sequence of this region in human RD1 is based on the rodent sequence in that it does not contain UCR1 and an incomplete UCR2 as the splice junction occurs downstream of the first exon encoding UCR2.

Based on this strategy the entire hRD1 open reading frame is contained within two fragments. One 87 base pairs long, encoding the unique N-terminal and another 1.8Kb long encoding the human common PDE4A region downstream of the splice junction for hRD1. Both fragments were cloned into separate expression vectors so that they could be sequenced. They were also engineered so that they could be ligated together at the splice junction and then the entire new gene sub-cloned into a different vector for expression.

The unique N-terminus was generated by annealing two long 87-mer oligonucleotides (synthesised by Cruachem). The resulting double stranded DNA was then cloned into the vector PK19 using the BamHI and SalI restriction sites. The common region (a region 1.8Kb long encoding the common HSPDE4A region downstream of the RD1 splice junction in UCR2) was amplified from DNA encoding the HSPDE46 sequence using primers 5', FB15a (AAG TTT AAA AGG ATG TTG AAC C) and 3', FB3'Sal1 (GTC GAC GAG GTC TGG GGA TCA GGT A). Cycling parameters were 25 cycles of 95°C for 30 seconds, 60°C for 30 seconds then 72°C for 2 minutes. The polymerase PWO was used to amplify this fragment due to its high proofreading fidelity and increased half-life at higher temperatures.

The 5' and 3' primers used to amplify this fragment were designed to introduce recognition sites for restriction endonucleases DraI and SalI respectively. This allowed

the fragment to be cloned into the vector pZERO Blunt (Invitrogen). Both of the fragments (the unique 87 base pair human RD1 N-terminal sequence and the 1.8Kb human PDE4A common region) were sequenced after cloning using the ABI prism 377 automated sequencer.

The full length construct was created by digesting the 1.8Kb common PDE4A sequence out of the pZERO Blunt vector using the DraI and SalI restriction endonuclease sites. This fragment was then sub-cloned into the vector pK19 already containing the unique N-terminus. This was achieved by digesting the pK19 vector using the unique internal DraI site in the N-terminal sequence and then the SalI site which had been placed next to it. This sub-cloning event produced a full length hRD1 construct in the vector pK19. The orientation of the sequence was confirmed using diagnostic restriction enzyme digestion.

3.1.7 Generation of a COS-7 cell expression Vector for hRD1

The next step was to investigate the properties of the protein encoded for by the human RD1 (hRD1) gene. In order to do this the sequence had to be expressed using an expression vector suitable for expressing proteins in a mammalian cell line. Once the protein was expressed in this type of system the location of the protein and the kinetic properties can be investigated.

The full length hRD1 construct was sub-cloned into the mammalian expression vector pcDNA3 for expression in COS-7 cells under the control of the CMV promoter which gives particularly good expression of proteins when transfected into mammalian cells.

This was achieved by cutting the hRD1 sequence out of the vector pK19 using the unique restriction enzyme sites BamHI and SalI. The vector pcDNA3 was digested with BamHI and then XhoI. The hRD1 sequence fragment was then ligated into the vector pcDNA3. This was consequently digested with NotI (a site between BamHI and XhoI in pcDNA3) in order to cut away empty vector. Diagnostic restriction enzyme digests were made to check the orientation of the construct in the vector and revealed that the BamHI site had been recreated but the SalI/XhoI sticky ends (which had been ligated at the 3' end) had been destroyed. This was further confirmed by sequence analysis (using the ABI 377 automated sequencer).

3.1.8 Cloning of the fragment encoding the unique N-terminal region of hRD1

As described previously direct amplification of the region encoding the unique N-terminal region of human RD1 using human cDNA as template proved unsuccessful due to the high GC content of the sequence. The C-terminal region of hRD1 is composed of sequence identical to HSPDE46, except that it lacks UCR1 and part of UCR2. hRD1 can therefore be created by placing sequence encoding its unique N-terminus directly upstream of the shared C-terminal sequence (PCR amplified from HSPDE46 DNA) at the point at which the splice junction occurs.

The following section describes how the unique N-terminal sequence was therefore synthesised from two 87 base pair oligonucleotides (one reverse and complimentary to the other) which were annealed together to form double stranded DNA. The unique N-

terminal sequence of human RD1 encodes for 22 amino acids (66 nucleotides). Additional nucleotides were required at either side of the coding region (8 at the C-terminal and 13 at the N-terminal) to provide restriction enzyme sites to be used for subsequent subcloning of the sequence.

The two long oligonucleotides encoding the N-terminus of hRD1 (synthesised by Cruachem) consisted of the following sequences: 5' primer encoding the upper (sense) sequence, hRD15'UP (GAT CCA CCA TGC CTT TGG TGG ATT TCT TCT GCG AGA CCT GCT CTA AGC CTT GGC TGG TGG GCT GGT GGG ACC AGT TTA AAC TTA AGG) and the 3' primer encoding the complimentary antisense sequence, hRD15'LOW (TCG ACC TTA AGT TTA AAC TGG TCC CAC CAG CCC ACC AGC CAA GGC TTA GAG CAG GTC TCG CAG AAG AAA TCC ACC AAA GGC ATG GTG).

This sequence was designed with a DraI restriction endonuclease site (TTT AAA from bases 75 to 80) at the N-terminal as this is the sequence encoding the region at which the splice junction for hRD1 occurs in the PDE4A sequence, which is specifically the first T in this sequence (or nucleotide number 899 in the HSPDE46 sequence L20965).

The preparation of this sequence for ligation onto the N-terminus of the common PDE4A sequence (which is the sequence shared by both the human RD1 and the long-form PDE4A HSPDE46) started with the digestion of the plasmid pk19 to create BamHI and SalI ends. Phenol chloroform extraction was used between each separate digest. Once the digestion was complete the linearised vector was purified by ethanol precipitation and resuspended for later use.

The two long oligonucleotides were now annealed to make double stranded DNA. This was done using 100mM stocks and mixing 1µl of each primer along with 93µl of water and 5µl of buffer H (total volume of 100µl). This mixture was incubated at 95°C for 2 minutes, 80°C for 5 minutes, 65°C for 5 minutes, 50°C for 5 minutes and then room temp for 5 minutes.

The resulting DNA was then ligated (overnight at 16°C) into the linearised pk19 (Kanamycin resistant) and the product was then transformed into TOP10 E.coli. A maxiprep was then made from the resultant colonies.

A diagnostic restriction enzyme digest was carried out to check that the long oligonucleotides (the insert) had been successfully ligated into the pk19 DNA. The insert contained the unique restriction enzyme site DraI and the vector contained the unique BglII site. If the insert is present this will produce two bands, one of 5-600bp and another of around 2.2-2.4Kb. The diagnostic restriction enzyme digest showed that colony number 7 contained the insert and this was selected to be prepared for sequencing (three other positive clones were also found).

Sequencing of the insert was necessary to verify that it had not mutated in any way and the two oligonucleotides had annealed correctly. This was carried out using the Vistra robot and Thermo Sequenase dye Primer sequencing kit with ET (energy transfer) dye primers. Universal and Reverse primers (which annealed to sequences in the vector) were used. Sequencing was carried out on the ABI prism 377 automated sequencer (see methods). This sequencing showed that the insert had been cloned into pk19 correctly and contained no errors on either the upper or the lower strand. The general cloning strategy can be seen in figure 17.

3.1.9 PCR amplification of common 4A region for hRD1

The following primer pairs were designed in order to amplify a region of sequence encoding the C-terminal sequence which is common to both hRD1 and HSPDE46 and contains the conserved catalytic domain. The primer pairs used were FBRD2, forwards with FB9, reverse and FBRD2 with 4A3'. The PCR conditions were optimised and different cycling parameters used but without success. Next the primer pair Smet1, FB9 and FB1, FB9 were used to produce fragments of 1054 and 853 respectively, which could be used in a second PCR reaction. These reactions were successful and the products of 1054 base pairs (Smet1, FB9) and 853 base pairs (FB1, FB9) were purified and resuspended in sterile water. 1 and 10μl of each of these fragments were used with the primer pair FB15, FB9 designed to amplify a region from the start of hRD1. Neither of these reactions worked so it was decided to use the primer FB15 but replace FB9 with 4A3' which is designed to anneal at the extreme C-terminal of the HSPDE46 coding region.

Two overlapping fragments containing the sequence of interest were to be amplified and then annealed together so that they could be used as template in a further PCR reaction. This reaction could work more efficiently as there would be less "unnecessary" or contaminating sequence in the reaction. The primer pairs used for this were Smet1, FB9 and FB4, 4A3'. The primers were added after the first round of amplification in the PCR machine to allow the fragments to ligate together. The diagram in figure 18 shows the general scheme.

All of these PCR reactions were carried out using the polymerase Pwo which has particularly good proofreading activity. DMSO (at a final concentration of 10%) was also added to the reaction mix to help disrupt secondary structure caused by GC-rich sequence. In this case a band of around the correct size of 1.2Kb was obtained. This was actually smaller than predicted which indicated an artefact (predicted size was around 1.8Kb) nevertheless this fragment was excised from the gel, purified and ligated into the vector pZero Blunt. This was done in order to analyse the sequence which had been amplified by this PCR reaction and to establish whether it was an artefact or not.

The pZero Blunt containing the PCR fragment was transformed into TOP10 *E.coli* and the colonies obtained (38 in total) were PCR screened using the primers MSU2 (a forwards Universal primer made by Mike Sullivan) and Zrev (a reverse primer for use with the pZero Blunt vector). Five positive clones were obtained and mini-prepped for sequencing. The Dynamic Universal and Mixed deaza ET Reverse primers were used for sequencing (see methods).

3.1.10 Sequencing the FB15, 4A3' fragment PCR amplified from two smaller fragments covering the hRD1 C-terminal (common PDE4A) domain

Sequencing of the clones containing the FB15, 4A3' fragment showed that the primer 4A3' was annealing to a region approximately 1.2Kb away from the 4A3' priming site. FB15 is not a particularly good primer as it is a GC-rich primer (over 60% GC content) so I believe that the primer 4A3' is out-competing any reaction involving FB15.

Therefore I determined to redesign the primer FB15 and also (later on) to redesign the primer 4A3' to make it more specific. The polymerase Pwo used in the reaction is actually helping the primer 4A3' to bind to a site which only contains the first three base pairs in common with its sequence. The primer FB15 was changed from: AAG TTT AAA AGG ATG TTG AAC C, to FB15a: TTT AAA AGG ATG TTG AAC CG. The last CG in the sequence would help it to bind to the first base in the target sequence (GC clamp). It was also decided to use DMSO (final concentration 10%) in the reaction and increase the annealing temperature which would hopefully increase the specificity of the reaction.

3.1.11 PCR reaction with new primer FB15 (FB15a) and redesigned 3' primers 4A3' Sal1/Sal2

At first the same piece of DNA composed of fragments A and B (from the PCR reactions Smet1, FB9 and FB15, 4A3' in the previous section) was used as template for the PCR reaction with primers FB15a (redesigned) and 4A3'. The same 1.2Kb band appeared so the primer 4A3' was redesigned. Two new primers were designed to replace 4A3' which would anchor at the extreme 3' end of the PDE4A coding region at a unique restriction enzyme site SalI. The new primers were FB3'Sal1 (GTC GAC GAG GTC TGG GGA TCA GGT TA) and FB3'Sal2 (GTC GAC GGA ACA GGG ACA GAG GGT). Both of these primers were now used in reactions with both primers FB15 and FB15a. The

reactions were carried out with and without DMSO (final concentration 10%) and all of them with the DNA polymerase Pwo.

In the first instance the template used was 10A DNA, but then we discovered that the new primers FB3'Sal1 and FB3'Sal2 anchored to sequence just outside the region which 10A encodes. The same reactions were then carried out using PDE46 DNA instead.

3.1.12 PCR amplification of the sequence encoding the common region of PDE4A

The PCR reactions using the newly designed primers FB15/FB15a and FB3'Sal1/FB3'Sal2 and PDE46 DNA as template were all successful. Each reaction (with or without 10% final concentration DMSO) produced a fragment of the predicted size of 1.8Kb. The photograph in figure 19 shows the 1.8Kb bands produced by each PCR reaction in each lane of the gel. Further reactions were carried out with an increased annealing temperature to increase specificity of the primer binding. Once again every reaction produced a fragment of the correct size. One of these bands was chosen to be excised from the gel and purified for ligation into a vector so that the sequence which had been PCR amplified could be checked to determine if it was correct or not.

3.1.13 Ligation of the PDE4A common region 1.8Kb fragment into pZero Blunt for sequencing.

One of the bands from the above reactions was chosen (reaction primers FB15a with FB3'Sal1) and excised from the agarose gel. The DNA was purified from the gel slice and used in a ligation reaction with pZero Blunt vector. This was ligated at 16°C for one hour. Half of the ligation mix was used to transform into TOP10 *E.coli* cells and plated out on LB/Kanamycin plates (see methods).

Ninety-six of the resultant colonies were screened for presence of the insert. The PCR screen was carried out using two primers whose sequence lies inside the PDE4A common region sequence. These were FB2 (forwards) and FB9 (reverse). The expected size of the fragment which these primers should produce is 657bp.

Most of the 96 colonies screened with the above primers showed a positive band of 657bp, indicating that they contained the 1.8Kb insert (see figure 20). The first five clones were picked for sequencing. Five clones were chosen because it was possible with the amplification of a large piece of DNA (1.8Kb) that mistakes or mutations could have been introduced, even though the high proofreading enzyme Pwo polymerase had been used.

All of the primers designed to internal sequence in the PDE4A common region downstream of the hRD1 splice junction were used in order to sequence the 1.8Kb fragment. Forwards primers used included: FB15a, FB2, FB3, FB4, 4AS1, 4AS3, 4AS5, 4AS7, 4AS8 and Universal primer to read in from the 5' vector sequence. The reverse primers which were used were as follows: FB7, FB6, FB5, FB9, 4AS2, 4AS4, 4AS6,

4AS9, 4AS10, 4A3' and Reverse primer to read in from the 3' vector sequence (see schematic in figure 15 and also figure 14 for specific location).

It was very important to read the sequence immediately adjacent to the vector sequence as it was crucial that the unique restriction enzyme sites designed into the primers had been reproduced exactly during the original PCR reaction. A clone with perfect sequence and with DraI and SalI restriction sites intact was required.

At the same time as the 1.8Kb common region was being sequenced, the annealed 87-mer oligonucleotides encoding the unique N-terminus of hRD1 which had been cloned into the pZero Blunt vector was sequenced again. This was to double check that the DNA had remained stable while in storage and it was found to have exactly the same sequence (namely 5'-GAT CCA CCA TGC CTT TGG TGG ATT TCT TCT GCG AGA CCT GCT CTA AGC CTT GGC TGG TGG GCT GGT GGG ACC AGT TTA AAC TTA AGG-3').

One clone encoding the PDE4A common region was also found to contain sequence which was 100% homologous to the C-terminal region common to both hRD1 and HSPDE46 (no mistakes had been introduced during the PCR reaction), and both the 3' and 5' unique restriction enzyme sites were intact. The plasmid DNA from both of these clones was maxi-prepped in order to be prepared for ligation.

3.1.14 Cloning of the 1.8Kb fragment encoding the PDE4A common region into pK19 containing the unique N-terminus of hRD1

Both the vectors containing either the 1.8Kb common region or the short unique hRD1 N-terminus were digested with the restriction enzymes DraI and then SalI (both unique restriction endonuclease sites in these constructs). Digesting the pZero Blunt vector containing the 1.8Kb PDE4A C-terminal region fragment with these restriction enzymes released the entire 1.8Kb insert. Digesting the vector (pK19) containing the unique hRD1 N-terminal domain linearised the vector at the point where the splice junction between the hRD1 N-terminal domain sequence and the catalytic C-terminal region sequence occurs. The linearised vector pK19 hRD1 5' has a size of 2.7Kb.

The products resulting from these restriction enzyme digestions were then subject to electrophoresis on an agarose gel and the bands of the correct sizes (the PDE4A common region of 1.8Kb and the linearised pK19 vector containing the unique hRD1 N-terminal region of 2.7Kb) were excised and the DNA was purified from the gel. The 1.8Kb fragment was ligated into the pK19 vector so as to place it downstream of the unique N-terminus.

Plasmid DNA was prepared from at least 10 of the resultant clones positive for the insert. Several diagnostic restriction enzyme cuts were carried out. These included SalI/Xho (to verify that the 1.8Kb fragment had been inserted), DraI/Bgl2 (to verify the orientation of the insert), and Bgl2 alone (to give an indication that the of the size of the final construct was as expected).

These restriction endonuclease digestions revealed that the 1.8Kb fragment encoding the C-terminal PDE4A domain common to both hRD1 and HSPDE46 had been successfully ligated downstream of the unique hRD1 N-terminal at the hRD1 splice junction. This had been achieved by cloning the 1.8Kb C-terminal domain into the vector (pK19) which already contained the unique hRD1 N-terminal sequence. The entire hRD1 coding region sequence was now contained within one vector. The general cloning strategy can be seen in figure 21.

3.1.15 Cloning of full length hRD1 into pcDNA3 (CMV promoter)

The full length hRD1 construct was cloned into the vector pcDNA3 which has a CMV promoter in order to increase expression of the gene in mammalian cells. This was chosen as it was intended to express hRD1 in COS-7 cells for biochemical analyses.

hRD1 was cloned into pcDNA3 using the following strategy. The full length hRD1 construct in the vector pK19 was cut out using restriction enzyme digestion with BamH1I and SalI. The vector pcDNA3 was prepared by digestion with BamHI and XhoI. These were separate digests rather than double digests and the products were cleaned up in between using a DNA Bind kit (see methods). The insert was ligated into the vector overnight at 16°C. The product was then digested with NotI which would cut any remaining empty vector therefore reducing the number of possible false positive colonies after transformation into *E.coli*.

Potential positive clones were PCR screened using the primers CMV5' (commercially available) and the internal 3' PDE4A primer FB7. Sequencing was carried out on the clones testing positive in the PCR screen and all of these had the correct sequence at the 5' and 3' ends directly adjacent to the vector. It was not necessary to sequence the entire insert as the cloning had been carried out using a simple "cut and paste" strategy and the risk of mistakes was thus eliminated except for the regions in which the digests had occurred and these were recreated.

3.1.16 Conclusion

The cloning of hRD1 represents the first identification of a human short-form PDE4A and confirmation of the existence of a major splice junction in the PDE4A. The splice junction occurs inside the UCR2 region towards the N-terminus so only includes two of the three exons encoding UCR2. The position of this splice junction is conserved between PDE4 family members.

The intronic region of rat forms of PDE4B and PDE4D between the first exon of UCR2 and the upstream exon is several thousand base pairs long, This indicates that there is plenty of scope in these two genes for the existence of alternative promoters and unique 5' exons to create other short-forms. The corresponding region of the PDE4A gene contains an intron which is only 138bp long which is obviously not large enough to accommodate either of these.

It would be interesting to know if the lack of one exon encoding UCR2 as well as the lack of UCR1 and LR1 in the short-form has an effect on the catalytic activity of the conserved domain. This would be very difficult to establish as the shorter UCR2 may be capable of interacting with the catalytic domain in the absence of the other regions and exerting an effect that way.

The cloning procedure employed to create hRD1 and the exploratory PCR reactions to try and identify TM3 highlighted just how difficult it is to amplify certain regions of PDE4A sequence due to the highly GC-rich sequence creating tertiary structure. However, several methods were employed and future difficulties could possibly be overcome using a combination of 5-10% DMSO in the reaction mix plus a polymerase with extended thermostability to resolve these difficulties.

3.1.17 Figures

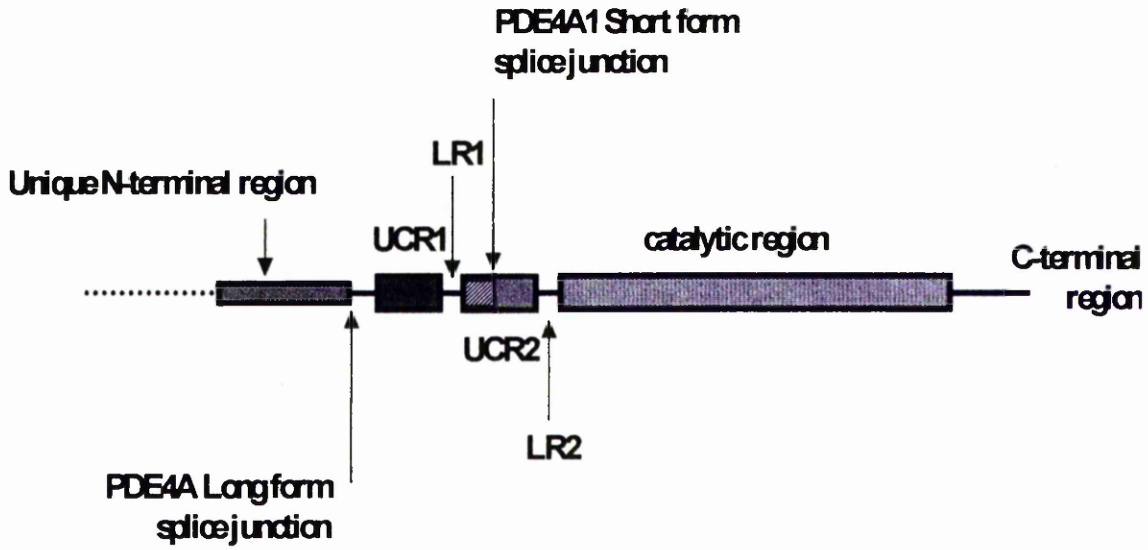

Figure 13. *The domain organisation of PDE4A isoforms. Also shown are the location of the long isoform splice junction and the short isoform splice junction within UCR2.*

Unique N-terminal Domain

ATG GAA CCC CCG ACC GTC CCC TCG GAA AGG AGC CTG TCT CTG

TCA CTG CCC GGG CCC CGG GAG GGC CAG GCC ACC CTG AAG CCT

CCC CCG CAG CAC CTG TGG CGG CAG CCT CGG ACC CCC ATC CGT

ATC CAG CAG CGC GGC TAC TCC GAC AGC GCG GAG CGC GCC GAG

CGG GAG CGG CAG CCG CAC CGG CCC ATA GAG CGC GCC GAT GCC

ATG GAC ACC AGC GAC CGG CCC GGC CTG CGC ACG ACC CGC ATG

FB11

TCC TGG CCC TCG TCC TTC CAT GGC ACT GGC ACC GGC AGC GGC

GGC GCG GGC GGA GGC AGC AGC AGG CGC TTC GAG GCA GAG AAT

GGG CCG ACA CCA TCT CCT GGC CGC AGC CCC CTG GAC TCG CAG GCG

UCR1

AGC CCA GGA CTC GTG CTG CAC GCC GGG GCG GCC ACC AGC CAG CGC

CGG GAG TCC TTC CTG TAC CGC TCA GAC AGC GAC TAT GAC ATG

FB10

TCA CCC AAG ACC ATG TCC CGG AAC TCA TCG GTC ACC AGC GAG

GCG CAC GCT GAA GAC CTC ATC GTA ACA CCA TTT GCT CAG GTG

CTG GCC AGC CTC CGG AGC GTC CGT AGC AAC TTC TCA CTC CTG

ACC AAT GTG CCC GTT CCC AGT AAC AAG CGG TCC CCG CTG GGC GGC

UCR2 FB1

CCC ACC CCT GTC TGC AAG GCC ACG CTG TCA GAA GAA ACG TGT CAG

FB8

CAG TTG GCC CGG GAG ACT CTG GAG GAG CTG GAC TGG TGT CTG

GAG CAG CTG GAG ACC ATG CAG ACC TAT CGC TCT GTC AGC GAG

FB15

ATG GCC TCG CAC AAG TTC AAA AGG ATG TTG AAC CGT GAG CTC

ACA CAC CTG TCA GAA ATG AGC AGG TCC GGA AAC CAG GTC TCA

FB2

GAG TAC ATT TCC ACA ACA TTC CTG GAC AAA CAG AAT GAA GTG

FB7

GAG ATC CCA TCA CCC ACG ATG AAG GAA CGA GAA AAA CAG CAA GCG

Catalytic Domain

CCG CGA CCA AGA CCC TCC CAG CCG CCC CCG CCC CCT GTA CCA CAC

TTA CAG CCC ATG TCC CAA ATC ACA GGG TTG AAA AAG TTG ATG CAT

AGT AAC AGC CTG AAC AAC TCT AAC ATT CCC CGA TTT GGG GTG

AAG ACC GAT CAA GAA GAG CTC CTG GCC CAA GAA CTG GAG AAC

CTG AAC AAG TGG GGC CTG AAC ATC TTT TGC GTG TCG GAT TAC

GCT GGA GGC CGC TCA CTC ACC TGC ATC ATG TAC ATG ATA TTC CAG

GAG CGG GAC CTG CTG AAG AAA TTC CGC ATC CCG GTG GAC ACG

ATG GTG ACA TAC ATG CTG ACG CTG GAG GAT CAC TAC CAC GCT

GAC GTG GCC TAC CAT AAC AGC CTG CAC GCA GCT GAC GTG CTG

CAG TCC ACC CAC GTA CTG CTG GCC ACG CCT GCA CTA GAT GCA

GTG TTC ACG GAC CTG GAG ATT CTC GCC GCC CTC TTC GCG GCT

GCC ATC CAC GAT GTG GAT CAC CCT GGG GTC TCC AAC CAG TTC

CTC ATC AAC ACC AAT TCG GAG CTG GCG CTC ATG TAC AAC GAT

GAG TCG GTG CTC GAG AAT CAC CAC CTG GCC GTG GGC TTC AAG

CTG CTG CAG GAG GAC AAC TGC GAC ATC TTC CAG AAC CTC AGC

AAG CGC CAG CGG CAG AGC CTA CGC AAG ATG GTC ATC GAC ATG

GTG CTG GCC ACG GAC ATG TCC AAG CAC ATG ACC CTC CTG GCT

GAC CTG AAG ACC ATG GTG GAG ACC AAG AAA GTG ACC AGC TCA

GGG GTC CTC CTG CTA GAT AAC TAC TCC GAC CGC ATC CAG GTC

CTC CGG AAC ATG GTG CAC TGT GCC GAC CTC AGC AAC CCC ACC

AAG CCG CTG GAG CTG TAC CGC CAG TGG ACA GAC CGC ATC ATG

GCC GAG TTC TTC CAG CAG GGT GAC CGA GAG CGC GAG CGT GGC

ATG GAA ATC AGC CCC ATG TGT GAC AAG CAC ACT GCC TCC GTG

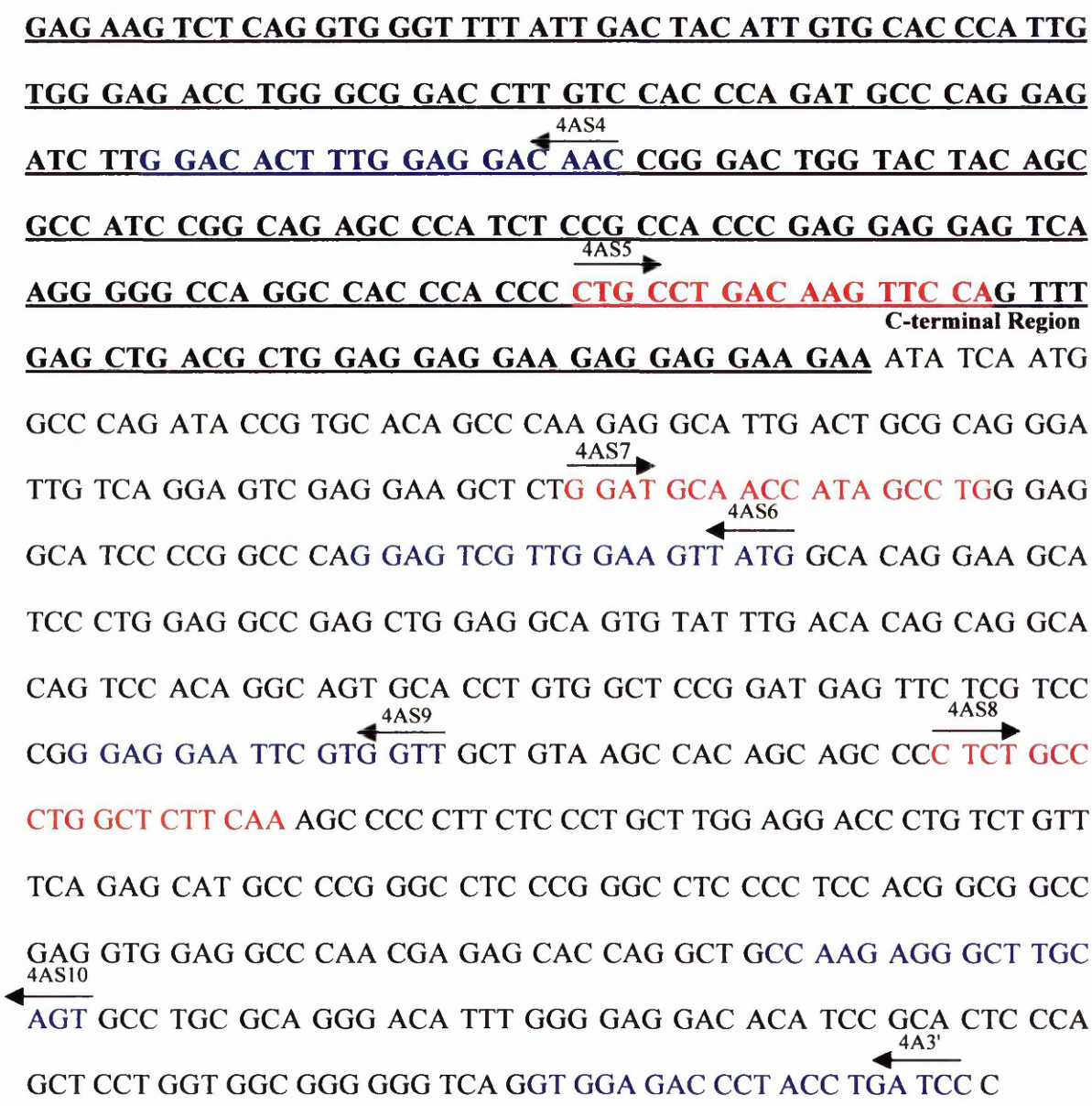

Figure 14. *This diagram shows where primers anneal to the HSPDE4A1A (h46) sequence L20965 showing sequence starting at nucleotide numbers 116 (the initiating ATG of PDE4A1AB, h46) to 2779 (end of the PDE4A1A open reading frame). These primers were designed to sequence within PDE4A1 (hRD1) that is common to both hRD1*

and PDE4A4B (h46). Forward (sense) primers are highlighted red and the reverse (antisense) primers are highlighted blue. The highlighted and underlined bold text in black shows the sequence encoding the various domains of PDE4A4B (unique N-terminal domain, UCR1, UCR2, the catalytic domain and the C-terminal region).

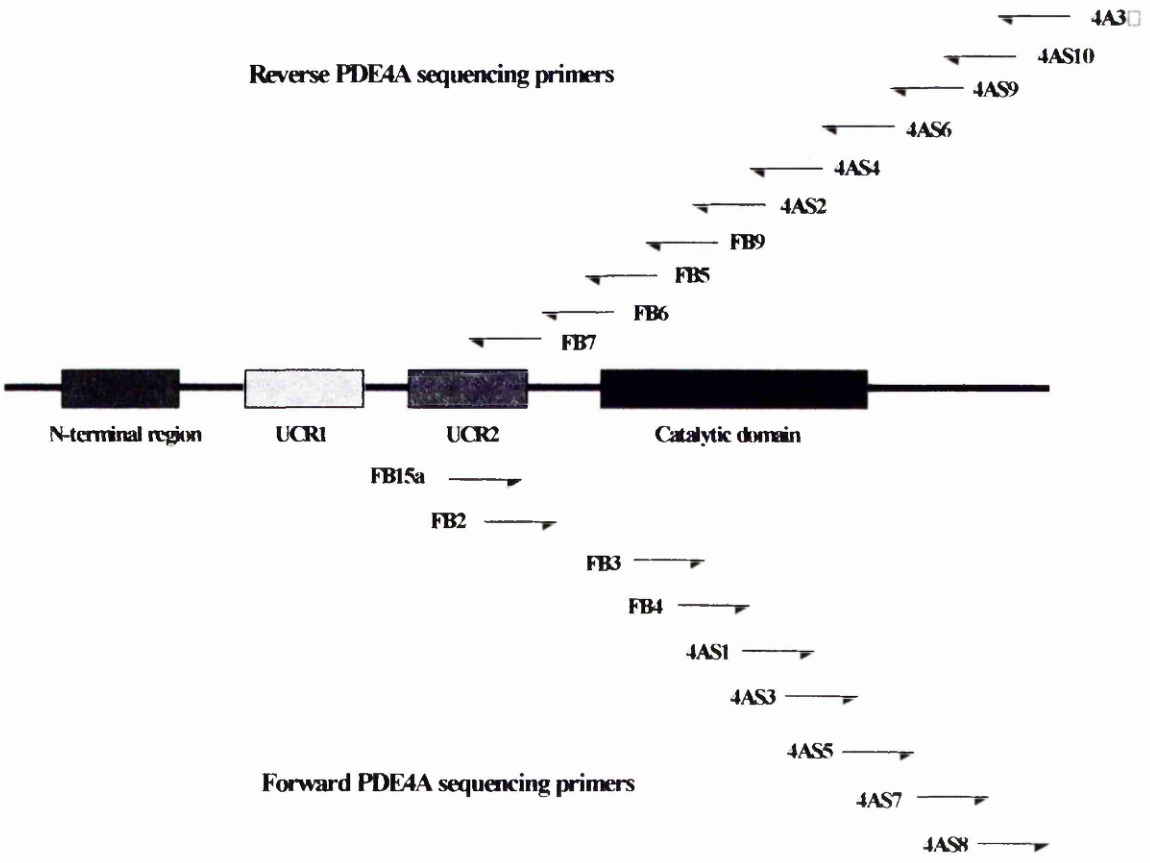

Figure 15. *Schematic diagram showing the approximate location of primers designed to anneal to sequence in the PDE4A common region downstream of the hRD1 splice junction for use in sequencing.*

FBRD1 CCA TGT AAC CAG GGC T

FBRD2 TCC ACT ACC CAC CTG C

FB8 CAG ACA CCA GTC CAG CTC

FB9 AGG TGG TGA TTC TCG AG

FB12 AGA CGC CTT CGG CTT C

4A3' GTC GAC GAT CAG GTA GGG TCT CCA C

SMET1 AGG ATC CAC CAT GTC ACC CAA GAC CAT G

SMET2 AGG ATC CAC CAT GTC CCG GAA CTC ATC G

Figure 16. *Sequence of primers used to screen for the presence of the PDE4A gene, hRD1 in human cDNAs.*

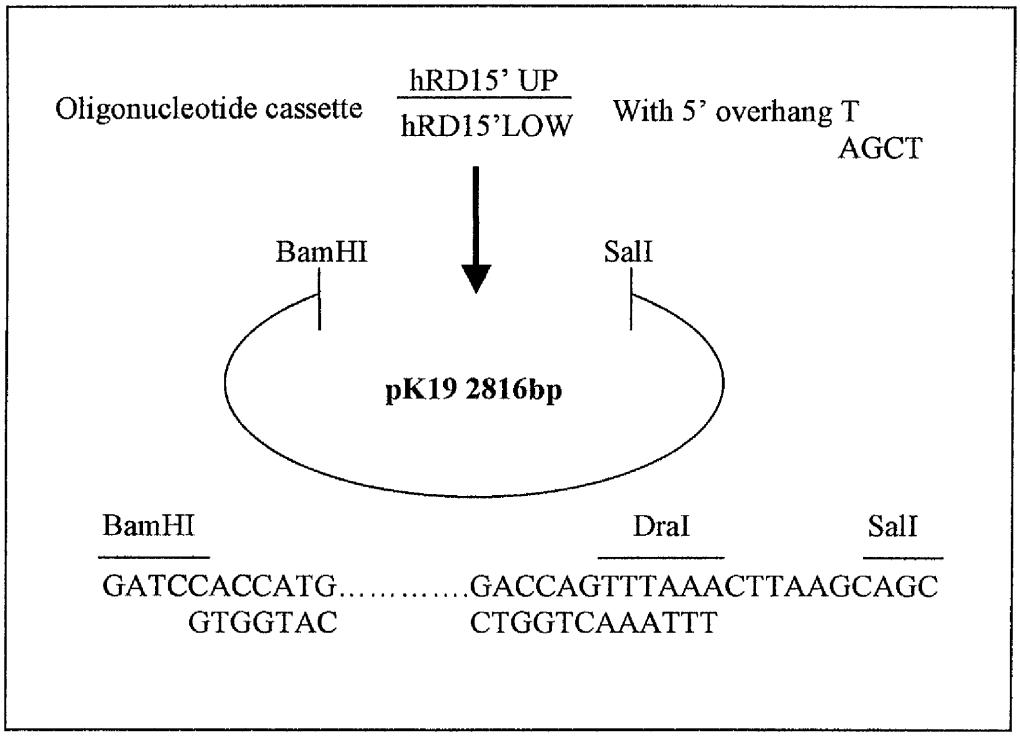

Figure 17. *General cloning strategy for cloning the two annealed long oligonucleotides encoding the unique N-terminal sequence of hRD1 into the vector pk19. The long primers have been designed so that the insert has the appropriate overhangs for the BamHI/SalI digested vector.*

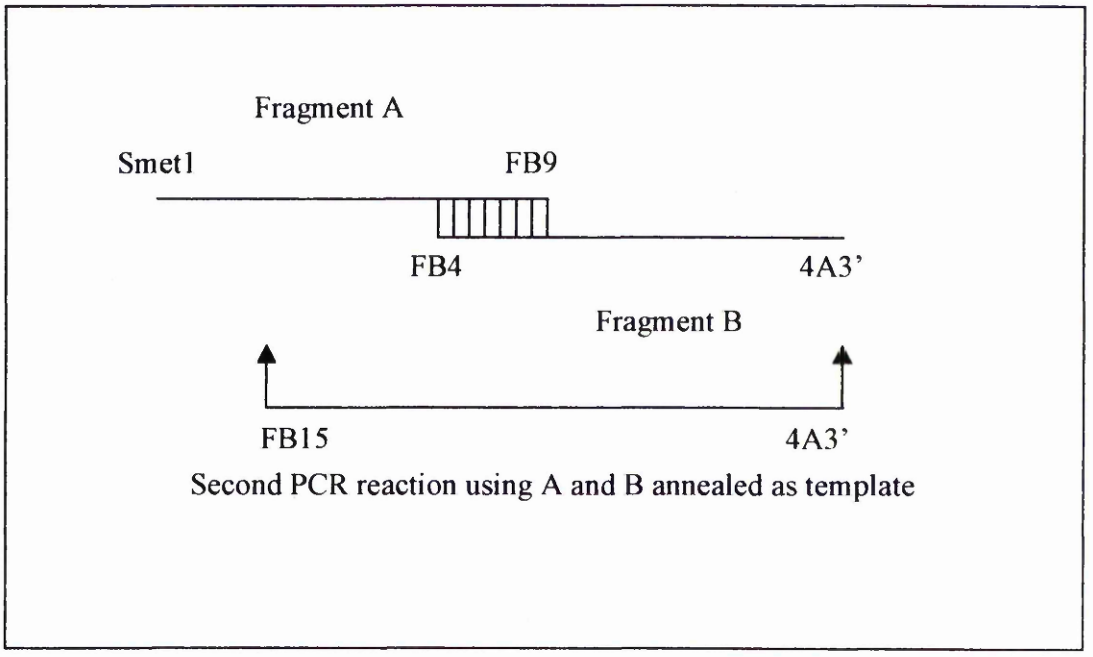

Figure 18. *Method used to create one single fragment from two overlapping smaller fragments of PCR amplified DNA (A and B). Fragments A and B overlap and cover the entire sequence encoding the C-terminal region common to both hRD1 and HSPDE46 downstream of the hRD1 splice site. The PCR reaction using the primer pair FB15 and 4A3' was carried out to amplify one continuous piece of DNA from the two smaller fragments A and B.*

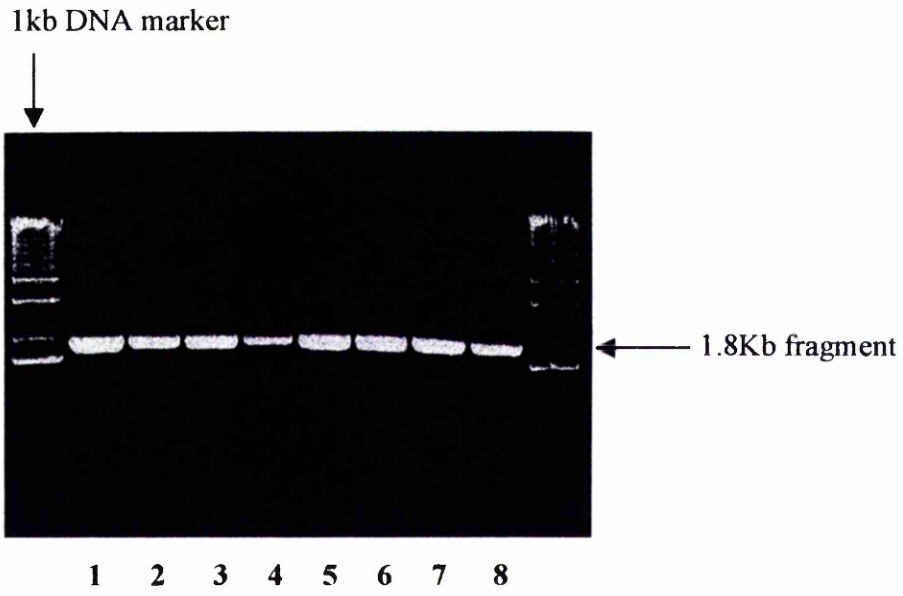

Figure 19. *The photograph above shows that every reaction with the primers FB15 or FB15a and FB3'Sal1 or FB3'Sal2 (with or without DMSO) produced a fragment of 1.8Kb which can be seen in every lane on this ethidium bromide stained agarose gel (1.8%). Lanes 1-4 show products obtained from primer pairs FB15a/Sal2, FB15a/Sal1, FB15Sal2, FB15Sal1 respectively all without DMSO present. Lanes 5-8 show the products obtained form primer pairs FB15a/Sal2, FB15a/Sal1, FB15/Sal2 and FB15/Sal1 all with 10% final concentration of DMSO in the reaction mix.*

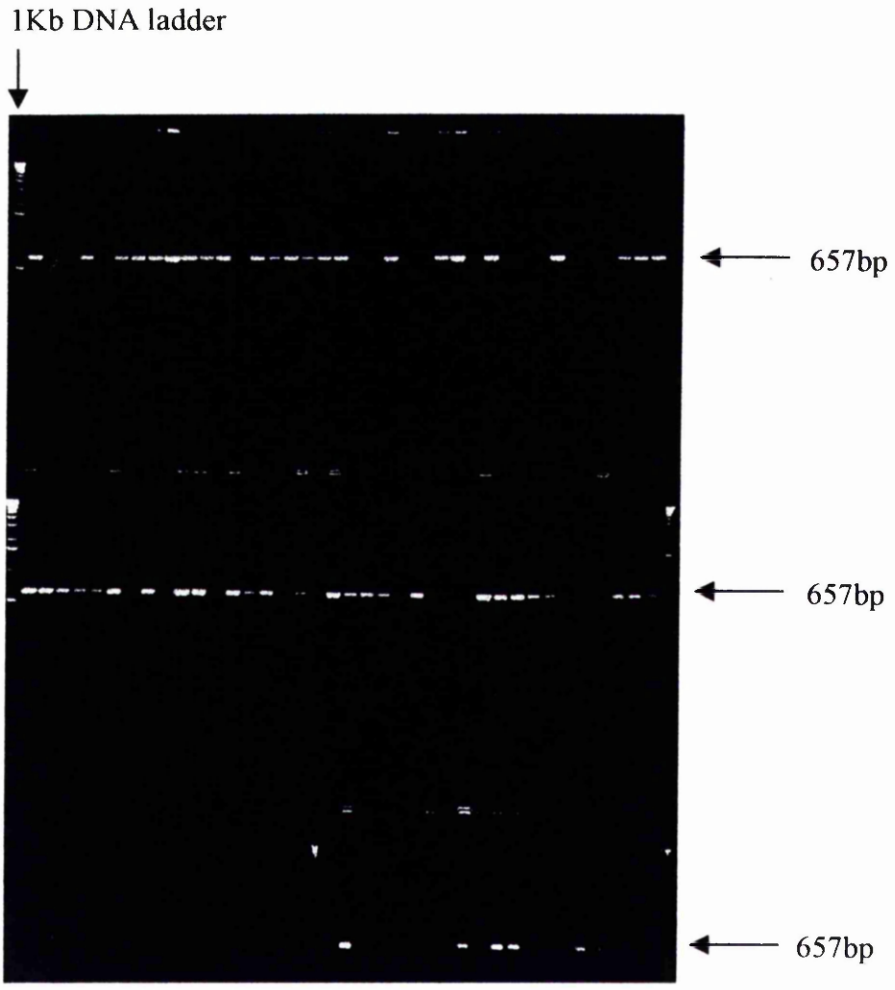

Figure 20. *This photograph shows the result of a 96 well PCR screen for the 1.8Kb insert encoding the PDE4A common region in the vector pZero Blunt. The internal 657bp fragment in the insert was amplified using primers FB2 (forwards) and FB9 (reverse).*

In fact most PDE4 isoforms appear to exhibit a similar aberrant behaviour on SDS/PAGE in migrating more slowly than would be predicted. One possibility is that the conserved poly (acidic) regions found towards the C-terminus of the catalytic region in these proteins lower the SDS binding and hence affect migration.

3.2.3 K_m values of hRD1

The phosphodiesterase assay described in the methods section was used to ascertain the level of PDE activity in each transfection using hRD1 DNA in COS-7 cells. Different amounts of protein from COS-7 cell fractions were assayed to establish the linear range of PDE activity in each separate transfection. Once this was known then the amount of hRD1 transfected COS-7 cell fraction which gave a reading of around 14,000 CPM in a PDE assay was used for further assays. The specific activity of the hRD1 expressed in each fraction was calculated from data in the linear range and these can be seen in figure 23.

Further assays included those investigating the kinetics of the enzyme encoded by the hRD1 sequence. First, the specific activity of the enzyme was established and then the K_m. This is a measure of the substrate concentration at half the maximum velocity of the enzyme. The K_m values for each fraction of hRD1 transfected COS-7 cells separately were obtained using the basic PDE assay but varying the amounts of substrate added to the assay (see figure 24) and in all instances were done over linear time courses. The amounts of cAMP added to the assay varied from 0.25 to 25 μM final concentration in

the assay. This range was used as saturation of the active site occurred at around 16 μM cAMP. The K_m values for hRD1 are shown in figure 25.

3.2.4 IC_{50} values of hRD1

The phosphodiesterase assay was also used to investigate the inhibition of hRD1 activity using the PDE4 selective inhibitor, rolipram. Final concentrations of rolipram used in the assay varied from 0.0001 to 100 μM and included samples containing no rolipram. Assays were again carried out at least three times on at least four separate transfections. The assays were also carried out at the cAMP concentration which corresponded to the K_m value for each particular fraction (see figure 27). Under such conditions and assuming rolipram acts as a simple competitive inhibitor then the IC_{50} values obtained are equivalent to the K_i values i.e. the affinity of the enzyme for the inhibitor (or ligand). The results obtained can be seen in figure 26.

3.2.5 Distribution of hRD1 phosphodiesterase activity in COS-7 cell fractions

hRD1 was successfully over-expressed in COS-7 cells and routinely accounted for ≥99% of the PDE cAMP hydrolysing activity detected in COS-7 cell fractions. As the graph in figure 28 shows, most of the PDE activity was found to be located in the P2 fraction

(44% +/-11). The remainder was shared between the P1 fraction (33% +/-10) and the S2 fraction (23% +/-8).

3.2.6 PCR screening of cDNA panel (Origene/Clontech) using primers for hRD1 plus RT-PCR and β-Actin controls

I decided to screen for the presence of hRD1 transcripts in human tissue in order to assess the distribution of this PDE4A gene product. The better the quality of cDNA, the higher the chance of detecting lower levels of message for the gene. Human brain cDNA library (Clontech) was prepared and screened using PCR to detect the presence of hRD1.

The primers used were specific to an N-terminal region found only in hRD1 and were as follows: 5' (AHR19) - TCG AAT TCT GAT GCC CTT GGT G and 3' (AHR20) - TGG ATC CCG GGG CTG TAA GTG. Cycling conditions were: 95°C for 1 minute, 55°C for 1 minute and then 72°C for one minute. Both negative and positive controls were carried out. The positive control was carried out on plasmid DNA containing the sequence for hRD1. Negative controls included the use of the above primers with plasmid DNA which contained sequences for two other PDE4As (PDE46 and 2EL). The β-Actin control primers were used to verify that the cDNA had been synthesised correctly and could be used to successfully amplify a region of DNA in a PCR reaction. None of the reactions using the PDE isoform specific primer pairs were successful in this instance.

3.2.7 Detection of a 276bp band - correct size for hRD1 in human brain cDNA (Y2H library)

Human brain cDNA was used as template to search for expression of the hRD1 gene. The two primers which were used in this PCR reaction were as follows: 5' primer, AHR19 (TCG AAT TCT GAT GCC CTT GGT G) the last 12 bases of which are specific to the hRD1 sequence, and the 3' primer, AHR20 (TGG ATC CCG GGG CTG TAA GTG) again, the last 12 base pairs of which are specific to the hRD1 sequence. This primer pair produced a band of 276 base pairs in size (see figure 29). The details of the PCR cycling conditions were as follows: 94°C for 30 seconds, 37°C for 30 seconds then 72°C for one minute, for a total of two cycles and then 25 cycles of 94°C for 30 seconds, 55°C for 30 seconds and then 72°C for one minute.

3.2.8 Screening Origene multiple choice cDNAs for the presence of hRD1 transcripts

Twelve different types of tissue cDNA were screened for the presence of hRD1. These included testis, ovary, small intestine, lung, muscle, prostate, leukocytes, brain, heart, kidney, spleen and liver. The primers used were AHR19 and AHR20 as described previously for detecting hRD1. The cycling conditions used were as follows 94°C for 30 seconds, 37°C for 30 seconds, 72°C for 1 minute for two cycles and then 94°C for 45 seconds, 55°C for 1 minute and then 72°C for 1 minute for a total of thirty five cycles.

Beta Actin primers were also used to check that the cDNA was good quality template and the PCR reaction should be working. The conditions for the β-Actin primers were as follows: 94°C for 45 seconds, 55°C for 1 minute, 72°C for 1 minute for 34 cycles and then one cycle of 94°C for 45 seconds, 55°C for 1 minute and then 72°C for 5 minutes. The β-Actin primers produced a band of 614 base pairs in size. The results of this screen were unclear and inconclusive.

3.2.9 Thermal denaturation

Proteins are normally thermolabile. Upon heating they are denatured and generally lose activity as a first order process (active to inactive) described as a single exponential. Thus a plot of log percentage activity remaining against time should be linear and can be used to calculate a half life from the time at which 50% of the original activity is remaining. Different proteins decay at different rates due to conformational differences. Indeed, conformational changes can alter the thermostability and thus calculation of half lives can be used to infer differences in conformation. I set out to: 1) evaluate if the half lives were different for hRD1 in the P1, P2 and supernatant fractions implying different conformational states and 2) to compare with half life values for rRD1 to see if differences in the common region between rat and human forms altered the conformation. Aliquots of each hRD1 transfected COS-7 cell fraction were immersed in a water bath at 50°C. The samples were placed in the water bath in a container with a stirrer to ensure even distribution of heat throughout the sample, giving a homogenous sample for

assaying. Samples were taken in duplicate every two minutes and removed to ice cold eppendorf tubes over a period of 40 minutes. The PDE activity assay was then carried out on these samples in the usual way at a substrate concentration of 1μM. The volume of the COS-7 cell fractions had been adjusted before the assay so that a 50μl aliquot would give a reading of around 14,000 CPM (i.e. within the linear range for the assay) before any heat was applied to the samples. The entire procedure was repeated at 55°C.

This experiment showed hRD1 to be remarkably thermostable. Even after 40 minutes at 50°C, or indeed 55°C, inactivation of the catalytic activity was still incomplete. The S2 fraction proved to be considerably more thermolabile than either the P1 or the P2 fractions (see figure 30).

The thermostability data is interesting as it shows distinct differences between the rat (RD1) and human (hRD1) forms of the enzyme (see figures 31 and 32). The human form has much higher thermostability at 55°C (approximately eight times higher). These two enzymes have a high degree of homology so the basis for this difference in thermostability might be associated with the hypervariable LR2 region encoded by exon 8 and the C-terminal region encoded by exon 15. The LR2 regions are all hydrophobic and consist of positively charged amino acids. The LR2 region of PDE4A has considerable predicted coil regions and it has been suggested that, along with LR1, this region may be able to confer conformational controls on UCR1/UCR2 interactions. There is also a higher percentage of proline residues in the human RD1 isoform and this residue is associated with conformational status. The linker regions may influence the orientation of the UCR1 and UCR2 domains with respect to each other and the catalytic core and also the orientation of the unique N-terminal regions.

It is also interesting to note the difference in thermostability between the two fractions of hRD1. The membrane bound fraction P2, displays a higher thermostability than the cytosolic fraction S2, (approximately five times higher). This difference might be accounted for by some membrane components or binding partners having a protective effect or else the binding itself has caused a conformational change in the hRD1 enzyme which makes it less heat labile.

3.2.10 High Salt/Triton X-100 treatment

Proteins can associate with the membrane in two ways. They can be peripheral, binding to other proteins at the membrane or the lipid headgroup in the lipid bilayer through electrostatic interactions. Alternatively they can be integrated into the lipid bilayer and interact with the lipids or other integral proteins in the bilayer. Detergent (Triton X-100) is required to extract integral proteins as this disrupts the interactions between lipids in the bilayer. Peripheral proteins, however, can be extracted by changes in ionic strength or the pH at the membrane which disrupts electrostatic interactions.

The first treatment involved changing the salt concentration. Increasing the salt up to a high level (from 0.001M to 2M) can be expected to cause disruption of ionic bonds. Adding Triton X-100 (0.5-5%) to membrane bound hRD1 would disrupt hydrophobic bonds.

Treatment of the particulate hRD1 with Triton X-100 led to the release of nearly all of the enzyme (>96%; n =3). The results can be seen in figure 33. Treatment with NaCl did not

release the enzyme and above a concentration of 0.001M interfered with the PDE assay so as to render the data unrepresentative. The effects of these treatments were assessed by PDE assay. These results indicate that the association of the hRD1 enzyme with the membrane is not due to charge but that hydrophobic interactions are required.

3.2.11 TNT cell-free expression of mature hRD1and COS-7 cell membrane binding

From the previous experiments it can be concluded that the hRD1 enzyme is integrated into biological membranes. To test this an *in vitro* assay was used. The mature hRD1 protein was produced using a cell-free transcription-translation system (Promega, see methods) and then mixed with membranes from COS cells to determine association. This may occur either as a result of insertion concomitant with translation or by post-translational insertion. As it appears that a small region is involved in membrane association of rat RD1 (Scotland and Houslay 1995) I decided to determine if mature hRD1 could bind to membranes. It has previously been shown that chimaeras of normally soluble enzymes engineered to posses the RD1 N-terminal region are able to bind to membranes in the same way as RD1. This is also the case when such chimaeras are produced as mature proteins in the cell-free transcription-translation system.

When hRD1 was produced in this way it was able to bind to COS-7 cell membranes. These experiments show that the ability to bind to membranes must be an inherent property of the N-terminal region of hRD1 as it has been shown previously that the core

or common region of the PDE4A protein does not bind to membranes (Scotland and Houslay 1995).

However, efficiency of insertion is seemingly not as good with hRD1 as with rat RD1. This may be due to the very different LR2 regions that, in human 4A4 have been shown to bind to SH3 domains containing proteins like LYN. Indeed 4A4 binds to LYN in COS cells. If such an association occurs for RD1 through the LR2 region then this might impair insertion efficiency. Alternatively in the case of hRD1 the reason may be technical as a low concentration detergent wash was used to clean up fractions after incubation with hRD1. In retrospect this might not have been a good idea as this could disrupt bonds formed during incubation. There is also current evidence from our laboratory suggesting that Ca^{2+} is required to promote insertion. The absence of added calcium may have decreased efficiency.

These blots (see figure 34) demonstrate the ability of hRD1 produced in the cell-free transcription-translation system to bind to COS-7 cell membranes. Blot A also shows that after treatment with a low concentration of Triton X-100 the protein loses the ability to bind to the membranes. This confirms the results observed using the Triton X-100 treatment detected using the PDE assay method.

3.2.12 Conclusion

The human form of RD1 and the rat form share 100% homology at their N-terminus. This provides a possibility to investigate the effects of the N-terminus of the rest of the

enzyme. These two enzymes do appear to have very similar kinetic properties. They have similar K_m values for the substrate cAMP, hRD1 at around 1.5 +/-0.5 μM compared to RD1 for which the K_m is around 4 +/- 2.3 μM (Shakur et al. 1993). The IC_{50} value of hRD1 for the inhibitor rolipram is slightly lower at 0.29 +/-0.09 μM than that of RD1 which is around 0.7 μM. This indicates that the N-terminal is interacting with the catalytic regions of hRD1 and RD1 in a very similar way.

The major difference is seen when the thermostability of hRD1 is compared to that of RD1 which is approximately eight times less thermostable. This difference must be due to conformational differences between the two isoforms with extra tertiary structure being formed in the human form conferring added stability on the catalytic domain through different types of bonds.

Both the human and rat forms have an intrinsic ability to bind to membranes. This must be a property contained within the N-terminus and not an element which is the product of post-translational modification. The cell-free transcription-translation experiments showed that no such modifications are required for hRD1 to form interactions with the membrane. Interestingly these interactions between hRD1 produced in the cell-free system and P2 membranes are disturbed by low concentrations of Triton X-100 in the same way as they are between hRD1 produced in COS-7 cells and the cell membranes.

It would be interesting to investigate the effects of the lack of UCR1, LR1 and part of UCR2 as these domains are thought to have regulatory effects on the catalytic domain. This could be investigated by producing a chimera which consists of the unique hRD1 N-terminus and a catalytic domain which includes the UCR1, LR1 and the missing exon encoding part of UCR2. This would in effect make it into a long-form PDE. The kinetic

properties of this enzyme could be compared to that of the short-form hRD1 and any differences attributed to the presence of these domains. Differences in the catalytic activity and inhibitor affinity of this chimera and h46 would then point to effects of the unique N-terminus on the catalytic domain.

3.2.13 Figures

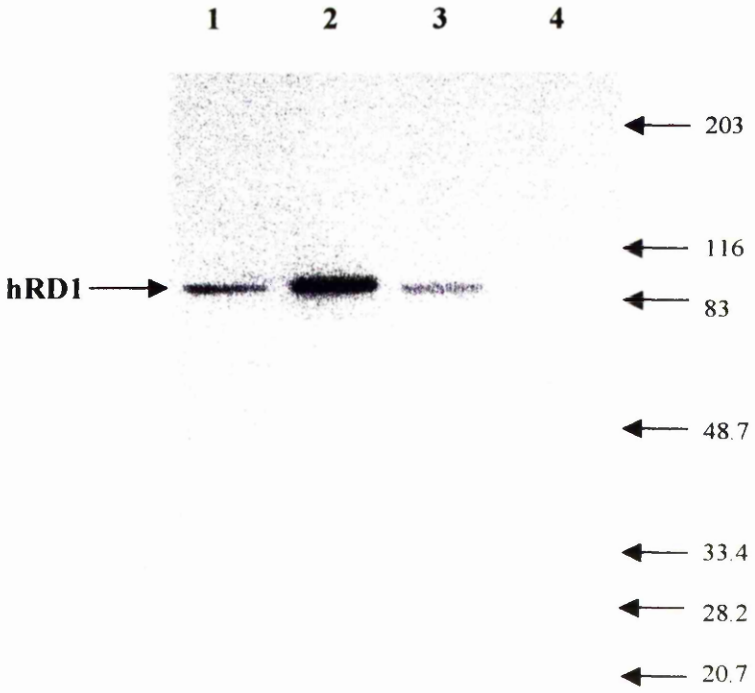

Figure 22. *Western Blot of hRD1 expressed in COS-7 cell fractions. Lane 1 contained 20μg of P1 fraction, lane 2: 5μg of P2 fraction, lane 3: 20μg of S2 fraction and lane 4 was loaded with 20μg of homogenate from the mock transfected COS-7 cells. Fractions were subject to SDS-PAGE with immunoblotting using a human PDE4A specific antiserum.*

	P1	P2	S2
nmol/min/mg prot.	0.9+/-0.2	12.1+/-0.8	0.8+/-0.1

Figure 23. *Table showing the specific PDE activity of hRD1 in each fraction (P1, P2 and S2) of COS-7 cells. This is expressed as nmol of cAMP hydrolysed per minute per mg of protein. Fractions from mock transfected (vector only) COS-7 cells were also tested and they had specific activities as follows: P1: 0.027+/-0.005, P2: 0.019+/-0.004, S2: 0.05+/-0.009 nmol cAMP/min/mg protein.*

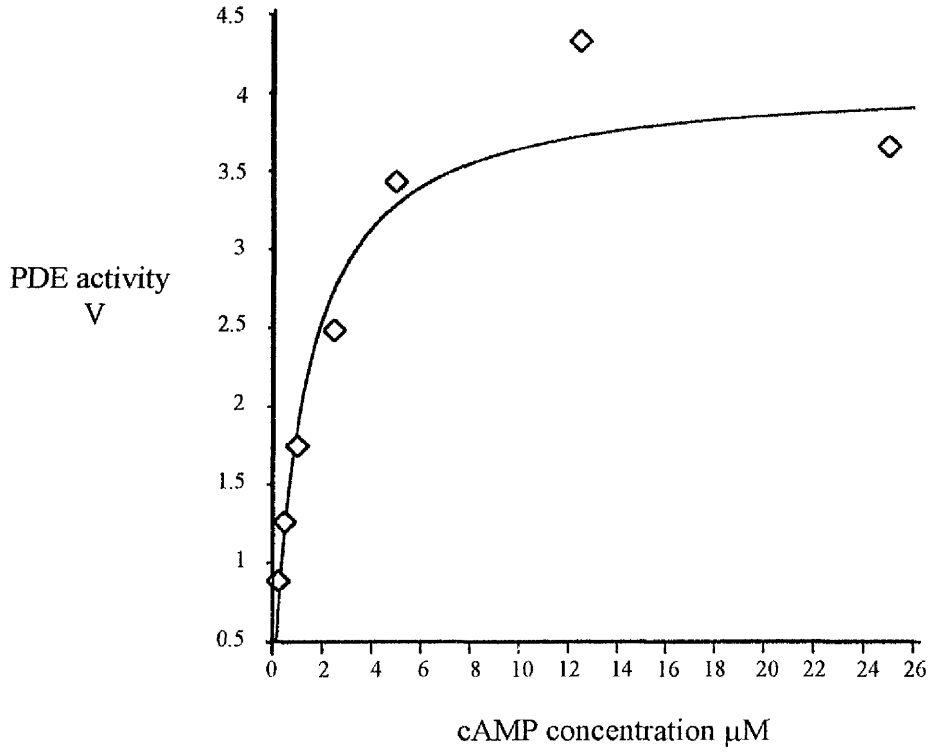

Figure 24. *Graph showing a Michaelis Menten plot describing the substrate dependence of hRD1 activity. These data were obtained using a transfected COS-7 cell P2 fraction. The curve shown is a least squares fit assuming simple Michaelis Menten kinetics, $V=VmaxS/(K_m+S)$, yielding a K_m of 1.2 μM.*

	P1	P2	S2
K_m cAMP (μM)	3.3 +/-2.0	1.5 +/-0.5	3.0 +/-1.5

Figure 25. *This table shows the K_m values for hRD1 expressed in various COS-7 cell fractions P1, P2 and S2. The values were obtained from PDE assays carried out at least three times on samples from at least four separate transfections of COS-7 cells and the standard errors (means +/-S.E.M. ; n=3) for each value are shown beside each one.*

	P1	**P2**	**S2**
IC_{50} Rolipram (μM)	0.36 +/-0.07	0.29 +/-0.09	0.52 +/-0.28

Figure 26. *Table of IC_{50} values for rolipram inhibition of hRD1 activity found in each fraction of hRD1 transfected COS-7 cells. Assays were carried out three times on at least four separate transfections. The graph below shows a typical inhibition plot of hRD1 found in COS-7 cell fractions in response to the inhibitor rolipram. These experiments were carried out using a cAMP concentration equal to that of the K_m for cAMP for each fraction.*

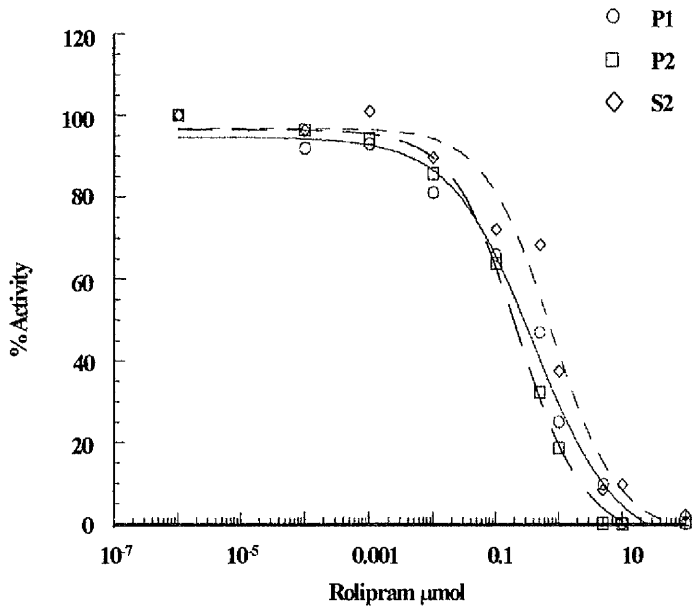

Figure 27. *Graph showing a typical inhibition curve (IC_{50}) for the response of hRD1 expressed in COS-7 cell fractions (P1, P2 and S2) in response to the inhibitor rolipram. Activity remaining at different inhibitor concentrations is expressed as a percentage of the maximum activity when no inhibitor is present in the assay. The cAMP concentration was at [K_m^{cAMP}].*

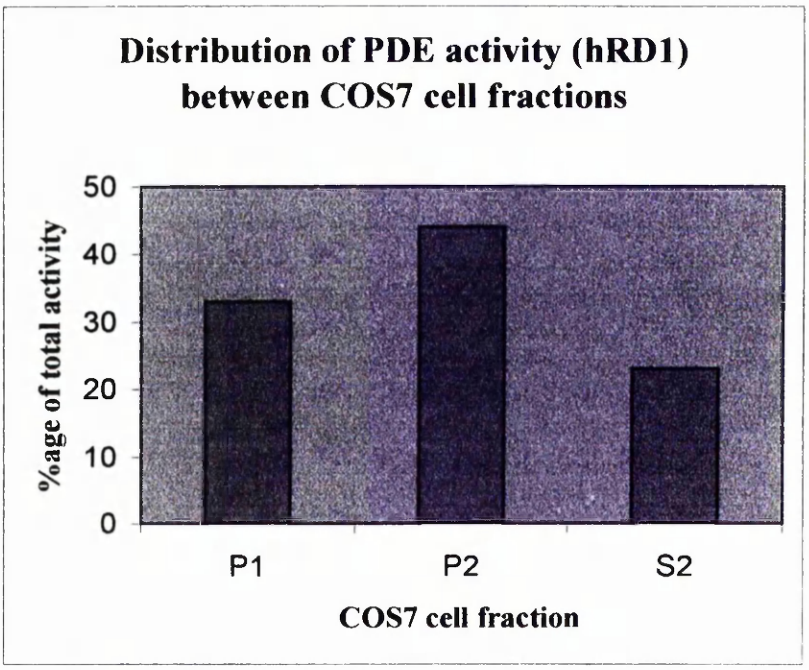

Figure 28. *This graph shows the amount of hRD1 phosphodiesterase activity distributed in each COS-7 cells fraction by volume alone. The P1 fraction contained 33%+/-10 of the total activity per volume, the P2 fraction 44% +/-11 and the S2 fraction 23% +/-8.*

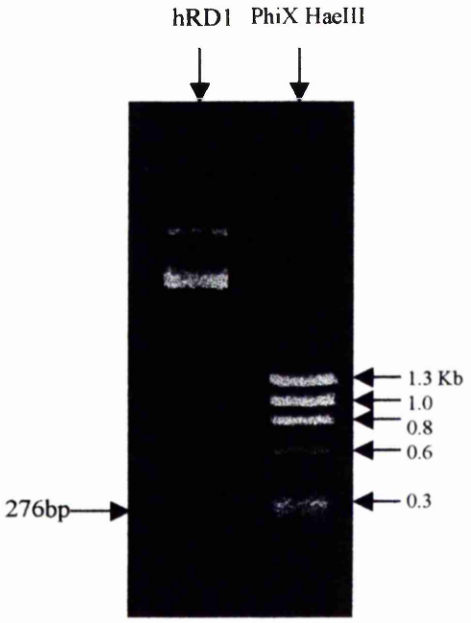

Figure 29. *Photograph of 276bp fragment of hRD1 PCR amplified from human brain cDNA.*

	$T_{0.5}$ (min) 50°C	$T_{0.5}$ (min) 55°C
P1	>120	93 +/-8.7
P2	>120	95 +/-5.5
S2	22 +/-4.5	7.3 +/-0.6

Figure 30. *This table shows the half lives for the hRD1 expressed in each COS-7 fraction when incubated at 50℃ and then 55℃ before being subject to PDE assay to assess the activity remaining. Each experiment was carried out three times on samples from three separate transfections.*

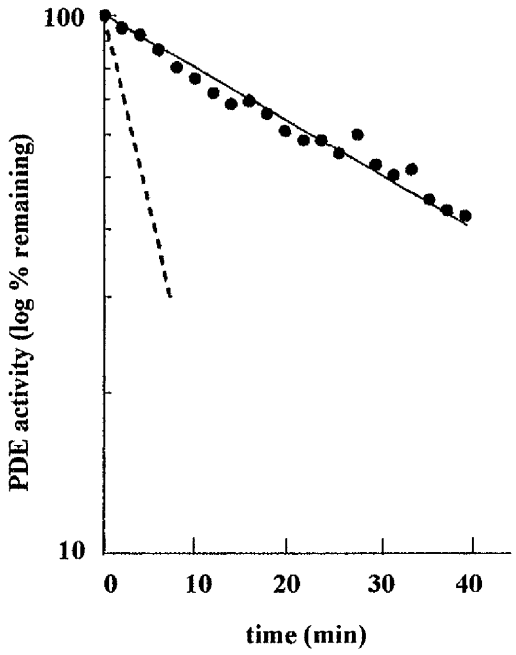

Figure 31. *Residual activity of P2 fraction from hRD1 transfected COS-7 cells incubated at 55℃. The dots indicate data obtained from COS-7 cells transfected with hRD1 DNA and the dashed line indicates data obtained from COS-7 cells transfected with RD1 DNA (from other data for rat enzyme). The logarithm of the percentage residual activity is plotted as a function of time. Thermal denaturation of proteins occurs as a first-order process which is defined as a single exponential. Thus for enzymes, semi-log plots of the residual activity against time will be linear and can be used to derive half lives (Shakur et al. 1993). Such analyses offers a simple way of ascertaining whether the human and rat RD1 forms are conformationally distinct.*

Temp °C	Fraction	Half life (min)	hRD1	RD1
55	P2		31+/-2	4

Figure 32. *Thermostability (shown as half life in minutes) of P2 hRD1 compared to that of P2RD1 at 55 ℃.*

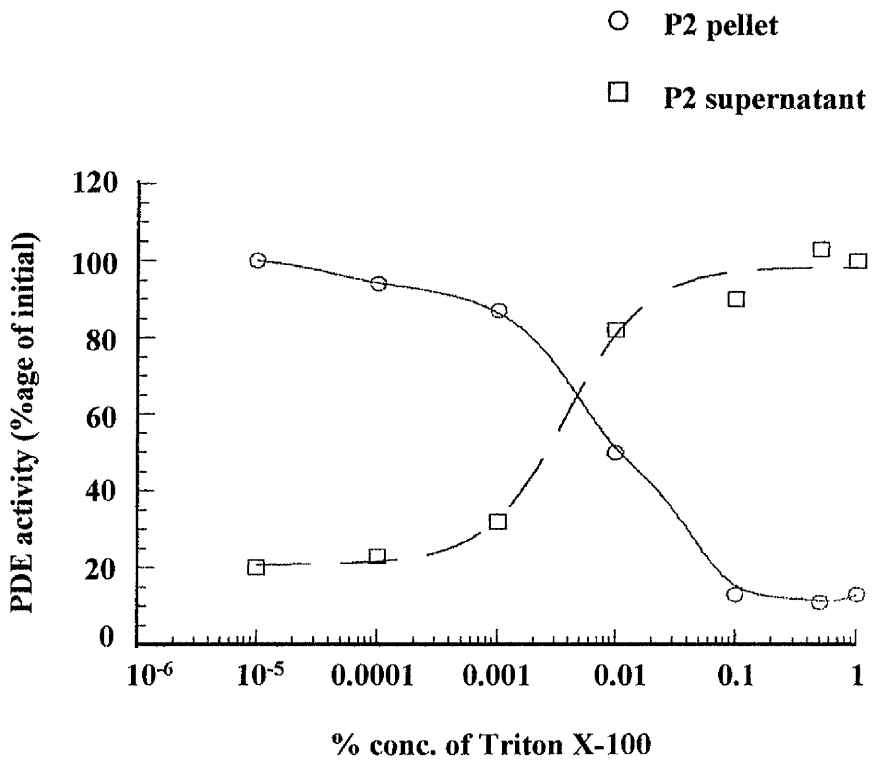

Figure 33. *Typical results of incubating hRD1 transfected COS-7 cell P2 fraction with increasing amounts of Triton X-100 for 30 minutes before centrifugation to produce a supernatant.*

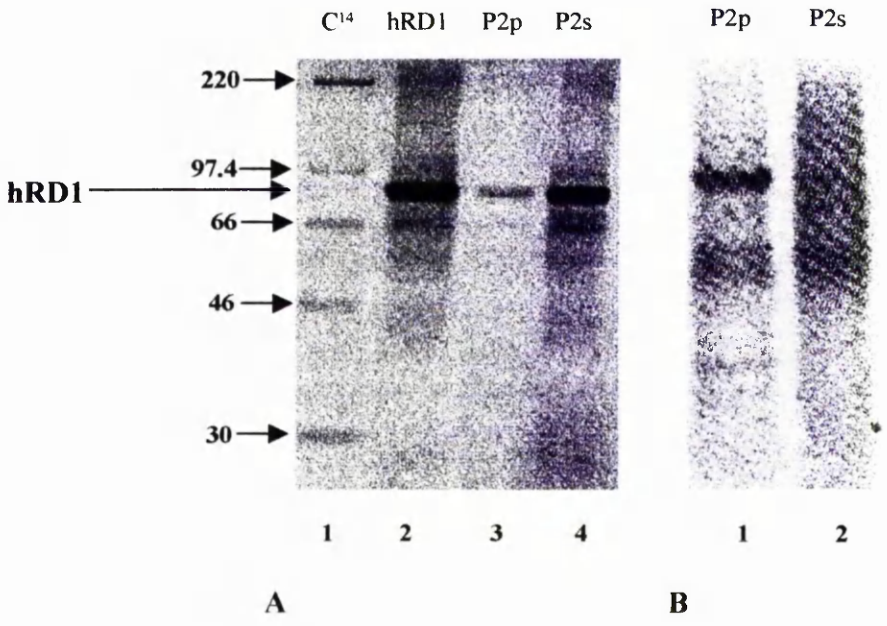

Figure 34. *Western blot of TNT hRD1. Blot A shows the results of incubating TNT hRD1 with P2 membranes and then subjecting them to a 0.001% Triton X-100 wash. After centrifugation the blot shows that the hRD1 is now present in the P2 supernatant fraction as opposed to binding to the P2 membranes. In blot B TNT hRD1 had been incubated with P2 membranes (with no subsequent Triton X-100 wash) and appears in the pellet fraction after centrifugation (lane 1).*

CHAPTER 4

4.1 Cloning and expression of PDE4A10

4.1.1 Introduction

Human PDE4A10, a long-form PDE isoform, was initially cloned in this laboratory by Graham Rena who based his cloning strategy on a rat cDNA that contained novel N-terminal sequence indicating a novel N-terminus. Using primers based on the rat sequence he was able to detect PDE4A10 in human cell lines using RT-PCR. He then used human cosmid clones containing sequence from the human PDE4A exons to reveal the sequence of a unique region plus sequence lying upstream of the unique 5' end of this splice variant. The upstream region lying between the 5' exon of PDE4A10 and the 5' exon of TM3 was thought to contain the promoter sequence for the gene (see figure 36). This investigation showed that the novel human N-terminal sequence represented the discovery of a novel PDE4A as the sequencing revealed the point at which the splice junction occurred (see figures 35, 36 and 37) and the common PDE4A region began (downstream of the unique N-terminus, see figure 37).

The sequence discovered by Graham Rena (which included 434 base pairs encoding the promoter region upstream of the unique N-terminus plus the unique N-terminus) was cloned into PCR2.1. This vector already contained the common (core) PDE4A region sequence starting from the PDE4A10 splice junction onwards. The novel sequence was cloned into the vector upstream of the PDE4A10 splice junction. The sequence was then expressed in COS cells.

At first it was thought that the open reading frame for PDE4A10 contained three (or four, including one situated too far upstream of the N-terminus to be a potential initiating ATG

for PDE4A10 but named ATG1 by Graham Rena nonetheless) potential in-frame ATG, methionine, transcriptional "start" sites (see figures 37 and 38). Further sequencing through this extremely GC-rich region revealed that only one of these "start" sites was a true ATG and this was ATG2. The others, ATG3 and ATG4 (at base pair numbers 46 to 48 and 52 to 54 respectively in the PDE4A10 sequence, see figures 38 and 42) were shown to in fact to be CTG. PDE4A10 was re-engineered so that the construct only contained the PDE4A10 ORF starting from the true ATG; ATG2 (see figure 42). This construct also contained an improved flanking Kozak sequence to enhance expression of the protein in mammalian cell lines. Studies carried out on the sequence flanking transcriptional start sites (ATG) showed that the presence of either a G or an A at the position 3 base pairs upstream of the ATG and the presence of G directly downstream of the ATG were crucial to maximizing translational efficiency of the ribosome (Kozak 1987a; Kozak 1987b). The presence of the G or A 3 base pairs upstream of the ATG was, however, not critical for efficient translation whereas the G downstream of the ATG was. This means that the sequence G(or A)CCATGG would form an optimal Kozak sequence flanking the ATG (see figure 38). ATG2 did not have an optimal Kozak sequence so it was changed from CCCATGC to CCCATGG, a single silent base pair change not changing the amino acid it encoded.

ATG1 in PDE4A10GR was too far away from the N-terminal sequence (840 base pairs upstream of ATG2) to be the true ATG, so was discounted but was still considered as ATG1 for the purposes of the study. ATG1 was discounted on the basis that it was found to be located in the promoter sequence, was not flanked by a Kozak sequence, and would have produced a protein of a predicted weight of 144 kDa taking into account the

aberrant migration of PDE4A10 on SDS-PAGE analysis. A major immunoreactive species of this molecular weight was not observed.

4.1.2 QuickChange primers designed to mutate PDE4A10 ATGs

Prior to the PDE4A10GR construct being sequenced, a strategy which could rapidly reveal the true initiating ATG of PDE4A10 was designed. This involved QuickChange mutational analysis (see methods) to silence ATGs 2, 3 and 4 in turn. The primers designed for this investigation are shown in figure 39. It was presumed that ATG3 was the most likely start site and had been chosen as such by Graham Rena as the sequence flanking it on either side was that which most resembled an optimal Kozac sequence. If ATG3 was the true initiating codon as presumed then mutating it should mean that no protein would be produced. Mutating either ATG2 or ATG4 would result in protein being made as ATG3 would be unaffected. This method presumed that translational was only occurring as the result of one ATG and was supported by the lack of a double band on SDS-PAGE and Western Blotting.

It was hoped that the QuickChange method would provide a rapid answer as to which ATG was the true initiating ATG. At this time sequencing had not progressed far enough to reveal that only one ATG actually existed. The QuickChange PCR reactions were not successful but the fact that this region was so GC-rich was interfering with all experiments involving PCR based strategies. The high fidelity DNA polymerase Pwo was

also used in conjunction with QuickChange to enhance the possibility of the reactions working but it did not produce any positives.

4.1.3 Sequencing Construct PDE4A10GR

The construct designated PDE4A10GR was the original construct made by Graham Rena in the vector pSV-SPORT. It was unclear what the precise sequence of this construct was. Thus I set out to sequence it in full, in order to reveal the sequence of the unique PDE4A10 5' N-terminal region which had been included in the construct therefore identifying the 5' exon of PDE4A10.

Sequencing of PDE4A10 was initially done using the SP6 primer which anneals upstream of the multiple cloning site in pSV-SPORT. The primers GR84, GR10 and GR11 were also used along with primer GR114 (see figure 40a). The exact sequences and positions of these primers can be seen in figure 37). GR10 was a primer which had been designed to rat sequence but matched the human sequence at certain points crucially at the start at finish of the primer sequence which are important for primer annealing (see figure 40b and c).

4.1.4 Attempt to sequence the N-terminal region of PDE4A10 protein

While awaiting sequencing data for the original PDE4A10GR construct to confirm the existence of the proposed ATGs an alternative approach to establish the true initiating ATG was also used. This involved expressing the protein PDE4A10 encoded by the sequence in the construct PDE4A10GR. By sequencing the protein this should tell us where initiation of transcription and translation starts.

In order to obtain sufficient protein for sequencing immuno-precipitation was used to maximise the amount of the PDE4A10 protein present. Immuno-precipitation was carried out using the antibody 97 which recognises a peptide sequence in the common region of PDE4A. The antibody was of a small enough molecular weight so that it would not interfere with the sequencing of the target protein PDE4A10. The protocols for the immuno-precipitation and the preparation of samples for protein sequencing can be found in the methods section.

Staining of the protein for sequencing was crucial in order to identify the particular band to be sequenced. The only stain available which was compatible with the type of membrane used to transfer the protein onto and the sequencing process was Coomassie Blue R. This unfortunately did not identify the band very strongly indicating that there was a low amount of immunoreactive protein present. It was decided that neither of the six or so attempts to isolate a PDE4A10 band had yielded enough protein for the sequencing to be successful.

4.1.5 First re-cloning strategy for PDE4A10 to start from ATG3

This cloning strategy was devised to dispense with the need to use Quick Change to mutate the ATGs as this strategy had been unsuccessful. It was decided to use ATG3 as the initiating methionine its flanking sequence best fitted the Kozac rule. Graham Rena had also decided that this must be the initiating ATG for the same reason. This re-cloning strategy would do two things at once. It would create a construct which started at ATG3 but also the new construct would not contain the sequence upstream of ATG3 making the new construct approximately 434bp smaller than PDE4A10GR. This additional 5' sequence could potentially interfere with expression of the protein. The general cloning strategy can be seen in figure 41.

Once the 1.3Kb fragment (with a KpnI site at the 5' end and a PaeR7I at the 3' end) had been amplified using primers PDE4A10FB21F and PDE4A10FB22R this was gel purified for ligation back into the vector. Before the 1.3Kb fragment was ligated into the vector pSV-SPORT it was digested with the restriction enzymes KpnI and PaeR7I thus removing a 1.7Kb fragment. This was replaced by the 1.3Kb fragment which started at ATG3.

Once this construct had been created further sequencing data became available which showed that ATGs 3 and 4 were in fact CTG and ATG2 was in fact the authentic initiating ATG. A further new cloning strategy had to be developed and the construct PDE4A10ATG3 was not used for biochemical analyses.

4.1.6 Second re-cloning strategy for PDE4A10 to start from ATG2

Sequencing of the original PDE4A10GR construct had been hampered by the high GC-rich regions it contained but new primers were used and revealed that two ATGs (3 and 4) were actually CTG instead. This is shown in figure 42. This meant that the construct PDE4A10ATG3 was in fact incorrect and would have to be re-engineered to start at ATG2, 45 base pairs further upstream of ATG3.

Engineering the construct so that it now started at ATG2 was straightforward and used the same strategy as the first re-cloning which produced PDE4A10ATG3. A new primer was designed to anneal in the region of ATG2 and contained a KpnI restriction site by changing the region GGC TCC to GGT ACC. The new forwards primer was called FBPDE4A10ATG2 (CGA CGG TAC CTG GCT ACC ATG CGC TCC GGT GCA GC) and was used with the existing reverse primer PDE4A10FB22R. The flanking sequence around ATG2 was also changed from CCC ATG GGC to ACC ATG CGC so that this better fit the Kozac rule and expression of this gene sequence would be enhanced. These primers produced a fragment of 1.335Kb (see figure 43). This fragment was gel purified and then Taq treated before ligation into the vector PCR2.1.

4.1.7 Sequencing of the 1.335kb fragment for PDE4A10ATG2 construct

Although the PCR reaction used to amplify the 1.335Kb fragment for PDE4A10ATG2 had been carried out using the high fidelity DNA polymerase Pwo it was vital to check

that the sequence had been amplified exactly and that no mistakes or mutations had occurred in the sequence. The sequencing was carried out using internal PDE4A primers including FB5, FB6, FB3, FB7, FB2, FB8 and FB1. The sequence and position of these primers can be seen in figure 14. One clone (29) was found to contain sequence homologous to the common PDE4A long-form region with no mistakes introduced by the PCR reaction.

4.1.8 Screening multiple choice cDNAs for presence of PDE4A10

The first round of screening for the presence of PDE4A10 in human tissues was carried out using Origene Multiple Choice cDNAs. These included cDNA from the following tissues: testis, ovary, small intestine, lung, muscle, prostate, leukocytes, brain, heart, kidney, spleen, liver. Plasmid DNA from 4A1GR pSV-SPORT, h46pSV-SPORT and cDNA from human brain library were also used as template with the PDE4A10 primers. The forwards primer (GR10) anneals to sequence in the unique N-terminus of PDE4A10 and the reverse primer (GR84) anneals in the common PDE4A region. These primers should produce a band of 224bp. β-Actin primers were also used to verify that the cDNA had been made correctly in the reverse transcriptase reaction. Many different PCR cycling parameters plus the addition of 5-10% final concentration DMSO were used in this reaction but no positive bands of the correct size were seen. The primers were able to amplify a band of the correct size from PDE4A10GR plasmid DNA and the negative controls produced no bands.

4.1.9 Screening cell lines for expression of PDE4A10

Previous experiments had shown PDE4A10 to be present in a number of different cells lines including Hek293, SK-N-SH, FTC 133, U118 and HeLa cells. Using RT-PCR for PDE4A10 in cell lines it was hoped to discover the true N-terminal sequence of native PDE4A10 so these cells were grown again along with other cell lines including U87, Jurkat, U937's, B cells, F442A, Molt 3 and HLA-60. When the cells reached confluency or a density of around $1X10^6$ cells per ml they were harvested and prepared for RNA extraction (see methods). cDNA was made using the RNA from the cell lines and any cDNA remaining was stored in the -80°C freezer. PCR was carried out the cDNA using the primer pairs GR10 and GR84 (224bp) or GR114 with GR84 which produced a larger fragment of 497bp. β-Actin primers were also used in each round of PCR to check that cDNA had been made successfully. The β-Actin controls were always positive but the primers were probably unable to amplify any sequence due to its high GC-rich nature.

4.1.10 Primer pairs for detecting presence of PDE46 and hRD1

The following primer pairs (see figure 44 for sequences) were designed and made to screen for the presence of either PDE4A4B (PDE46) or PDE4A1 (hRD1). The PDE4A4B primers were designed in order that if screening for PDE4A10 was successful then it would be possible to verify that PDE4A10 rather than PDE4A4B had been PCR amplified. The PDE4A1 primer pair was designed so that a complimentary screening

study could be carried out at the same time. However, as the screens for PDE4A10 were unsuccessful there was always some doubt as to the quality of the cDNA and the focus remained on screening for PDE4A10 rather than any other PDE4A isoforms. The N-terminal (forwards) primer in each case is designed to anneal to a region in the unique N-terminal sequence of each isoform and the C-terminal (reverse) primer is designed to anneal to common PDE4A sequence. In this way a fragment spanning across the splice junction is created. The primer pairs for each isoform can be seen in figure 44. These primer pairs may be of use for future screening.

4.1.11 RT-PCR using GR29, a PDE4A10 specific primer to make cDNA

Due to the lack of signal after RT PCR using cDNA from cell lines with PDE4A10 specific primers many different PCR conditions and cycling parameters were used to see if this would effect the outcome. The primer used in the reverse transcriptase element of the procedure (to produce the cDNA) was also changed. A "random" NotI d-(T) primer which produces fragments of cDNA of varying lengths wherever it anneals to a NotI site had been used with the first strand cDNA synthesis kit (see methods). This was replaced with the primer GR29 (sequence CCACGATGTGGACCACCCTG synthesised reverse and complimentary for the reverse transcriptase reaction) which is designed to anneal downstream from the unique PDE4A10 sequence and produce cDNA covering this region (see figure 40a for position). This should increase the percentage of target DNA in the resulting cDNA, however, the outcome did not change in this case.

4.1.12 RT-PCR using IM primer to produce longer fragment

Another strategy which was used to amplify a PDE4A10 specific band from cell line cDNA was to use primers which were further away from the unique region. This would result in the primers annealing to sequence which was less GC-rich and therefore have a better chance to read through the more GC-rich areas. The primers used in this case were 5'PDE4A10at3' (forwards) GCA CCC TCC GGG CAG ATC TGT C which was designed to anneal at the 3' end of the unique N-terminus and out with the most GC-rich region in that area. The reverse primer was rtCATPDE4A10at5' AGT GTG TCA GGC TGT TAC TA which together with the forwards primer would produce a band of 750bp. The forward primer 5'PDE4A10at3' could also be used with common 4A primers FB10 (406bp) or FB8 (190bp). Once again none of the reactions using these primer pairs produced positive bands with the cell line cDNA.

4.1.13 RT-PCR detects PDE4A10 transcripts in RNA from human tissue

The sense primer IM1 (TCC GGG CAG ATC TGT CAG CTT; position 120 to 140 in HSPDE4A10) was used with the antisense primer ESH4 (ACT GGG AAC GGG CAC ATT GGT; HSPDE4A common region, position 412 to 432 of HSPDE4A10) in order to amplify a 313bp region in HSPDE4A10 (see figure 40a for relative positions). This primer pair was to probe a panel of human tissue RNA samples ("Panel 1" RNA from Clontech; cat. K4000-1). Both positive (using HSPDE4A10 plasmid DNA) and negative

(using water) PCR reaction were also carried out at the same time. HSPDE4A10 transcripts were detected in all of the various tissue types analysed (see figure 45). The strongest signal was detected in heart although it must be noted that this analysis is qualitative only and not quantitative.

4.1.14 Expression of the sequence encoding PDE4A10GR

When DNA encoding the PDE4A10GR sequence was transfected into COS-7 cells it was found to have a very low level of expression. This had not previously been a problem when Graham Rena has expressed PDE4A10 from the vector PCR2.1. The decrease in expression levels could have been due to changes in the COS-7 cells. New COS-7 cells were used but the expression levels did not increase. The low levels of PDE4A10 expression also meant that the overall specific activity of the enzyme was unrepresentative as the endogenous PDE activity can become significant, making kinetic studies invalid. This could have been overcome by immunoprecipitating PDE4A10 prior to kinetic analyses. In order to avoid this expression levels could be increased by re-engineering the construct to contain a Kozak sequence which would give optimum expression of the gene. The strategy of optimising the Kozak sequence is often employed during the cloning of genes and in this case proved very successful leading to high levels of the expression of the PDE4A10 gene.

Western blotting of the PDE4A10GR protein after SDS-PAGE showed, as for all known PDE4 enzymes, that the expressed protein migrated at a higher molecular weight than

predicted from the amino acid sequence. PDE4A10 appeared to migrate in a similar fashion to HSPDE4A4B (PDE46). However, its predicted molecular weight is 9kDa less than that of HSPDE4A4B (see figure 46). This is a small difference and higher resolving gels are needed to discriminate between the two proteins.

As discussed above, PDE enzymes characteristically migrate more slowly on SDS-PAGE than predicted by their amino acid sequence. This can be a result of the conserved poly (acidic) regions found towards the C-terminus of the catalytic region. Another possible reason for aberrant migration on SDS-PAGE is that the enzyme might be phosphorylated. The degree to which phosphorylation could be a contributing factor could be investigated using a simple de-phosphorylation experiment.

4.1.15 De-phosphorylation of PDE4A10

As described in the previous section phosphorylation due to motifs present in the unique N-terminus of PDE4A10GR could be a cause of aberrant migration of PDE4A10 on SDS-PAGE. These included the motifs PESL (β-adrenergic receptor kinase), TGPE and SDED (casein kinase 2) none of which are present in PDE4A4B. There was also an additional TRR motif (protein kinase C) in the PDE4A10 N-terminal sequence although PDE4A4B (PDE46) also contains several protein kinase C motifs in the common region shared with PDE4A10.

A simple experiment to demonstrate whether this was the case involved using a phosphatase treatment to de-phosphorylate the protein. COS-1 cells which had been

transfected with PDE4A10GR DNA were serum starved overnight prior to treatment. Alkaline phosphatase was used either alone or after pre-treatment of cells with Protein Kinase C inhibitor (see methods). The results can be seen in figure 47. It is possible that the MW of PDE4A10GR was reduced slightly by the de-phosphorylation but further experiments were unable to clarify this. Thus a more intensive investigation needed to be carried out as a separate project to evaluate this.

4.1.16 Expression of PDE4A10ATG2 in COS-1 cells

Once the final construct ATG2 was made three clones were used for expression in COS-7 cells. COS-1 cells were chosen as the expression system for characterisation of the protein as PDE4A10 appeared to be expressed more efficiently in these than in COS7 cells. Indeed ≥98% of total PDE activity was due to recombinant enzyme. Thus any endogenous PDE activity would not interfere with the characterisation of PDE4A10. These data were then compared to the other PDE4A long-form PDE4A4B (PDE46).

Figure 48 shows how the predicted molecular weights of the three proteins PDE4A4B (PDE46), PDE4A10ATG3 and PDE4A10ATG2 compared. This was done on the basis of the amino acid sequence obtained from the sequence making up the open reading frame of gene. From the number and type of amino acids in the sequence it is possible to calculate the approximate molecular weight of the protein and how they should compare when resolved by SDS-PAGE.

Using the traditional 8% cross-linked SDS-polyacrylamide gels to resolve PDE4A10 meant that its size could not be distinguished from that of PDE4A4B by eye as the separation was not particularly good. To obtain higher resolution in order to resolve these proteins a new range of pre-cast Tris-Acetate 3-8% polyacrylamide gels (Novex) was used. These were designed to separate proteins in the size region of around 125kDa i.e. exactly in the region required (see figure 49).

Not only was it now possible to show a difference in size between PDE4A4B and PDE4A10 (see figure 50) but also this confirmed that ATG2 was the initiating methionine in that both constructs PDE4A10GR (wild type) and PDE4A10ATG2 encoded similarly migrating species. The construct PDE4A10ATG3 contained 15 fewer amino acids and also produced a smaller protein which was visible only with this particular system.

While the predicted ATG2 was the correct one it was only a prediction. Thus to elucidate it I generated constructs that would encode either only an ATG2 start or only an ATG3 start. These gave single bands on SDS PAGE that migrated differently from each other. Secondly I used a "native" construct that had cloned the entire "presumed" 5' exon of PDE4A10 plus the presumed 5' intron (this was later considered to contain part of the putative PDE4A10 promoter sequence). It follows therefore that all possible ATG starts were made available in this construct. However, only one band appeared and this migrated with the protein encoded for in the ATG2 construct rather than the ATG3 construct. This is excellent evidence for my contention that ATG2 provides the PDE4A10 initiating "start" codon.

4.1.17 Conclusion

The original construct encoding PDE4A10 produced a protein which when over expressed in COS-1 cells appeared to have a much higher molecular weight than expected. Most PDE4s migrate aberrantly slowly on SDS-PAGE which could be as a result of structural motifs, post-translational modifications or phosphorylation. In the original PDE4A10 construct there was additional sequence upstream of the presumed initiating codon. This was thought to also perhaps be having an effect on the production of the protein.

The first step in clarifying the situation was to make a construct which started immediately at the initiating codon. De-phosphorylation of the protein produced was also used to see if these reduced the size of the protein therefore accounting for its higher molecular weight. This did result in a slight reduction.

Additional sequencing showed that the presumed initiating codon was in fact not an ATG. The difficulty in sequencing this region once again reflected the GC-rich nature of some of the N-terminal regions of PDE4s. The protein produced from the sequence starting from the true initiating ATG interestingly produced a protein of identical molecular weight to the original construct which contained additional 5' sequence. This showed that none of the upstream sequence had been influencing the production of the PDE4A10 protein. Any increase in molecular weight above that expected was therefore likely to be intrinsic due to the nature of the residues, in particular the conserved poly-acidic regions present in the C-terminal region, or some kind of post-translational modification.

The cloning of the gene encoding PDE4A10 represents the discovery of a new long-form PDE which shares the same splice junction as PDE46 as well as a homologous catalytic C-terminal domain although the N-terminal region of h46 is some 61 amino acids longer.

4.1.18 Figures

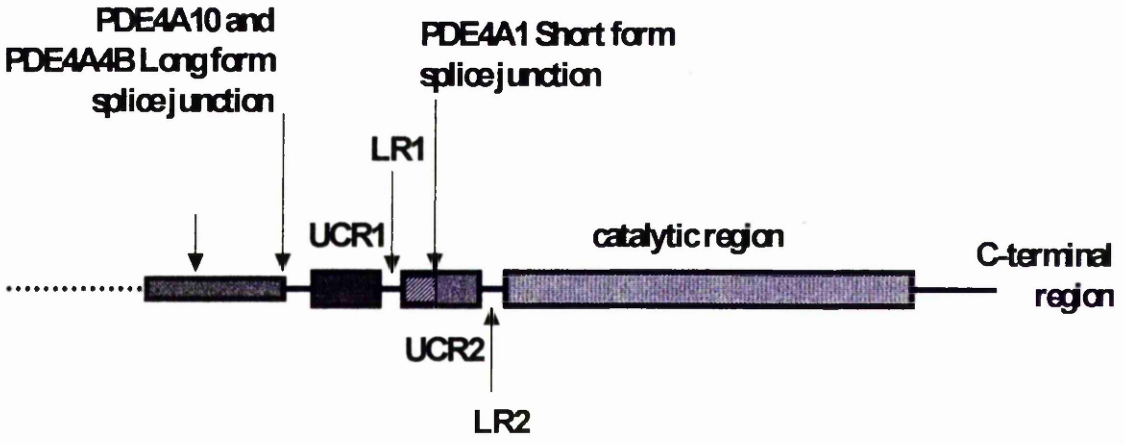

Figure 35. *Schematic diagram of location of the PDE4A10 long-form N-terminal splice junction. This position is shared with the other human PDE4 long isoform PDE4A4B (h46). Also shown are the positions of the internal regions UCR1, UCR2, linker regions 1 and 2 (LR1 and LR2) and the catalytic region which are all common to both PDE4A10 and PDE4A4B.*

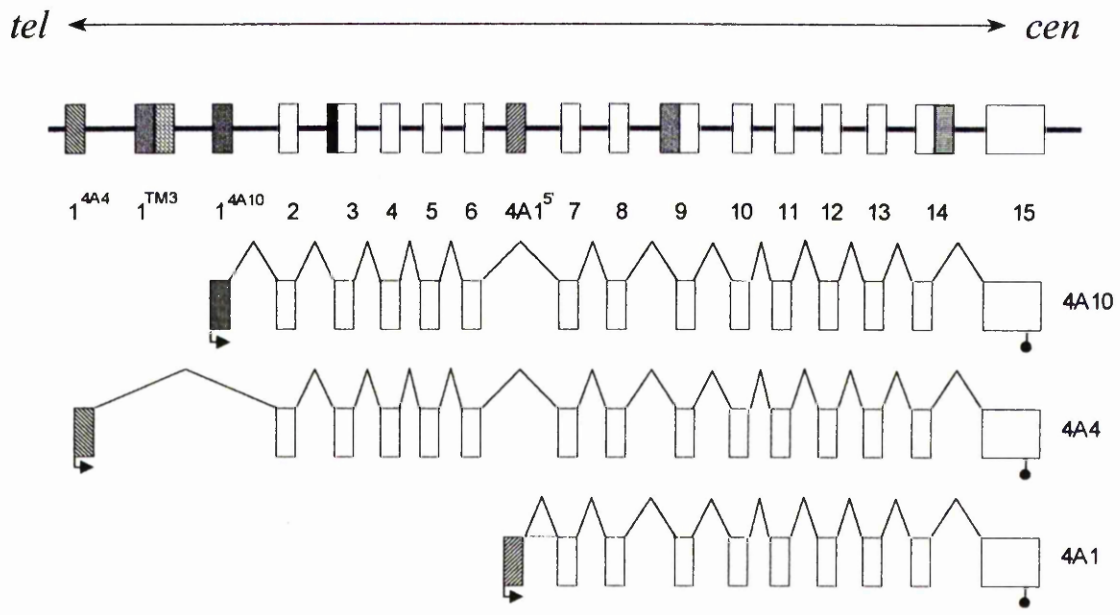

Figure 36. *Schematic diagram of position of the PDE4A10 5' exon encoding the unique N-terminal region in the HSPDE4A gene. Also shown are the relative positions in the HSPDE4A gene of the 5' exons encoding the unique N-terminal regions of PDE4A4 (h46) and 4A1 (hRD1).*

GR11

G GGG GGG AAA TTG GTC CGA TTC CGC AGG ACC CCT GCA GGG GGA GGC

AGA CAG AGC GCC CGT GCG CTC CCT TCC CCC GTG CAG ACC CGG GAA

CGT TCG ACC GCC CGG GGC TGT CCC TGG GGG GGT CAC CAG AGG CGT

GGA GGC GGT GCC GGC AGT GGA GGC CGC AGA CAC CTT GGG CCT GGC

CAG CAG CGC GCC CAC ACC GCC CTG CCG CCG TCC CCA TGC GCG CCC

2 Novel 5' region

CGA CGA CGG CGC TTG GCT CCC ATG CGC TCC GGT GCA GCG CCC CGG

3 GR10 4

GCC CGG CCC CGG CCC CCT GCC ATG GCA ATG CCC CCC ACG GGC

CCC GAG TCC CTG ACC CAC TTC CCC TTC AGC GAT GAG GAC ACC

GR11

CGT CGG CAC CCT CCG GGC AGA TCT GTC AGC TTC GAG GCA GAG AAT

GGG CCG ACA CCA TCT CCT GGC CGC AGC CCC CTG GAC TCG CAG GCG

UCR1

AGC CCA GGA CTC GTG CTG CAC GCC GGG GCG GCC ACC AGC CAG CGC

GR8

CGG GAG TCC TTC CTG TAC CGC TCA GAC AGC GAC TAT GAC ATG

TCA CCC AAG ACC ATG TCC CGG AAC TCA TCG GTC ACC AGC GAG

GCG CAC GCT GAA GAC CTC ATC GTA ACA CCA TTT GCT CAG GTG

CTG GCC AGC CTC CGG AGC GTC CGT AGC AAC TTC TCA CTC CTG

ACC AAT GTG CCC GTT CCC AGT AAC AAG CGG TCC CCG CTG GGC GGC

UCR2

CCC ACC CCT GTC TGC AAG GCC ACG CTG TCA GAA GAA ACG TGT CAG

CAG TTG GCC CGG GAG ACT CTG GAG GAG CTG GAC TGG TGT CTG

GAG CAG CTG GAG ACC ATG CAG ACC TAT CGC TCT GTC AGC GAG

ATG GCC TCG CAC AAG TTC AAA AGG ATG TTG AAC CGT GAG CTC

ACA CAC CTG TCA GAA ATG AGC AGG TCC GGA AAC CAG GTC TCA

GAG TAC ATT TCC ACA ACA TTC CTG GAC AAA CAG AAT GAA GTG

GAG ATC CCA TCA CCC ACG ATG AAG GAA CGA GAA AAA CAG CAA GCG

CCG CGA CCA AGA CCC TCC CAG CCG CCC CCG CCC CCT GTA CCA CAC

TTA CAG CCC ATG TCC CAA ATC ACA GGG TTG AAA AAG TTG ATG CAT

Catalytic region

AGT AAC AGC CTG AAC AAC TCT AAC ATT CCC CGA TTT GGG GTG

AAG ACC GAT CAA GAA GAG CTC CTG GCC CAA GAA CTG GAG AAC

CTG AAC AAG TGG GGC CTG AAC ATC TTT TGC GTG TCG GAT TAC

GCT GGA GGC CGC TCA CTC ACC TGC ATC ATG TAC ATG ATA TTC CAG

GAG CGG GAC CTG CTG AAG AAA TTC CGC ATC CCG GTG GAC ACG

ATG GTG ACA TAC ATG CTG ACG CTG GAG GAT CAC TAC CAC GCT

GAC GTG GCC TAC CAT AAC AGC CTG CAC GCA GCT GAC GTG CTG

CAG TCC ACC CAC GTA CTG CTG GCC ACG CCT GCA CTA GAT GCA

GTG TTC ACG GAC CTG GAG ATT CTC GCC GCC CTC TTC GCG GCT

GCC ATC CAC GAT GTG GAT CAC CCT GGG GTC TCC AAC CAG TTC

CTC ATC AAC ACC AAT TCG GAG CTG GCG CTC ATG TAC AAC GAT

GAG TCG GTG CTC GAG AAT CAC CAC CTG GCC GTG GGC TTC AAG

CTG CTG CAG GAG GAC AAC TGC GAC ATC TTC CAG AAC CTC AGC

AAG CGC CAG CGG CAG AGC CTA CGC AAG ATG GTC ATC GAC ATG

GTG CTG GCC ACG GAC ATG TCC AAG CAC ATG ACC CTC CTG GCT

GAC CTG AAG ACC ATG GTG GAG ACC AAG AAA GTG ACC AGC TCA

GGG GTC CTC CTG CTA GAT AAC TAC TCC GAC CGC ATC CAG GTC

CTC CGG AAC ATG GTG CAC TGT GCC GAC CTC AGC AAC CCC ACC

AAG CCG CTG GAG CTG TAC CGC CAG TGG ACA GAC CGC ATC ATG

GCC GAG TTC TTC CAG CAG GGT GAC CGA GAG CGC GAG CGT GGC

ATG GAA ATC AGC CCC ATG TGT GAC AAG CAC ACT GCC TCC GTG

GAG AAG TCT CAG GTG GGT TTT ATT GAC TAC ATT GTG CAC CCA TTG

TGG GAG ACC TGG GCG GAC CTT GTC CAC CCA GAT GCC CAG GAG

ATC TTG GAC ACT TTG GAG GAC AAC CGG GAC TGG TAC TAC AGC

GCC ATC CGG CAG AGC CCA TCT CCG CCA CCC GAG GAG GAG TCA

AGG GGG CCA GGC CAC CCA CCC CTG CCT GAC AAG TTC CAG TTT

C-terminal region

GAG CTG ACG CTG GAG GAG GAA GAG GAG GAA GAA ATA TCA ATG

GCC CAG ATA CCG TGC ACA GCC CAA GAG GCA TTG ACT GCG CAG GGA

TTG TCA GGA GTC GAG GAA GCT CTG GAT GCA ACC ATA GCC TGG GAG

GCA TCC CCG GCC CAG GAG TCG TTG GAA GTT ATG GCA CAG GAA GCA

TCC CTG GAG GCC GAG CTG GAG GCA GTG TAT TTG ACA CAG CAG GCA

CAG TCC ACA GGC AGT GCA CCT GTG GCT CCG GAT GAG TTC TCG TCC

CGG GAG GAA TTC GTG GTT GCT GTA AGC CAC AGC AGC CCC TCT GCC

CTG GCT CTT CAA AGC CCC CTT CTC CCT GCT TGG AGG ACC CTG TCT GTT

TCA GAG CAT GCC CCG GGC CTC CCG GGC CTC CCC TCC ACG GCG GCC

GAG GTG GAG GCC CAA CGA GAG CAC CAG GCT GCC AAG AGG GCT TGC

AGT GCC TGC GCA GGG ACA TTT GGG GAG GAC ACA TCC GCA CTC CCA

GCT CCT GGT GGC GGG GGG TCA GGT GGA GAC CCT ACC TGA TCC C

Figure 37. *Complete coding sequence for PDE4A10. The regions highlighted and underlined indicate sequence encoding distinct domains within this PDE. These regions include 1) the novel N-terminal domain, 2) UCR1, 3) UCR2, 4) the catalytic domain and 5) the C-terminal region. The position of ATGs 2, 3 and 4 are also highlighted in red.*

Also indicated are the positions and sequences of the primers used to sequence the construct PDE4A10GR.

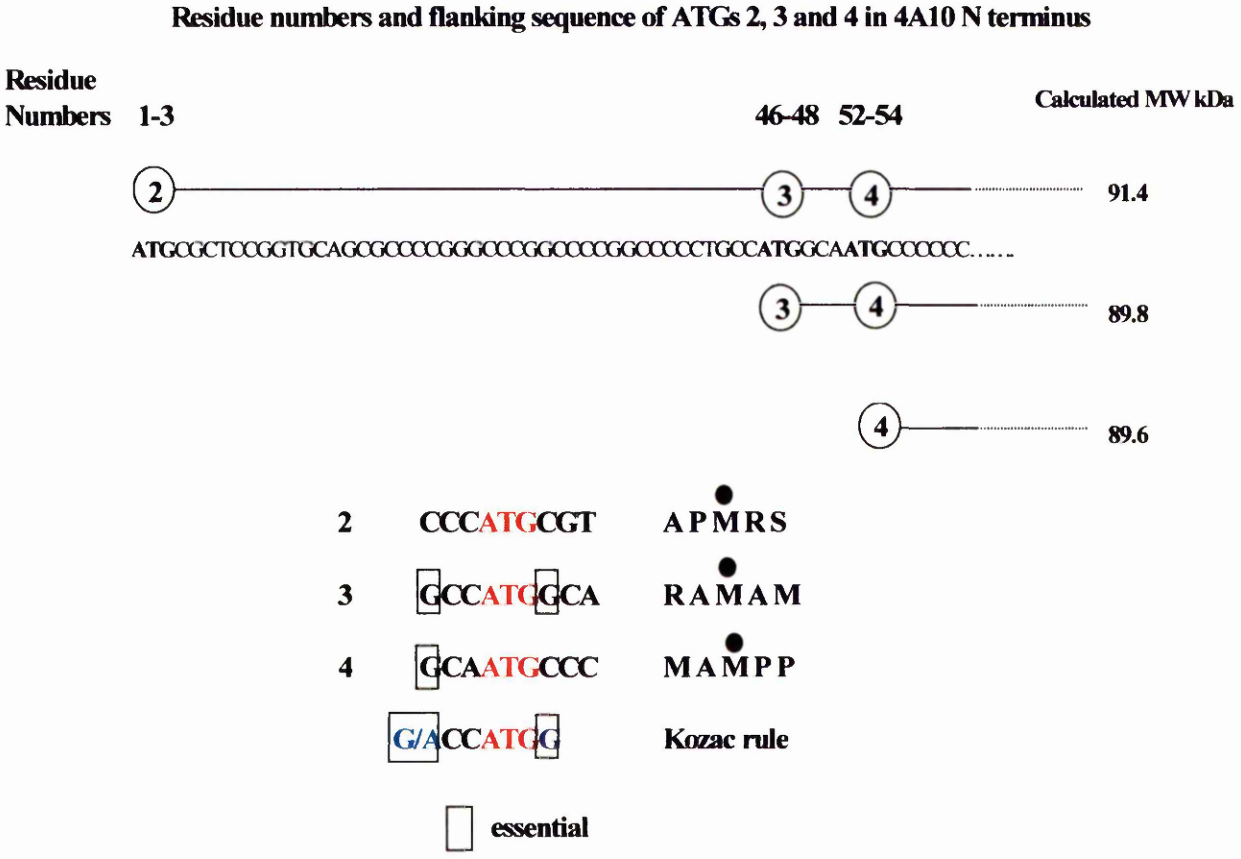

Figure 38. *The relative positions of PDE4A10 ATGs 2, 3 and 4 and their flanking sequence in comparison to the Kozak rule sequence.*

Primers pairs designed to mutate ATGs 2, 3 and 4 from ATG to GCG

FBQC1 →
TTGGCTCCCGCGCGTTCCGGTGCAGCGCCCCGG
← FBQC2
CCGGGGCGCTGCACCGGAACGCGCGGGAGCCAA
FBQC3 →
CCGGCCCCGTGCCGCGGCAATGCCCCCCACCGG
← FBQC4
CCGTGGGGGGCATTGCCGCCGCACGGGGCCGG
FBQC5 →
CCCGTGCCATGGCAGCGCCCCCCACGGGCCCCG
← FBQC6
CGGGGCCCGTGGGGGGCGCTGCCATGGCACGGG

Figure 39. *List of QuickChange primers used to mutate PDE4A10ATGs 2 (FBQC1/FBQC2), 3 (FBQC3/FBQC4) and 4 (FBQC5/FBQC6) and the position of the desired change from ATG to GCG.*

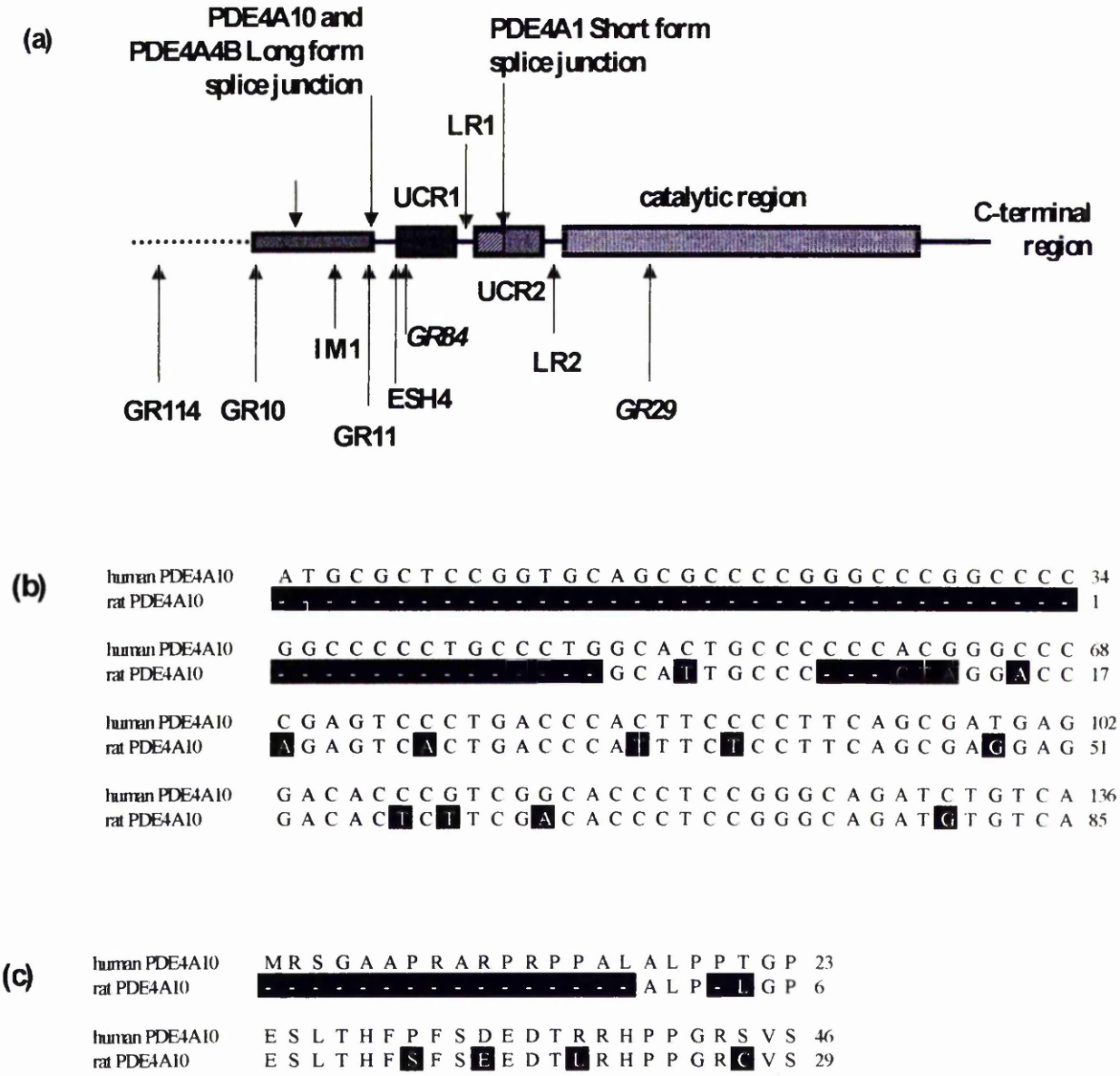

Figure 40. *Position of PDE4A10 sequencing primers. Diagram (a) shows the approximate positions of the primers (including the PDE4 specific primer IM1) used to sequence the N-terminal portion of the construct PDE4A10GR. Primer GR10 was*

designed to rat PDE4A10 sequence and diagrams (b) and (c) show the regions of similarity that the human and rat nucleotide and amino acid sequences share.

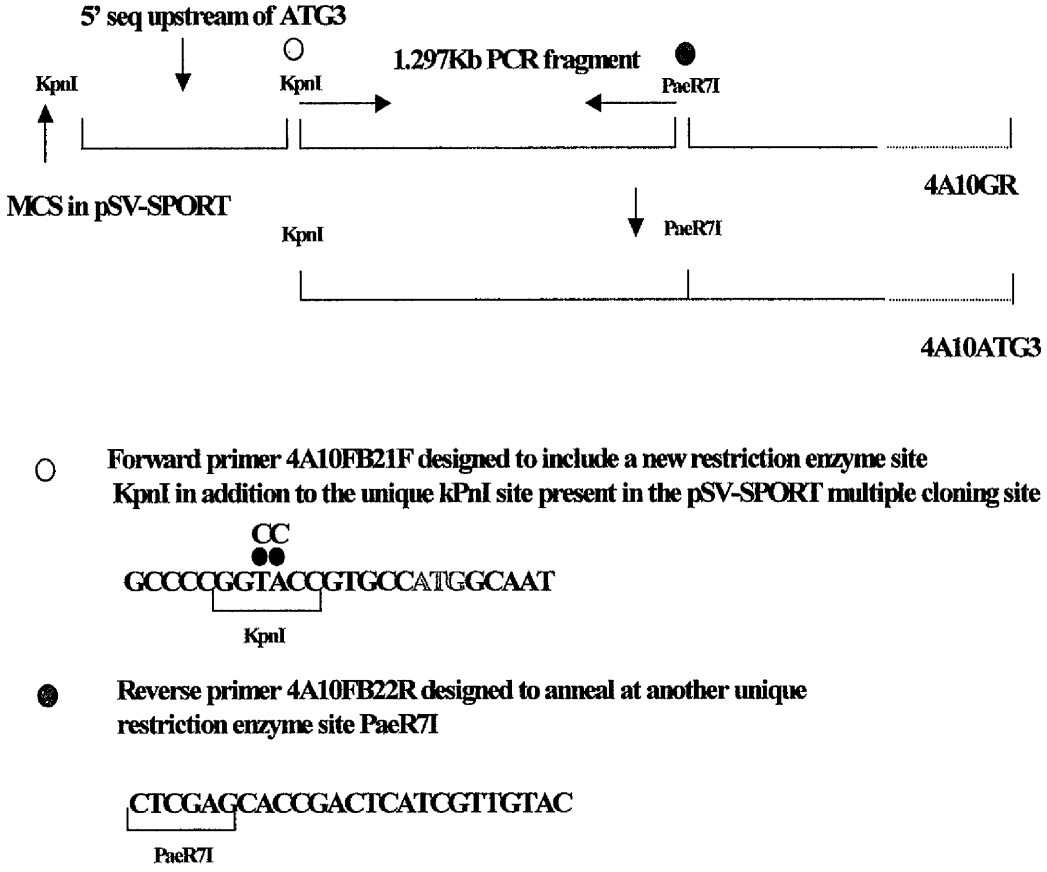

Figure 41. *This diagram shows how the construct PDE4A10GR pSV-SPORT was re-engineered to start at ATG3. This involved designing a primer 434bp downstream of the start of the insert sequence which included a KpnI restriction site (as does the multiple cloning site in the vector) and another 1.3Kb downstream of it to PCR amplify this region.*

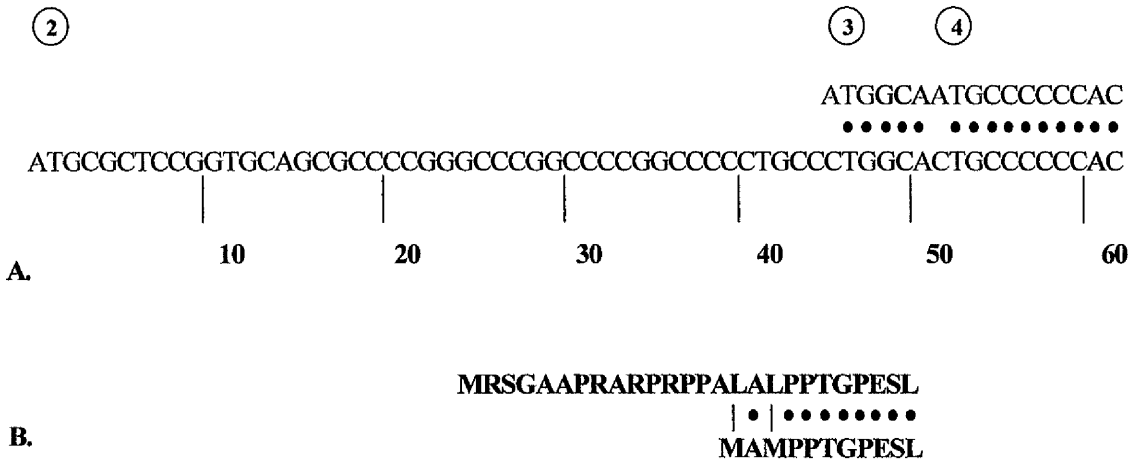

Figure 42. *Diagram A shows the position of ATGs 2, 3 and 4 and the sequence change from ATG to CTG in ATGs 3 and 4. Diagram B also shows how the nucleotide differences change the amino acid sequence in this region.*

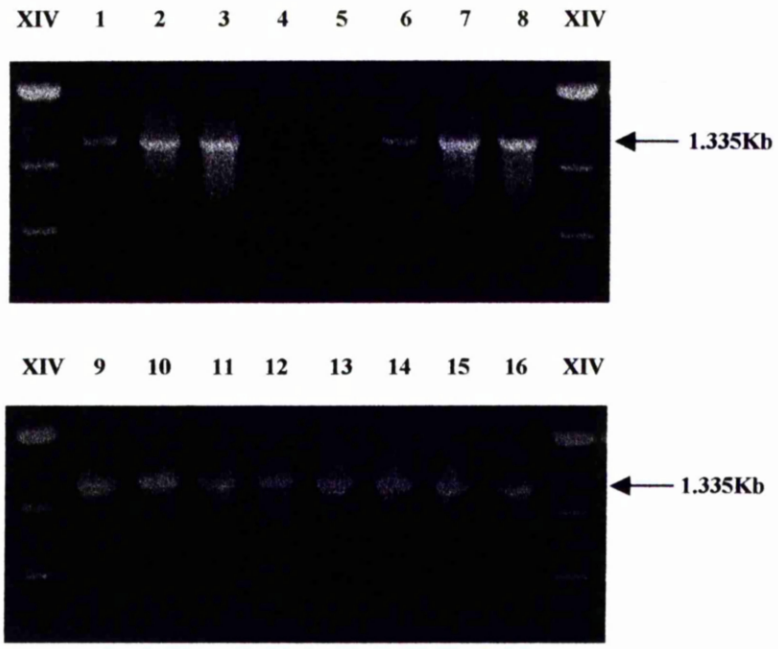

Figure 43. *The 1.335Kb bands obtained using the primers FBPDE4A10ATG2 and PDE4A10FB22R. Lanes 1 to 4, 5 to 8, 9 to 12 and 13 to 16 show bands obtained with varying $MgCl_2$ concentrations (0.5, 1.0, 1.5 and 2μl stock per 25 μl reaction volume from left to right in each set). Reactions 1 to 8 were carried out using Taq DNA polymerase: 1 to 4 contained no DMSO and 5 to 8 contained 2% DMSO. Reactions 9 to 16 were carried out using Pwo DNA polymerase with or without DMSO as before.*

		Band Size
h463' →	AGCCTGTCTCTGTCACTGC	
h465' ←	TGAGCGGTACAGGAAGGACT	**419**
hRD15' →	GAGACCTGCTCTAAGCCTTG	
hRD13' ←	TGGTAGTGATCCTCCAG	**538**

Figure 44. *Primer pairs used to amplify fragments of the PDE4A isoforms PDE4A4B (h46) or PDE4A1 (hRD1). In each case the N-terminal (forwards) primer is specific to the isoform and the N-terminal (reverse) primer is a generic 4A primer.*

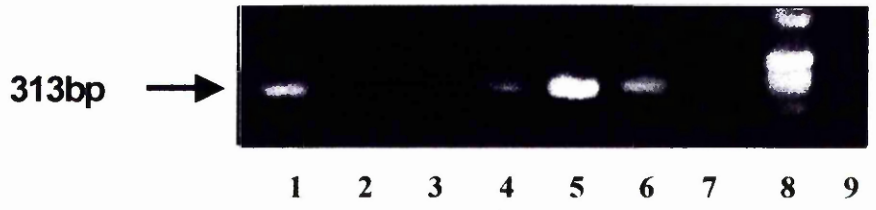

Figure 45. *Bands of predicted size (313bp) amplified by RT-PCR using PDE4A10 primers IM1 and ESH4 from human tissue RNA. Lanes 1 to 9 show the bands obtained from this RT-PCR reaction carried out in the following samples: 1) +ve control, 2) liver, 3) trachea, 4) brain, 5) heart, 6) lung, 7) kidney, 8) DNA size markers, 9) -ve control. Data kindly supplied by Ian McPhee.*

Gene	Amino acids	Predicted MW kDa
PDE4A4B	886	98.5
PDE4A10	810	89.79

Figure 46. *Number of amino acids which make up PDE4A4B (PDE46) and PDE4A10ATG2 compared to their predicted molecular weight.*

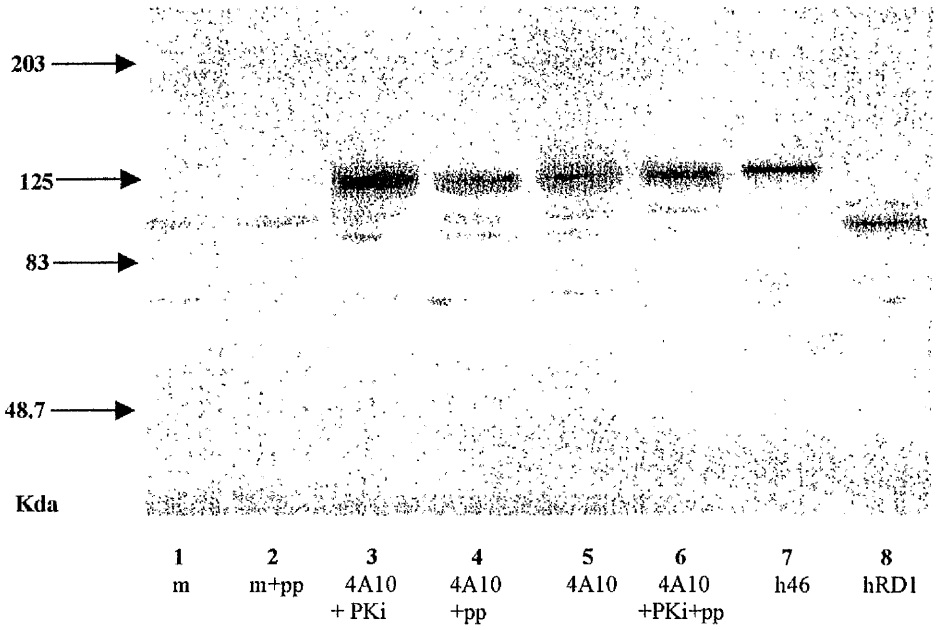

Figure 47. *The above blot shows the effect of incubating PDE4A10 expressed in COS-7 cells with phosphatase on the subsequent mobility of the protein on SDS-PAGE. The key under the lane numbers denotes the following treatments/samples: m=mock COS-1 cells, pp=phosphatase treated, Pki=pre-treatment with protein kinase C inhibitor. PDE4A1 (hRD1) and PDE4A4B (PDE46) are used as standards.*

Construct	Size bp (ORF)	Total aa	Predicted MW kDa
PDE4A10ATG3	2433	811	89.79
PDE4A10ATG2	2478	826	91.4
HSPDE4A4B	2661	887	98.15

Figure 48. *Predicted sizes (kDa) of constructs HSPDE4A4B, PDE4A10ATG2 and PDE4A10ATG3 from the sequence in their open reading frames.*

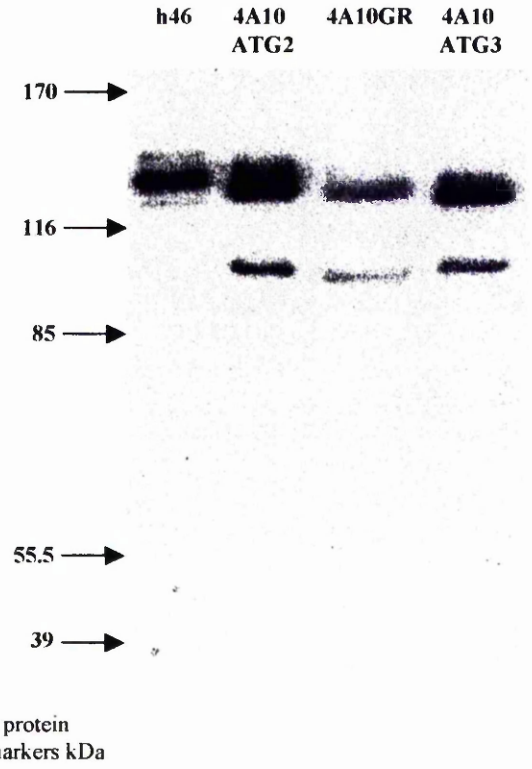

Figure 49. *Western Blot showing the differences in MW between the proteins PDE4A10GR (there is no assumption as to the correct ATG in this protein therefore it should be considered "native"), PDE4A10ATG2 and PDE4A10ATG3 compares to PDE4A4B using the pre-cast Tris-Acetate 3-8% polyacrylamide minigel system from Novex. All of the above were expressed in COS-1 cells. The amounts of protein (from left to right 2, 2, 30 and 2μg) loaded in each well varied in the attempt to achieve bands of similar immunoreactivity.*

Protein	Size kDa	Standard error
PDE4A4B	124.9	0.59
PDE4A10GR	120.9	0.52
PDE4A10ATG3	119.4	1.18
PDE4A10ATG2	120.7	0.36

Figure 50. *Molecular weights of HSPDE46, PDE4A10GR, PDE4A10TAG3 and PDE4A10TAG2 observed when resolved on Novex Tris-Acetate 3-8% polyacrylamide minigels (n=4). The figures presented here show no significant difference but this is evidently clear on the gels.*

4.2 Biochemical Analysis of PDE4A10ATG2

4.2.1 Separation of two distinct PDE4A10 immunoreactive bands

After subjecting all PDE4A10 constructs to SDS-PAGE and Western blotting there appeared to be two distinct immunoreactive bands present. These appeared when PDE4A10 DNA was over-expressed in both COS-1 and COS-7 cells. The major band was the full length protein with a molecular weight of around 120kDa and the smaller band was around 83kDa. It was important to establish whether the smaller band was the result of protease cleavage and whether it displayed any PDE activity which may interfere with or mask the true enzymatic nature of PDE4A10 during characterisation experiments. The smaller band did, however, appear when mock-transfected cells were included in the same SDS-PAGE Western blot but this band was intensified in the cells over-expressing the PDE4A10 protein.

It was unlikely that the smaller band was a truncation product of the larger protein as none of the other PDEs produce truncation products.

In order to separate these two bands an ion exchange column was used. Approximately 2mg of COS-1 cell cytosolic fraction (where most of the PDE4A10ATG2 was expressed) was applied to a Superose 6 column. Fraction volumes of 0.5ml were collected and assayed for PDE activity in order to detect the level of activity in each fraction. The results can be seen in figure 51 which shows a peak of activity in fraction 29.

This fraction corresponded to a molecular weight of around 250kDa (see curve for the markers in this column in figure 52) which is approximately twice the size of PDE4A10 when resolved by SDS-PAGE and Western blotting.

The procedure was repeated using PDE assay buffer as before but with an increased NaCl concentration (to 125mM) to decrease the possibility of the enzyme sticking to the column. The same result was seen again with a peak of activity appearing in the fraction corresponding to a molecular weight of 250kDa. On interpretation of these results the indication is that PDE4A10ATG2 may form a dimer. The localisation of PDE activity to one fraction also indicated that the smaller protein did not display any PDE activity so would not be interfering with PDE assays to establish the enzymatic characteristics of PDE4A10ATG2. This meant that I could therefore go ahead with biochemical analyses.

4.2.2 ELISA of PDE4A10ATG2 and h46 to establish relative immuno-reactivity

Calculating the percentage of PDE activity on the basis of volume in each fraction may give an indication of where the majority of the PDE activity is located in the cell but does take into consideration the relative levels of expression the two isoforms PDE4A4B and PDE4A10ATG2 which can vary from one transfection to another. In order to compare the expression levels of these two proteins in COS-1 cells an ELISA assay was used. ELISA plates were prepared by incubating increasing amounts of COS-1 cell fractions (P1, P2 and S2) from either PDE4A10ATG2 or PDE4A4B transfected cells (see methods). The ELISA used a common PDE4A antibody to target the two isoforms which

recognises a peptide sequence of the common region present in both enzymes. The antibody (in this case Ab 97) should bind in proportion to the amount of PDE present in each well and a range of concentrations are tested in order to ensure that readings are taken from within the linear range for binding.

After detection of the antibody the colour development is read in the plate reader. Expression levels can be compared by converting absorbance units to immunosorbant-enzyme units and then calculating the enzyme units per μg of protein in the well. The table in figure 53 shows the percentage of isoforms PDE4A10ATG2 and PDE4A4B expressed in each fraction of COS-1 cells. Using the ELISA method the majority (82.8% +/-7.8) of the immunoreactive PDE PDE4A10ATG2 was found to be located in the S2 fraction, 12.8% +/-5.5 associated with the P1 fraction and 4.3% +/-2.3 with the P2. In the case of PDE4A4B the majority (66.45% +/-6.5) of the immunoreactive protein was also found in the S2 fraction, 20.1% +/-2.23 was associated with the P1 fraction and 13.6% +/- 7.4 was found to be associated with the P2 fraction.

4.2.3 Relative distribution of PDE4A10ATG2/PDE4A4B activity by volume

The distribution of activity was also calculated on the basis of volume i.e. in a volume of 1ml what percentage of the total PDE activity present was within each fraction. This gives an approximate view of the location of the majority of the PDE activity on the cell. The data for this calculation was taken when the PDE assay was in the linear range. PDE activity due to over expression of PDE4A10ATG2 DNA in COS-1 cells was found to be

mainly located in the S2 fraction (82.8% +/-7.8) and the remainder was shared between the P1 fraction (12.8% +/-5.5) and the P2 fraction (4.2% +/-2.3). Roughly the same distribution of activity was seen with PDE4A4B DNA expressed in COS-1 cells with the majority being located in the S2 fraction (66.15% +/-6.5) and the remainder being shared between the P1 fraction (20.18% +/-2.23) and the P2 fraction (13.6% +/-7.4). The results can be seen in figure 54.

The pre-cast Tris-Acetate 3-8% polyacrylamide minigels from Novex were also used to show the approximate distribution of PDE4A10ATG2 expressed in COS-1 cells on the basis of volume (2μl of each fraction were loaded in each well). This can only be an approximation as the S2 fraction contains far more immunoreactive PDE4A10ATG2 protein than the other two lanes which in comparison are barely visible using this system (see figure 55).

4.2.4 Western Blot showing native PDE4A10 immunoreactive bands in cell lines

Protein samples from a range of different cells lines (Hek, COS-1, U118, FTC and SK) were subject to SDS-PAGE (using the pre-cast Tris-Acetate 3-8% polyacrylamide minigel system from Novex) and subsequent Western Blotting using a common PDE4A antibody (Ab 97). Protein standards run alternately alongside each cell sample were HSPDE4A1 (h46) protein or HSPDE4A10 protein obtained from over-expressed HSPDE4A1 or HSPDE4A10 DNA in COS-1 cells. Up to 50 μg of cell-line sample protein was run in each lane and around 0.1 μg of the PDE4A1 and PDE4A10 protein

standards. This was due to the detectable level of native protein being anticipated to be very low. It was necessary to over-expose the Western blot in order to detect any native PDE4A10 in this way. The amount of PDE410 and PDE4A1 standard protein therefore had to be very low in order not to obscure the detection of any native protein on over-exposure of the blot.

A faint band of around 125kDa was observed in the lane containing SK cell protein (see figure 56). This corresponds to the band seen in the lane containing the PDE4A10 standard. This result could be confirmed if an antibody specific for the unique N-terminal region of PDE4A10 were to become available.

4.2.5 K_m value of PDE4A10

Once it had been established that the kinetic characteristics of PDE4A10ATG2 would not be confused by the existence of a smaller active PDE the kinetic analyses could proceed starting with establishing the K_m for its substrate cAMP. All of the characterisation assays were carried out at least three times on fractions from at least three separate transfections to eliminate differences due to expression levels and to present a more accurate picture of the kinetic properties of PDE4A10ATG2 expressed in this system compared to PDE4A4B.

To determine the K_m value of PDE4A10ATG2 PDE assays were conducted using cAMP concentrations over a range from 0.01μM to 50μM. The graph in figure 57 shows a typical Michaelis-Menten plot. This data was fitted by regression analysis to the

Michaelis-Menten equation ($v=V_mS/(K_m+s)$) in order to calculate the K_m value for the PDE4A10ATG2 found in the S2 fraction of COS-1 cells. K_m values were also calculated for PDE4A4B in order to compare the two enzymes.

During analyses to establish the kinetic characteristics of PDE4A10ATG2 the PDE activity found in mock transfected COS-1 cells was also measured. The level of activity from this source was always below background or $\leq$ 1% of the activity found in PDE4A10ATG2 transfected COS-1 cells which was then subtracted from the activity data for PDE4A10ATG2. Figure 58 gives the K_m values calculated for the PDE4A10ATG2 enzyme found in COS-1 cell fractions P1, P2 and S2 compared to those calculated for the enzyme PDE4A4B. These K_m values are very similar to those observed for other PDE isoforms. The two other long PDE4A isoforms, HSPDE4A4B and the rat isoforms RNPDE4A5 (RPDE6) and RNPDE4A8 (RPDE39) each have K_m values of 2, 2 and 3 μM cAMP respectively. K_m values for PDE4As short and long-forms vary from 2 to 6 μM cAMP. The PDE subtypes B, C and D all display K_m values of 3 μM cAMP or below, all K_m values for group D are around 1.3-1μM cAMP.

4.2.6 V_{max} of PDE4A10ATG2 relative to PDE4A4B

Using the ELISA data to work out the relative expression levels of each type of PDE in the various COS-1 cell fractions it was then possible to calculate the relative V_{max} values of the two enzymes PDE4A10ATG2 and PDE4A4B. Figure 59 shows how these values compare on the basis of activity per immunoreactive enzyme unit.

4.2.7 Specific activities of PDE4A4B and PDE4A10ATG2

The specific activities of the two enzymes PDE4A4B and PDE4A10ATG2 were calculated from data obtained from PDE assays during the linear phase of the experiments. These values do not take into account the level of expression of the enzyme but is interesting to note that the higher level of activity is found in the fraction where the majority of the enzyme is expressed. Figure 60 displays the specific activities of the two enzymes PDE4A4B and PDE4A10ATG2 and figure 61 shows the ratios for this activity relative to each other and the ratio of activity in different fractions relative to that found in the cytosolic fraction. In other studies which have compared distribution of activity in cell fractions the two long rat form PDE4As (RNEPDE4A5 and RNPDE4A8) had particulate/cytosolic activity ratios of 0.7 and 2 respectively. Studies carried out on PDE4B isoforms also found values of around the same level in that the isoforms HSPDE4B1, HSPDE4B2 and HSPDE4B3 each had particulate/cytosolic activity ratios of 0.3, 0.4 and 1 respectively. This shows that the ratio of activity obtained for PDE4A10 while being fairly low compared to other isoforms is at a similar level.

4.2.8 Inhibition of PDE4A10ATG2 by rolipram (IC_{50})

The PDE4 inhibitor rolipram was used in order to determine the IC_{50} value of PDE4A10ATG2 for this particular inhibitor. Rolipram is a cAMP analogue and therefore binds at the active site on the enzyme and is a competitive inhibitor in all studies done to

date (Bolger et al., 1996; Houston et al., 1996; McPhee et al., 1995; Muller et al., 1996; Owens et al., 1997).

Rolipram was dissolved in 100% DMSO as a 10mM stock and diluted in the PDE assay buffer (20mM Tris/HCl/10mM $MgCl_2$ at a final pH of 7.4) to provide a range of concentrations from 0.001μmol to 50μmol. IC_{50} values were determined using a substrate concentration (cAMP) equal to the K_m value of each fraction. Under such conditions the IC_{50} equals the K_i assuming simple competitive inhibition. Once again any activity found in mock transfected COS-1 cells was either below background levels or it was subtracted from the PDE4A10ATG2 activities. Figure 62 shows how the IC_{50} values for the enzymes PDE4A4B and PDE4A10ATG2 compare and figure 63 shows a typical rolipram inhibition curve.

4.2.9 Conclusion

The cloning of PDE4A10 by engineering a construct starting from ATG2 showed that the protein produced by the construct GR was initiated from the same ATG. This was made possible using the Novex mini-gel system which gave particularly good resolution of proteins at a particular molecular weight depending on the gel used.

It was also possible to show that PDE4A10 is most probably produced as a dimer using the column fractionation method. This was not initially investigated from this point of view but because of fears that a smaller immunoreactive band seen on the Western blots

would be contributing activity during kinetic assays on PDE4A10. It would be interesting to run the same experiment using PDE4A4B to see if this is also a dimer.

PDE4A10 differs from PDE4A4B solely in the N-terminal region where as well as being 61 amino acids shorter is also quite different in sequence. It also contains several potential phosphorylation motifs not present in the PDE4A4B amino acid sequence.

The kinetic properties displayed by PDE4A10 are slightly different to that of PDE4A4B. For example although their K_m values are more or less equivalent the IC_{50} value of PDE4A10 found in the cytosolic fraction is approximately 66 times lower than that of PDE4A4B. This difference may be a reflection of the unique N-terminus of PDE4A10 having some kind of influence over the rolipram binding site within the catalytic region perhaps by changing the conformation of this region slightly. The IC_{50} value of the PDE4A10 found in the cytosolic fraction is a lot lower than that of any other PDE4A (values range from 0.2 to 1 μM cAMP) isoform expressed in the cytosolic fraction, however, it is a similar range to isoforms of PDE type B, C and D which are expressed in the cytosol (which vary from 0.02 to 0.14 μM cAMP). The IC_{50} value of the PDE4A10 in the particulate fraction is comparable to the values found for the other PDE4A isoforms which range from 0.2-1.2 μM cAMP).

PDE4A10 like PDE4A4B is found mainly in the cytosol (82.8% +/- 7.8 of PDE4A10 compared to 66.45 +/- 6.5% of PDE4A4B) and although some is found associated with the P2 membranes this is probably an effect of overexpression of the protein in the cell. It is interesting to note that the specific activity of both PDEs is also higher in the cytosolic fraction, perhaps a reflection of their endogenous expression pattern.

The RT-PCR analyses of cell lines and tissue and the Western blot showing native PDE4A10 both confirm the existence of this PDE isoform and the native blot shows that the molecular weight of the endogenous protein is very similar to that seen in the COS-1 expression system. This could reinforce the theory that additional weight is caused by features intrinsic to the protein and not because of post-translational modifications. This could be confirmed using an *in-vitro* cell-free transcription-translation system where post-translational modification due to the surrounding cellular machinery is excluded.

4.2.10 Figures

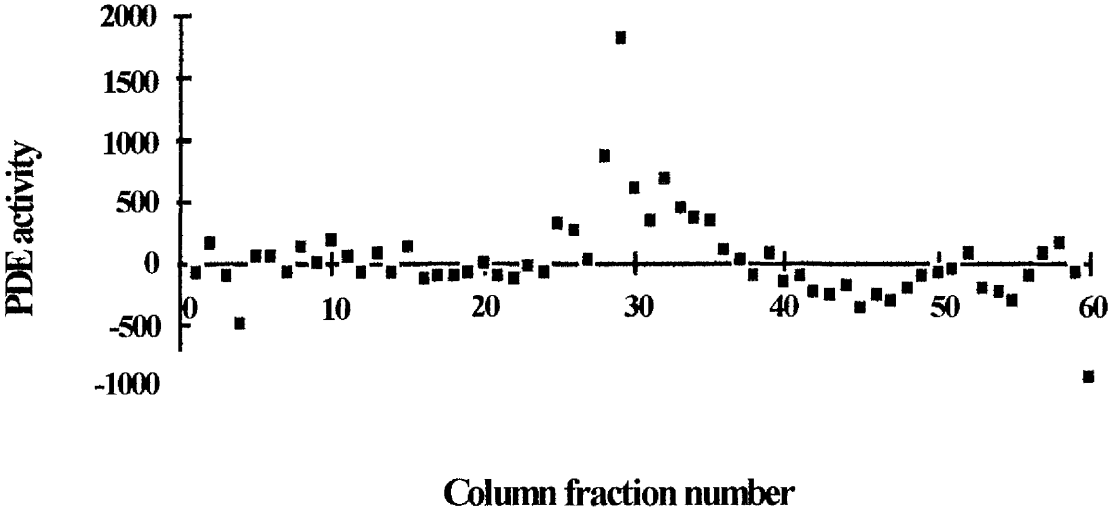

Figure 51. *PDE activity found in 0.5ml fractions separated on the basis of molecular weight through a Sepharose 6 ion exchange column. A peak of PDE activity is observed in the fraction corresponding to 250kDa. The sample applied to the column was COS-1 cell S2 fraction containing over-expressed PDE4A10ATG2 protein.*

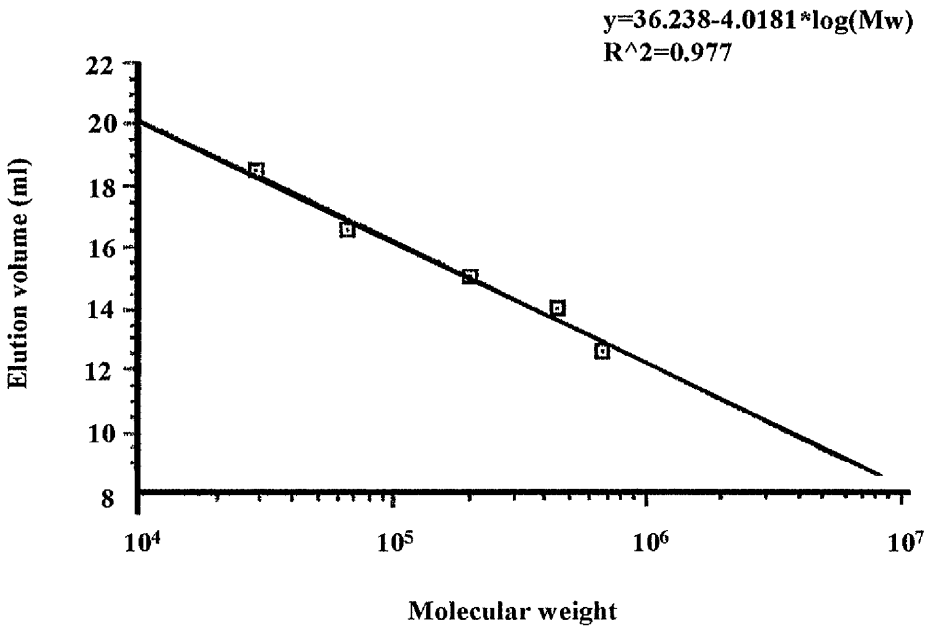

Figure 52. *Elution curve for the Superose 6 HR10/30 ion exchange column and displaying the elution volume (which corresponds to fraction number) against the molecular weight of the standard molecular weights (375kDa, 325kDa, 282kDa, 244kDa and 230kDa) which are also run with the column.*

COS-1 cell fraction	Percentage of activity PDE4A10ATG2	Percentage of activity PDE4A4B
P1	13 +/-6	20 +/-2
P2	4.3 +/-2.3	13.6 +/-7.4
S2	83 +/-8	66 +/-7

Figure 53. *Percentage expression of isoforms PDE4A10ATG2 and PDE4A4B in each fraction (P1, P2 and S2) of COS-1 cells calculated from ELISA data. Experiments were carried out three times on fractions from three separate transfections.*

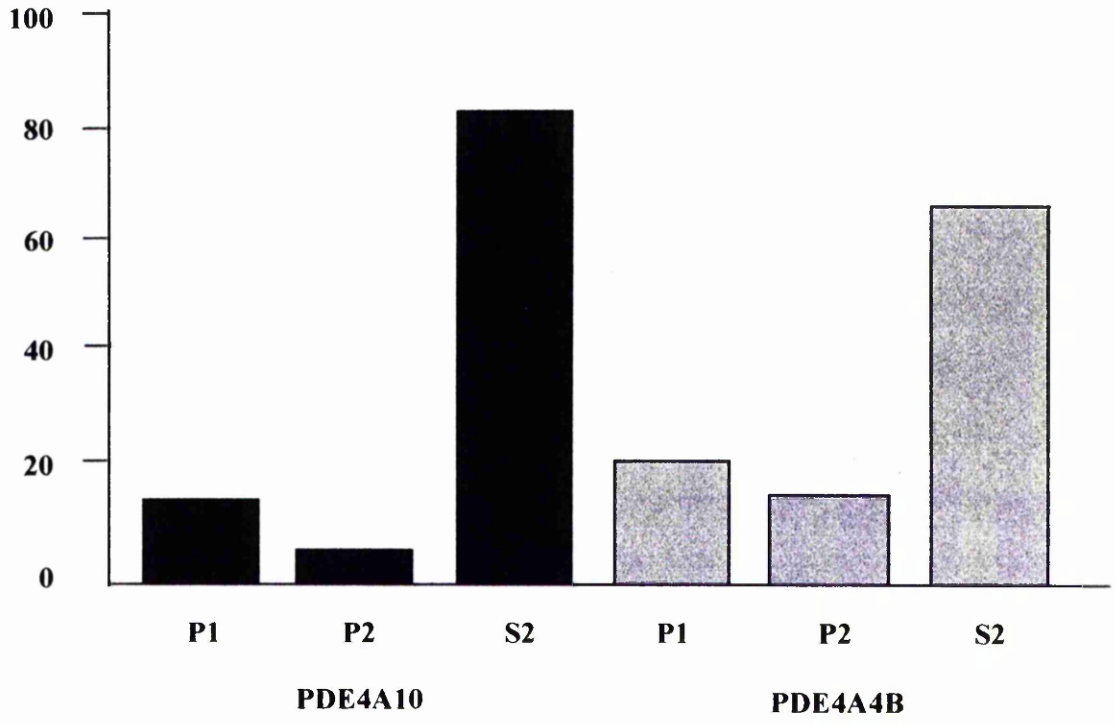

Figure 54. *Percentage of PDE activity in each fraction of COS-1 cells due to over-expression of PDE4A10ATG2 DNA compared to that of PDE4A4B DNA on the basis of volume.*

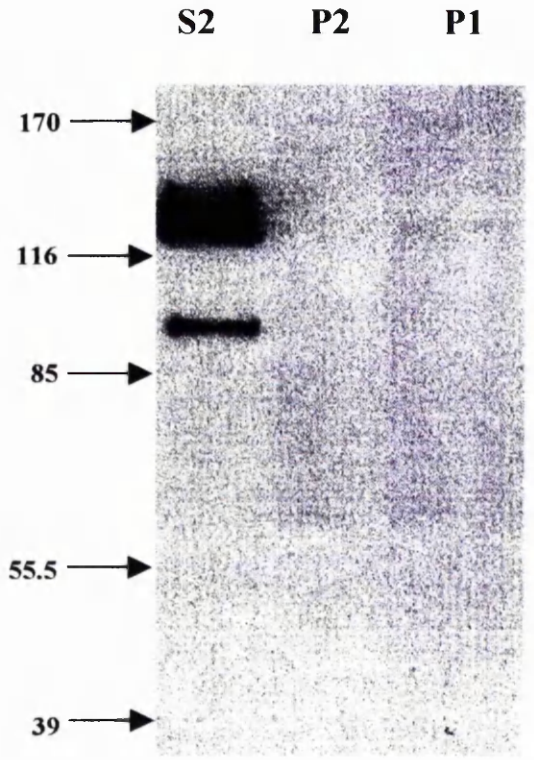

Figure 55. *Western Blot showing the distribution of PDE4A10ATG2 expressed in COS-1 cell fractions (2µml per lane) resolved using the Novex Tris-Acetate minigel system.*

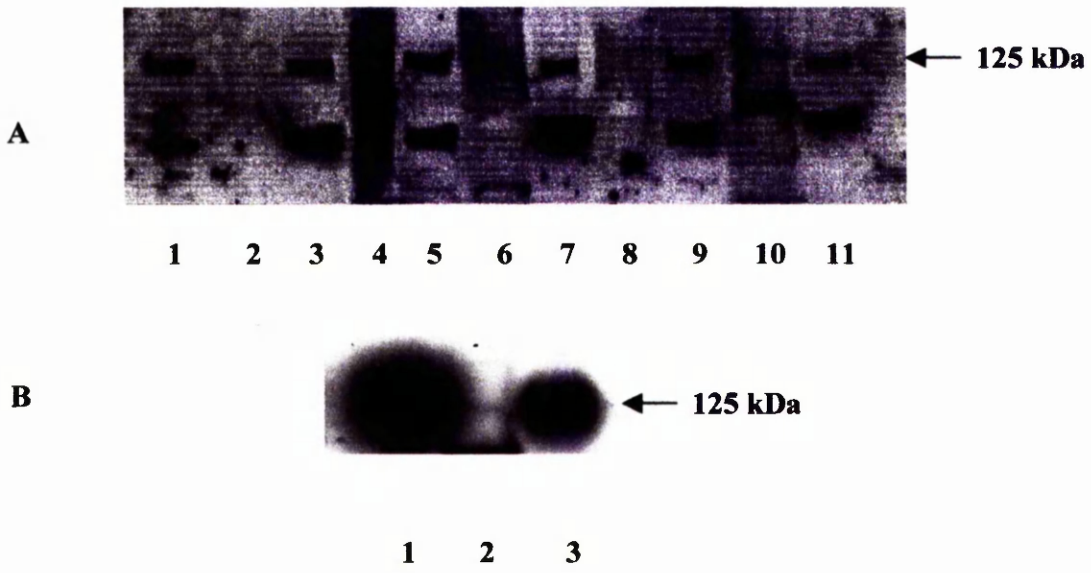

Figure 56. *A. Photograph of Western blot used to detect the presence of HSPDE4A10 protein in cell lines. Lanes 1, 5, and 9 contain 0.1μg of HSPDE4A1 protein and lanes 3, 7 and 11 contain 0.1μg of HSPDE4A10 protein run as standards. These proteins were obtained from PDE4A1 and PDE4A10 DNA over-expressed in COS-1 cells. Samples from cell lines in the other lanes were as follows: 2) Hek, 4) COS-1, 6) U118, 8) FTC and 9) SK.* ***B.*** *Portion of same Western blot at a higher exposure. The samples in the lanes are as follows: 1) HSPDE4A1 standard, 2) SK cells and 3) HSPDE4A10 standard. Up to 50μg of protein was run in each lane containing cell samples. This analysis was carried out using the pre-cast Tris-Acetate 3-8% polyacrylamide minigel system from Novex.*

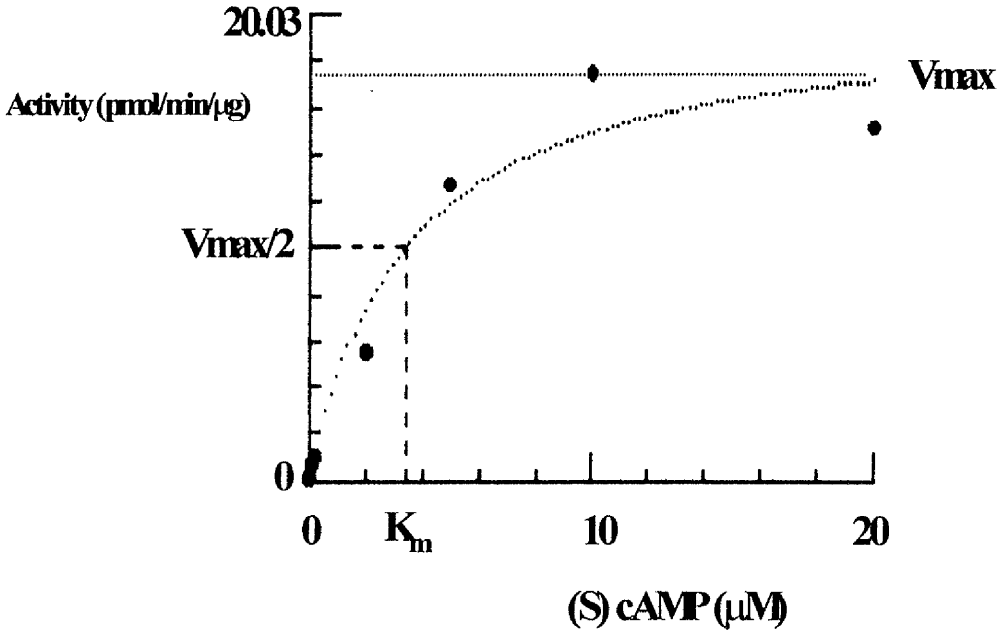

Figure 57. *Hyperbolic Regression used to calculate the K_m value of the enzyme PDE4A10ATG2. The data for this calculation was obtained from PDE4A10ATG2 over-expressed in the S2 fraction of COS-1 cells and is typical of the curves obtained in these experiments. In this particular case the K_m calculated for PDE4A10ATG2 present in the S2 fraction was 3.4 μm cAMP.*

PDE4A10	K_m (μM cAMP)	PDE4A4B	K_m (μM cAMP)
P1	4.1+/-0.5	**P2**	1.9+/-0.3
P2	3.8+/-1.1	**S2**	2.6+/-0.6
S2	2.9+/-0.6		

Figure 58. *K_m values for PDE4A10ATG2 in COS-1 cell fractions P1, P2 and S2 compared to those calculated for PDE4A4B.*

Fraction	PDE4A4B	PDE4A10ATG2	Ratio (unity)
P1	1	1.7	1.7
P2	1	1.25	1.25
S2	1	1.7	1.7

Figure 59. *V_{max} ratios for the two enzymes PDE4A4B and PDE4A10ATG2 based on PDE activity (pmol substrate/min) per immunoreactive PDE unit.*

	P1 (pmol/min/μg)	P2 (pmol/min/μg)	S2 (pmol/min/μg)
PDE4A10ATG2	0.9+/-0.1	0.4+/-0.01	1.9+/-0.4
PDE4A4B	2+/-0.1	1.6+/-0.6	3.9+/-0.1
Ratio PDE4A10:PDE4A4B	1:2	1:4	1:2

Figure 60. *Specific activity of PDE4A4B and PDE4A10ATG2 (pmol cAMP hydrolysed per minute per μg of protein assayed). The table also shows the ratio of specific activity (PDE4A10:PDE4A4B) found in each COS-1 cell fraction.*

	P1/S2	P2/S2
PDE4A10ATG2	0.47	0.22
PDE4A4B	0.52	0.42

Figure 61. *Ratio of PDE activity in the P1 and P2 COS-1 cell fractions relative to that found in the S2 (cytosolic) fraction.*

PDE4A10ATG2	IC_{50}	PDE4A4B	IC_{50}
P1	0.93+/-0.20	**P2**	0.19+/-0.03
P2	0.31+/-0.08	**S2**	1.6+/-0.3
S2	0.02+/-0.01		

Figure 62. *IC_{50} values of enzymes PDE4A4B and PDE4A10ATG2 for the inhibitor rolipram in the various COS-1 cell fractions.*

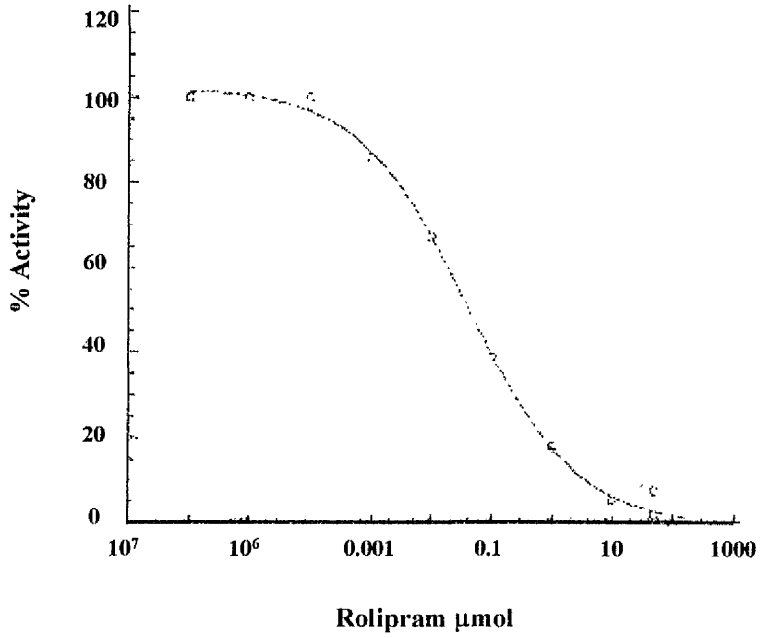

Figure 63. *Typical inhibition curve (IC_{50}) for the response of PDE4A10 expressed in the S2 fraction of COS-1 cells in response to the inhibitor rolipram. Activity remaining at different inhibitor concentrations is expressed as a percentage of the maximum activity when no inhibitor is present in the assay. The cAMP concentration was at [K_m^{cAMP}].*

CHAPTER 5

5 Discussion

The research presented here has shown the existence and characterisation of two novel PDE4As. One a short-form, the other a long-form. This also confirms and demonstrates the complex nature of the organisation of the PDE4A gene. Not only does the gene encode many isoforms but it is capable of producing significantly shorter and different isoforms due to alternative splicing sites within it.

The variation produced by this alternative splicing which creates both short and long-forms each with novel N-termini, has also been demonstrated through biochemical means. Different exons making up each PDE area also able to confer different properties upon it. This is particularly distinct when the two N-termini of hRD1 and PDE4A10 are compared. The sequences encoding these regions are not homologous although the two isoforms have identical catalytic regions. hRD1 is targeted to the cell membrane due to its N-terminus which has been the subject of much investigation. It has been shown that using the N-terminal sequence alone this is able to confer membrane association on the normally soluble bacterial protein chloramphenicol acetyl transferase (CAT) when the two are produced as a chimera (Scotland and Houslay 1995).

These experiments were carried out using the rat RD1 but the human form is identical in the N-terminal region. Studies on the rat form defined the residues in the N-terminal which are responsible for targeting to the first 23. This was confirmed using chimeras as before with CAT. Chimeras consisting of 1-25 RD1-CAT and another of 1-100 RD1-CAT were both expressed in COS-1 cells and found to associate with the membrane. However when the first 25 residues were excluded (26-100 RD1-CAT) the resulting

protein was found to be expressed exclusively in the cytosol. Due to the rat and human N-terminal sequences of RD1 and hRD1 being identical it can be presumed that the same residues are responsible for the targeting of the human form. There would therefore be very little basis on which to produce an hRD1-CAT chimera and carrying out the same mutational studies.

The ability of hRD1 to bind to COS-7 cell membranes was confirmed by incubating hRD1 expressed in a cell-free transcription-translation system with COS-7 cell membranes (from the high speed P2 fraction). This demonstrated that the ability of the protein to bind COS-7 cell membranes must be an intrinsic feature of the protein itself rather than due to post-translational modifications. The expression of hRD1 in the cell-free transcription-translation system produced a protein of comparable molecular weight to that expressed in COS-7 cells (81 +/- 3 kDa compared to 83 +/- 1 kDa respectively). These proteins both display significantly lower mobility on SDS-PAGE analysis than the predicted from their amino acid sequence (72 kDa). This lower mobility must therefore be a feature of the enzyme itself (probably due to the conserved poly-acidic regions found towards the C-terminus of the catalytic region) and supports the theory that little or no post-translational modification of the enzyme occurs when expressed in COS-7 cells. However, this may not reflect the true state of the enzyme *in-vivo* and any post-translational modification may be dependent on cell type.

It would be interesting to investigate how and if indeed the mass of endogenous hRD1 varies depending on cell type. This would, however, be dependent on the ability to detect native hRD1 in human tissue which would in turn depend on the level of expression of

hRD1 in a particular cell type. This particular investigation would also reveal whether hRD1 is targeted to the membrane in different cell types.

Investigations into the nature of hRD1 binding to membranes revealed that the enzyme was almost completely released (≥ 96%) by low concentration of the detergent Triton X-100 (0.01-1%) whereas treatment with 1M NaCl did not cause release of the enzyme. This indicates that the nature of hRD1 association with its membrane anchor is due to hydrophobic interactions which is supported by structural and mutational studies on RD1. These revealed that the region of the N-terminal region that interacts with membranes is highly hydrophobic (Smith et al. 1996).

Thermal denaturation experiments carried out on hRD1 produced some interesting results. The human isoform (hRD1) has a much higher half life than the rodent isoform. The activity of the rodent form is halved after 4 minutes at 55°C whereas the activity of the human isoform is halved after around 30 minutes. The N-terminal sequences of these two isoforms are identical therefore the sequences of their C-terminal domains must encode proteins with different structures.

However, investigations into the catalytic properties of hRD1 revealed that they were comparable to that of RD1. hRD1 enzyme found in the P2 fraction of transfected COS-7 cells had a K_m for cAMP of 1.5 +/- 0.5 μM and RD1 had a K_m for cAMP (also COS-7 P2 fraction) of +/- 2.3 μM. Their IC_{50} values for inhibition by rolipram are also comparable, hRD1 having a slightly lower IC_{50} value of 0.29 +/- 0.09 μM compared to 0.7 μM for RD1 (both values obtained for enzyme expressed in the P2 fraction of COS-7 cells). This indicates that the differences in thermostability of the two enzymes are due to structural differences found in regions outside of the catalytic domain. It is possible that the

structural interactions in or around the catalytic domain of the human isoform are less easily de-stabilised by heat so the active site of this enzyme is intact for longer at 55°C.

Structural studies have so far been limited to the N-terminal region of RD1. Further structural investigation into the C-terminal regions of PDE4A isoforms may reveal the nature of the proposed interactions between the linker regions LR1, LR2, the Upstream Conserved regions UCR1 and UCR2 and the catalytic domain.

PDE4A10 is the second human long PDE4A isoform to be cloned and characterised. It shares the same splice junction as PDE4A4B but its unique N-terminal region is 46 amino acids in length compared to the 107 which make up the unique N-terminal region of PDE4A4B. Expression of PDE4A10 cloned by Graham Rena in COS-7 cells revealed a protein that co-migrated with PDE4A4B. This protein seemed to have a much lower mobility on SDS-PAGE than predicted from its amino acid sequence. However, the construct used for expression in this case also contained sequence upstream of the PDE4A10 initiating codon. In fact the location of the initiating codon and therefore the exact sequence encoding PDE4A10 were unclear.

It was postulated that phosphorylation of residues in the PDE4A10 unique N-terminal region may be contributing to the aberrant migration of PDE4A10 on SDS-PAGE. De-phophorylation experiments showed a very slight reduction in observed molecular weight but not enough to account for the aberrant migration of PDE4A10.

Many attempts were made to sequence the N-terminal protein expressed by the construct PDE4A10GR and this would have quickly revealed the initiating ATG. However, these attempts were unsuccessful. Only when further DNA sequencing was carried out using

sequencing primers designed to read through the very GC-rich regions of sequence in the N-terminal region of PDE4A10 that the location of the initiating ATG was revealed.

The hypothesis that this ATG represented the location of the endogenous initiating ATG (ATG2 in Graham Rena's original sequence) for PDE4A10 was supported by the identification of a band in SK cells co-migrating with PDE4A10 on SDS-PAGE.

The aberrant migration of PDE4A10 on SDS-PAGE may be due to residues located in the unique N-terminal region as its C-terminal region sequence shows 100% homology with PDE4A4B. It has been proposed previously that aberrant migration of PDE4A isoforms on SDS-PAGE is due to conserved poly-acidic regions found towards the C-terminus of the PDE4A catalytic region. This would not account for the difference in mobility on SDS-PAGE in this case. It is possible that post-translational modifications within the cell are responsible for this. The expression of PDE4A10 in a cell-free transcription-translation system and subsequent SDS-PAGE analysis of the protein produced would reveal whether or not this could be the case.

RT-PCR analysis to detect the presence of PDE4A10 transcripts in human tissue RNA proved rather difficult due to the high GC-rich nature of PDE4A10. Many different primer pairs were used along with an internal RT primer to increase the level of possible target in samples. Eventually the primer pair IM1 and ESH4 (data provided by Ian McPhee) were able to detect the presence of PDE4A10 transcripts in a range of human tissue RNA samples including liver, trachea, brain, heart, lung and kidney. This showed that PDE4A10 has a relatively wide distribution in human tissues. Future work could use RT-PCR analysis to identify PDE4A10 transcripts in cell lines. The identification of an

endogenous PDE4A10 in a cell line and subsequent biochemical and distribution analysis may be more representative of the characteristics of the enzyme in an *in-vivo* situation.

PDE4A4B and PDE4A10 display very similar distribution in COS-1 cells with the majority (detected either using phosphodiesterase assays or immunoreactivity in ELISA assays) found in the cytosolic fraction. Around 83% of PDE4A10 expressed in COS-1 cells is found in the cytosol compared to 66% of PDE4A4B. Previous studies have shown that PDE4A4B association with cytoskeletal components of the cell could be due to the SH3 binding domains found in the unique N-terminal region of this isoform. The interaction of SH3 domains with binding proteins occurs through proline-rich motifs in the form of PxxPxxR which are present in the N-terminal region of PDE4A4B. PDE4A10 does not contain proline-rich motifs in this particular context, although it does contain a proline rich LR2 region in the context PRxRPRPP. This within the extreme N-terminal region could account for the lower level of this isoform detected in the membrane fractions of COS-1 cells.

A simple way to investigate the nature of PDE4A10 membrane association would involve treatment of membranes with the detergent Triton X-100 and high ionic strength solutions. If PDE4A10 enzyme activity is not released by either treatment this would indicate strong interactions with cytoskeletal components in a similar fashion to PDE4A4B. Subsequent investigations into the ability of PDE4A10 to bind SH3 domains would reveal whether the proline rich region of this particular isoform contributes to membrane association.

PDE4A10 and PDE4A4B have comparable K_m values for cAMP (both around 2 μM for enzyme found in the cytosolic fraction) but exhibit markedly different IC_{50} values for the

inhibitor rolipram (0.02 μM and 1.6 μM respectively). This must be due to differences in their unique N-terminal regions as the sequence encoding their C-terminal and catalytic domains are 100% homologous. The N-terminal region of PDE4A10 must be exerting some kind of regulatory effect on the catalytic activity of this enzyme. The structure of the unique N-terminal region may be influencing the orientation of the UCR domains (UCR1 and UCR2) which are also thought to have a regulatory influence on catalytic activity. The structure and position of the PDE4A10 N-terminal domain may also be able to interact in some way with the rolipram binding site.

Further investigations into the inhibition of PDE4A10 activity could be investigated through mutational analysis to identify particular residues interacting with the C-terminal regions.

The discovery of new PDE inhibitors with general clinical use is dependent on the identification and characterisation of the many PDE isoforms. It is crucial to identify their distribution within tissues and their intracellular locations and binding partners. One novel approach to inhibiting PDE function involves the use of small molecules to disrupt their interactions of specific isoforms with their binding proteins. The effects of this tailored approach would be two fold. The PDE function would presumably be lost if it is no longer correctly positioned with regard to other signalling molecules and the specificity of this action would hopefully reduce many of the adverse side-effects seen with current PDE inhibitors.

The data presented in this thesis makes a significant contribution to our understanding of the range, location and function of PDE4A isoforms. This will aid the design of novel PDE4A inhibitors and our understanding of the influence of PDEs in cell signalling.

References

References

1. Aceves-Pina, E. O., Booker, R., Duerr, J. S., Livingstone, M. S., Quinn, W. G., Smith, R. F., Sziber, P. P., Tempel, B. L. and Tully, T. P. (1984). *Cold Spring Harbour Symposium in Quantitative Biology* 48, 831-840.

2. Adams, S. R., Harootunian, A. T., Buechler, Y. J., Taylor, S. S. and Tsien, R. Y. (1991). *Nature* 349, 694-697.

3. Altenbach, C., Yang, K., Farrens, D., Farahbakhsh, Z., Khorana, H. and Hubbell, W. (1996). *Biochemistry* 35, 12470-12478.

4. Alvarez, R., Sette, C., Yang, D., Eglen, R. M., Wilhelm, R., Shelton, E. R. and Conti, M. (1995). *Molecular Pharmacology* 48, 616-622.

5. Altschul, S. F., Gish, W., Miller, W., Myers, E. W. and Lipman, D. J. (1990). *Journal of Molecular Biology* 215, 403-410.

6. Bacskai, B. J., Hochner, B., Mahaut-Smith, M., Adams, S. S., Kaang, B. K., Kandel, E. R. and Tsien, R. Y. (1993). *Science* 260, 222-226.

7. Baehr, W., Champagne, M. S., Lee, A. K. and Pittler, S. J. (1991). *FEBS Letters*

278, 107-114.

8. Baldwin, J., Schertler, G. and Unger, V. (1997). *Journal of Molecular Biology* 272, 144-164.

9. Banner, K. H. and Page, C. P. (1995). *European Respiratory Journal* 8, 996-1000.

10. Barnette, M. S., Grous S., Cieslinski L. B., Burman M., Christensen, S. B. and Torphy, T. J. (1995). *The Journal of Pharmacology and Experimental Therapeutics* 273, 1396-1402.

11. Barsony, J. and Marks, S. J. (1990). *Proceedings of the National Academy of Science USA* 87, 1188-1192.

12. Beavo, J. A. (1995). *Physiology Review* 75, 725-748.

13. Beavo, J. A. (1988). *Advances in Second Messenger and Phosphoprotein Research* 22, 1-38.

14. Beavo, J. A., Conti, M. and Heaslip, R. J. (1994). *Molecular Pharmacology* 46, 399-405.

15. Beavo, J. A., Hansen, R. S., Harrison, S. A., Hurwitz, R. L., Martins, T. J. and

Mumby, M. C. (1982). *Molecular and Cellular Endocrinology* 28, 387-410.

16. Beavo, J. A., Hardman, J. G. and Sutherland, E. W. (1971). *Journal of Biological Chemistry* 246, 3841-3846.

17. Beavo, J. A. and Reifsnyder, D. H. (1990). *Trends in Pharmacological Science* 11, 150-155.

18. Beebe, S. J. and Corbin, J. D. (1986) in *The Enzymes* (Boyer P.D., ed.), *Academic Press, Orlando, FL* 17, 44-100.

19. Beltman, J., Becker, D. E., Butt, E., Jensen, G. S., Rybalkin, S. D., Jastorff, B. and Beavo, J. A. (1995). *Molecular Pharmacology* 47, 330-339.

20. Bentley, J. K. and Beavo, J. A. (1992). Regulation and function of cyclic nucleotides. *Current Opinion in Cell Biology* 4, 233 240.

21. Bentley, J. K., Kadlecek, A., Sherbert, C. H., Seger, D., Sonnenburg, W. K., Charbonneau, H., Novack, J. P. and Beavo, J. A. (1992). *Journal of Biological Chemistry* 267, 18676-18682.

22. Bloom, T. J. and Beavo, J. A. (1996). *Proceedings of the National Academy of Science USA* 93, 14188-14192.

23. Bluml, K., Schnepp, W., Schroder, S., Beyermann, M., Macais, M., Oschkinat., H. and Lohse, M. (1997). *EMBO Journal* 16, 4908-4915.

24. Bol, G. F., Gros, C., Hulster, A., Bosel, A. and Pfeuffer, T. (1997). *Biochemical and Biophysical Research Communications* 237, 251-256.

25. Bolger, G. B. (1994). *Cellular Signalling* 6 (8), 851-859.

26. Bolger, G. B., Erdogan, S., Jones, R. E., Loughney, K., Scotland, G., Hoffman, R., Wilkinson. I., Farrell, I. C. and Houslay, M. D. (1997). *Biochemical Journal* 328, 539-548.

27. Bolger, G. B., McPhee, I. and Houslay, M. D. (1996). *Journal of Biological Chemistry* 271, 1065-1071.

28. Bolger, G., Michaeli, T., Martins, T., St John, T., Steiner, B., Rodgers, L., Riggs, M., Wigler, M. and Ferguson, K. (1993). *Molecular and Cellular Biology* 13, 6558-6571.

29. Borisy, F. F., Ronnett, G. V., Cunningham, A. M., Juilfs, D., Beavo, J. and Snyder, S. H. (1992). *Journal of Neuroscience* 12, 915-923.

30. Bregman, D. B., Bhattacharayya, N. and Rubin, C. S. (1989). *Journal of Biological Chemistry* 264, 4648-4656.

31. Bregman, D. B., Hirsch, A. H. and Rubin, C. S. (1991). *Journal of Biological Chemistry* 266, 7207-7213.

32. Burns, F. and Pyne, N. J. (1992). *Bichemical and Biophysical Research Communications, 189, 1389-1396.*

33. Burns, F, Rodger, I. W. and Pyne, N. J. (1992). *Biochemical Journal* 283, 487-491.

34. Butt, E., Beltman, J., Becker, D. E., Jensen, G. S., Rybalkin, S. D., Jastorff, B. and Beavo, J. (1994). *Molecular Pharmacology* 47, 340-347.

35. Byers, D., Davis, R. L. and Kigler, J. A. (1981). *Nature* 289, 79-81.

36. Cannizzaro, G., Gagliano, M., La Rocca, S., Novara, V. Flugy, A. (1989). *Pharmacological Research* 21, Suppl 1:53-54.

37. Charbonneau, H. (1990). *Cyclic Nucleotide Phosphodiesterases*, ed. Beavo, J. and Houslay, M. D. 2, 267-298. Chichester, John Wiley.

38. Charbonneau, H., Beier, N., Walsh, K. A. and Beavo, J. A. (1986). *Proceedings of the National Academy of Science USA* 83, 9308-9312.

39. Charbonneau, H., Kumar, S., Novack, J. P., Blumenthal, D. K., Griffin, P. R., Shabanowitz, J., Hunt, D. F., Beavo, J. A. and Walsh, K. A. (1991). *Biochemistry* 30, 7931-7940.

40. Chen, C., Denome, S. and Davis, R. L. (1986). *Proc. Natl, Acad. Sci. USA* 83, 9313-9317.

41. Chen, J., DeVivo, M., Dingus, J., Harry, A., Li, J., Siu, J., Carty, D., Blank. J., Exton, J., Stoffel, R., Inglese, J., Lefkowitz, R., Logothetis, D., Hildebrandt, J. and Iyengar, R. (1995). *Science* 268, 1166-1169.

42. Chen, Y., Harry, A., Li, J., Smit, M. J., Bai, X., Magnusson, R., Pieroni, J. P., Weng, G. and Iyengar, R. (1997). *Proceedings of the National Academy of Science USA* 94, 14100-14104.

43. Chen, Y., Weng, G., Li, J., Harry, A., Pieroni, J., Dingus, J., Hildebrandt, J., Guarnieri, F., Weinstein, H. and Iyengar, R. (1997). *Proceedings of the Nationsl Academy of Science USA* 94, 2711-2714.

44. Cheung, P. P., Xu, H., McLaughlin, M. M., Ghazaleh, F. A., Livi, G. P. and

Colman, R. W. (1996). *Blood* 88, 1321-1329.

45. Chidiac, P., Herbert, T. E, Valiquette, M., Dennis, M. and Bouvier, M. (1994). *Molecular Pharmacology* 45, 490-499.

46. Clapham, D. and Neer, E. (1997). *Annual Review of Pharmacological Toxicology* 37, 167-203.

47. Colicelli, J., Nicolette, C., Birchmeier, C., Rodgers, L., Riggs, M. and Wigler, M. (1991). *Proceedings of the National Academy of Sciences USA* 88, 2913-2917.

48. Conti, M. and Jin, S. L. (1999). *Progress in Nucleic Acid Research & Molecular Biology* 63, 1-38.

49. Conti, M., Jin, S. L. C., Monaco, L., Repaske, D. R. and Swinnen, J. V. (1991). *Endocrinology Review* 12, 218-234.

50. Conti, M., Nemoz, G., Sette C. and Vicini E. (1995). *Endocrinology Review* 16, 370-389.

51. Cooper, D. M. F. (1998). *Advances in Second Messenger Phosphoprotein Research* 32.

52. Cooper, D. M. F., Mons, N. and Karpen, J. M. (1995). *Nature* 374, 421-424.

53. Corbin, J. D. and Keely, S. L. (1977). *Journal of Biological Chemistry* 252, 910-918.

54. Corbin, J. D., Keely, S. L. and Park, C. R. (1975). *Journal of Biological Chemistry* 250, 218-225.

55. Corbin, J. D., Soderling, T. R. and Park, C. R. (1973). *Journal of Biological Chemistry* 248, 1813-1821.

56. Cvejic, S. and Devi, L. A. (1997). *Journal of Biological Chemistry* 272, 26959-26964.

57. Davis, R. L. and Kauvar, L. M. (1984). *Advances in Cyclic Nucleotide Research and Protein Phosphorylation* 16, 393-402.

58. Davis, R. L., Takayasu, H., Eberwine, M. and Myers, J. (1989). *Proceedings of the National Academy of Science USA* 86, 3604-3608.

59. Degerman, E., Manganiello, V. C., Newman, A. H., Rice, K. C. and Belfrage, P. (1988). *Second Messenger Phosphoproteins* 12, 171-182.

60. Dell'Acqua, M. L. and Scott, J. D. (1997). *Journal of Biological Chemistry* 272, 20, 12881-12884.

61. Deterre, P., Bigay, J., Forquet, F., Robert, M. and Chabre, M. (1988). *Proceedings of the National Academy of Sciences USA* 85, 2424-2428.

62. Dias, J. A., Lindau-Shepard, B., Hauer, C. and Auger, I. (1998). *Biological Reproduction* 58, 1331-1336.

63. Dixon, R. A., Kobilka, B. K., Strader, D. J., Benovic, J. L., Dohlman, H. G, Frielle, T., Bolanowski, M. A., Bennett, C. D., Rands, E., Diehl, R. E., et al. (1986). *Nature* 321, 75-79.

64. Doublie, S., Tabor, S., Long, A. M., Richardson, C. C. and Ellenberger, T. (1998). *Nature* 392, 251-258.

65. Dudai, Y., Jan, Y. N., Byers, D., Quinn, W. G. and Benzer, S. (1976). *Proceedings of the National Academy of Science USA* 73, 1684-1688.

66. Edelman, A. M., Blumenthal, D. K. and Krebs, E. G. (1987). *Annual Review of Biochemistry* 56, 567-613.

67. Engels, P., Fitchel, K. and Lubbert, H. (1994). *FEBS Letters* 350, 291-295.

68. Engels, P., Sullivan, M., Muller, T. and Lubert (1995). *FEBS Letters* 358, 305-310.

69. Fantozzi, D. A., Taylor, S. S. , Howard, P. W., Maurer, R. A., Feramisco, J. R. and Meintkoth, J. L. (1992). *Journal of Biological Chemistry* 267, 16824-16828.

70. Farrens, D., Altenbach, C., Yang, K., Hubbell, W. and Khorana, H. (1996). *Science* 274, 768-770.

71. Fawcett, L., Baxendale, R., Stacey, P., McGrouther, C., Harrow, I., Soderling, S., Hetman, J., Beavo, J. A. and Phillips, S. C. (2000). *Proceedings of the National Academy of Science USA* 97, 3702-3707.

72. Fisher, D. A., Smith, J. F., Pillar, J. S., St. Denis, S. H. and Cheng, J. B. (1998a). *Journal of Biological Chemistry* 273, 15559-15564.

73. Fisher, D. A., Smith, J. F., Pillar, J. S., St. Denis, S. H. and Cheng, J. B. (1998b). *Biochemical and Biophysical Research Communications* 246, 570-577.

74. Francis, S. H. and Corbin, J. D. (1994). *Annual Review of Physiology* 56, 237-272.

75. Gamm, D. M., Baude, E. J. and Uhler, M. D. (1996). *Journal of Biological*

Chemistry 271, 15736-15742.

76. Gailey, D. A., Jackson, F. R. and Siegl, R. W. (1982). *Genetics* 102, 771-782.

77. Genain, C. P., Roberts, T., Davis, R. L., Nguyen, M., Uccelli, A., Faulds, D., Li, Y., Hedgpeth, J. and Hauser, S. L. (1995). *Proceedings of the National Academy of Sciences USA,* 92, 3601-3605.

78. Gether, U. and Kobilka, B. K. (1998). *The Journal of Biological Chemistry* 273, 29, 17979-17982.

79. Gibbs, C. S., Knighton, D. R., Sowadski, J. M., Taylor, S. S. and Zoller, M. J. (1992). *Journal of Biological Chemistry* 267, 4806-4814.

80. Gillespie, P. G. and Beavo, J. A. (1988). *Journal of Biological Chemistry* 263, 8133-8141.

81. Giembycz, M. A. (1996). *Trends in Pharmacological Sciences* 17, 331-336.

82. Glantz, S. B., Amat, J. A. and Rubin, C. S. (1992). *Molecular Biology of the Cell* 3, 1215-1228.

83. Glantz, S. B., Li, Y. and Rubin, C. S. (1993). *Journal of Biological Chemistry* 268,

12796-12804.

84. Gonzalez, G. A. and Montminy, M. R. (1989). *Cell* 59, 675-680.

85. Gordon, L. A., Bergman, A., Christensen, M., Danganan, L., Lee, D. A., Ashworth, L. K., Nelson, D. O., Olsen, A. S., Mohrenweiser, H. W., Carrano, A. V. and Brandriff, B. F. (1995). *Genetics* 30, 187-194.

86. Grossmann, M., Weintraub, B. and Szkudlinski, M. (1997). *Endocrinology Reviews* 18, 476-501.

87. Gutkind, J. S. (1998). *The Journal of Biological Chemistry* 273, 4, 1839-1842.

88. Hagiwara, M., Brindle, P., Harootunian, A., Armstrong, R., Rivier, J., Vale, W., Tsien, R. and Montminy, M. R. (1993). *Molecular Cell Biology* 13, 4852-4859.

89. Hanoune, J. , Pouille, Y., Tzavara, E., Shen, T. S., Lipskaya, L., Miyamoto, N., Suzuki, Y. and Defer, N. (1997). *Molecular and Cellular Endocrinology* 128, 179-194.

90. Han, P., Zhu, X. and Michaeli, T. (1997). *Journal of Biological Chemistry* 272, 16152-16157.

91. Harhammer, R., Gohla, A. and Schultz, G. (1996). *FEBS Letters* 399, 211-214.

92. Harrison, S. A., Reifsnyder, D. H., Gallis, B., Cadd, G. G. and Beavo, J. A. (1986). *Molecular Pharmacology* 29, 506-514.

93. Hausken, Z. E., Coghlan, V. M., Hasting, C. A. S., Reimann, E. M. and Scott, J. D. (1994). *Journal of Biological Chemistry* 269, 24245-24251.

94. Hausken, Z. E., Dell'Acqua, M. L., Coghlan, V. M. and Scott, J. D. (1996). *Journal of Biological Chemistry 271, 29016-29022.*

95. Hausken, Z. E., Coghlan, V. M. and Scott, J. D. (1997). In *Protein Targeting Protocols* (R. A. Clegg, ed.) 47-64, *Humana Press, Totowa, NJ.*

96. Hayshi, M., Matsushima, K., Ohashi, H., Tsunoda, H., Murase, S., Kawarada, Y. and Tanaka, T. (1998). *Biochemical and Biophysical Research Communications* 250, 751-756.

97. Henkel-Tigges, J. and Davies, R. L. (1990). *Molecular Pharmacology* 37, 7-10.

98. Herbert, T. E., Moffett, S., Morello, J. P., Loisel, T. P., Bichet, D. G., Barret, C. and Bouvier, M. (1996). *Journal of Biological Chemistry* 271, 16384-1639.

99. Hirsch, A. H., Glantz, S. B., Li, Y., You, Y. and Rubin, C. S. (1992). *Journal of Biological Chemistry* 267, 2131-2134.

100. Hoffman, R., Wilkinson, I. R., McCallum, J. F., Engels, P. and Houslay, M. D. (1998). *Biochemical Journal* 333, 139-149.

101. Horton, Y. M., Sullivan, M. and Houslay, M. D. (1995). *Biochemical Journal* 308, 683-691.

102. Houslay, M. D. (1996). *Biochemical Society Transactions* 24, 980-986.

103. Houslay, M. D and Kilgour, E. (1990). *Cylcic Nucleotide Phosphodiesterases* ed. J. A. Beavo and M. D. Houslay, 2, 185-226. Chichester, uk, John Wiley & Sons Ltd.

104. Houslay, M. D. and Marchmont, R. J. (1981). *Biochemical Journal* 198, 703-706.

105. Houslay, M. D. and Milligan, G. (1997). *Trends in Biochemistry* 22, 6, 217-224.

106. Houslay, M. D., Scotland, G., Pooley, L., Spence, S., Wilkinson, I., McCallum, F., Julien, P., Rena, N. G., Michie, A. M., Erdogan, S., Zeng, L., O'Connell, J. C., Tobias, E. S. and McPhee, I. (1995). *Biochemical Society Transactions* 23, 393-398.

107. Houslay, M. D., Sullivan, M. and Bolger, G. B. (1998). *Advances in Pharmacology* 44, 225-342.

108. Hurley, J. H. (1999). Structure, mechanism and regulation of mammalian adenylyl cyclase. *The Journal of Biological Chemistry* 274, 12, 7599-7602.

109. Huston, E., Pooley, L., Julien, J., Scotland, G., McPhee, I., Sullivan, M., Bolger, G. and Houslay, M. D. (1996). *Journal of Biological Chemistry* 271, 31334-31344.

110. Ichimura, M. and Kase, H. (1993). *Biochemical and Biophysical Research Communications* 193, 985-990.

111. Jacobitz, S., McLaughlin, M. M., Livi, G. P., Burman, M. and Torphy, T. J. (1996). *Molecular Pharmacology* 50, 891-899.

112. Jacobitz, S., Ryan, M. D., McLaughlin, M. M., Livi, G. P., DeWolf, W. E. and Torphy, T. J. (1997). *Molecular Pharmacology* 51, 999-1006.

113. Ji, T. H., Grossmann, M. and Ji, I. (1998). *The Journal of Biological Chemistry* 273, 28, 17299-17302.

114. Ji, T. H., Murdoch, W. J. and Ji, I. (1995). *Endocrine* 3, 187-194.

115. Jin, S. L. C., Swinnen, J. V. and Conti, M. (1992). *Journal of Biological Chemistry* 267, 18292-18939.

116. Kayusa, J., Goko, and Fujita-Yamaguchi (1995). *Journal of Biological Chemistry* 270, 14305-14312.

117. Kemp, B. E., Bylund, D. B., Huang, T. S., and Krebs, E. G. (1975). *Proceedings of the National Academy of Science USA* 72, 3448-3452.

118. Kemp, B. E., Graves, D. J., Benjamini, E. and Krebs, E. G. (1977). *Journal of Biological Chemistry* 252, 4888-4894.

119. Kemp, B. E. and Pearson, R. B. (1990). *Trends in Biochemical Sciences* 15, 342-346.

120. Kenakin, T. (1997). *Trends in Pharmacological Sciences* 18, 416-417.

121. Khramtsov, N. V., Feshchenko, E. A., Suslova, V. A., Schmukler, B. E., Terpugov, B. E., Rakitina, T. V., Atabekova, N. V. and Lipkin, V. M. (1993). *FEBS Letters* 327, 275-278.

122. Kiefer, J. R., Mao, C., Braman, J. C. and Beese, L. S. (1998). *Nature* 392, 304-

307.

123. Kincaid, R. L., Stith-Coleman, I. E. and Vaughn, M. (1985). *Journal of Biological Chemistry* 260, 9009-9015.

124. Kisselev, O., Pronin, A., Ermolaeva, M. and Gautam, N. (1995). *Proceedings of the National Academy of Science USA* 92, 9102-9106.

125. Kovala, T., Sanwal, B. D. and Ball, E. H. (1997). *Biochemistry* 36, 2968-2976.

126. Kozak, M (1987a). *Journal of Molecular Biology* 196 (4), 947-950.

127. Kozak, M (1987b). *Nucleic Acids Research* 15 (20), 8125-8148.

128. Krause, W., Kuhne, G. and Sauerbrey, N. (1990). *European Journal of Clinical Pharmacology* 38, 71-75.

129. Krupinski, J., Coussen, F., Bakalyar, H., Tang, W. J., Feinstein, P. G., Orth, K., Slaughter, C., Reed, R. R. and Gilman, A. G. (1989). *Science* 244, 1558-1564.

130. Lambright, D. G., Noel, J. P., Hamm, H. E. and Sigler, P. B. (1994). *Nature* 369, 621-628.

131. Lambright, D., Sondek, J., Bohm, A., Skiba, N., Hamm, H. and Sigler, P. (1996). *Nature* 379, 311-319.

132. Lavan, B. E., Lakey, T. and Houslay, M. D. (1989). *Biochemical Pharmacology* 38, 4123-4136.

133. Lefkowitz, R. (1998). *Journal of Biological Chemistry* 273, 18677-18680.

134. Lefkowitz, R. J., Cotecchia, S., Samama, P. and Costa, T. (1993). *Trends in Pharmacological Science* 14, 303-307.

135. Leiser, M., Rubin, C. S. and Erlichman, J. (1986). *Journal of Biological Chemistry* 261, 1904-1908.

136. Levin, L. R. and Reed, R. R. (1995). *Journal of Biological Chemistry* 270, 7573-7579.

137. Li, T. S., Volpp, K and Applebury, M. L. (1990). *Proceedings of the National Academy of Science USA* 87, 293-297.

138. Li, Y. and Rubin, C. S. (1995). *Journal of Biological Chemistry* 270, 1935-1944.

139. Lipkin, V. M., Khramtsov, N. V., Vasilevskaya, I. A., Atabekova, N. V., Muradov,

K. G., Gubanov, V. V., Li, T., Johnston, J. P., Volpp, K. J. and Applebury, M. L. (1990). *Journal of Biological Chemistry* 265, 12955-12959.

140. Liu, Y., Ruoho, A. E., Rao, V. D. and Hurley, J. H. (1997). *Proceedings of the National Acadamy of Science USA* 94, 13414-13419.

141. Livi, G. P., Kmetz, P., McHale, M. M., Cieslinski, L. B., Sathe, G. M., Taylor, D. P., Davis, R. L., Torphy, T. J. and Balcarek, J. M. (1990). *Molecular and Cellular Biology* 10, 2678-2686.

142. Lobban, M., Shakur, Y., Beattie, J. and Houslay, M. D. (1994). *Biochemical Journal* 304, 399-406.

143. Lochhead, A., Nekrasova, E., R., Arshavsky, V. Y. and Pyne, N. J. (1997). *Journal of Biological Chemistry* 272, 18397-18403.

144. Lohmann, S. M., DeCamili, P., Enig, I. and Walter, U. (1984). *Proceedings of the National Academy of Science USA* 81, 6723-6727.

145. Loughney, K., Snyder, P. B., Uher, L., Rosman, G. J., Ferguson, K. and Florio, V. A. (1999). *Gene* 234, 109-117.

146. Luo, Z., Shafit-Zagardo, B. and Erlichman, J. (1990). *Journal of Biological*

Chemistry 265, 21804-21810.

147. MacPhee, C. H., Harrison, S. A. and Beavo, J. A. (1986). *Proceedings of the National Academy of Science USA* 83, 6660-6663.

148. Manganiello, V. C., Murata, T., Taira, M., Belfrage, P. and Degerman, E. (1995a). *Archives of Biochemistry and Biophysics* 322, 1-13.

149. Manganiello, V. C., Taira, M., Degerman, E. and Belfrage, P. (1995b). *Cellular Signalling* 7, 445-455.

150. Marchmont, R. J., Ayad, S. R. and Houslay, M. D. (1981). *Biochemical Journal* 195, 645-6652.

151. Marchmont, R. J. and Houslay, M. D. (1980). *Biochemical Journal* 187, 381-392.

152. Martin, E. L., Rens-Domiano, S., Schatz, P. J. and Hamm, H. E. (1996). *Journal of Biological Chemistry* 271, 361-366.

153. McAllister-Lucas, L. M., Haik, T. L., Colbran, J. L., Sonnenburg, W. K., Seger, D., Turko, I. V., Beavo, J. A., Francis, S. H. and Corbin, J. D. (1995). *Journal of Biological Chemistry* 270, 30671-30679.

154. McAllister-Lucas, L. M., Sonnenburg, W. K., Kadlecek, A., Seger, D., Trong, H. L., Colbran, J. L., Thomas, M. K., Walsh, K. A., Francis, S. H., Corbin, J. D. (1993). *Journal of Biological Chemistry* 268, 22863-22873.

155. McHale, M. M., Cieslinski, L. B., Eng, W. K., Johnson, R. K., Torphy, T. J. and Livi, G. P. (1991). *Molecular Pharmacology* 39, 109-113.

156. McLaughlin, M. M., Cieslinski, L. B., Burman, M., Torphy, T. J. and Livi, G. P. (1993). *Journal of Biological Chemistry* 268, 6470-6476.

157. McPhee, I., Pooley, L., Lobban, M., Bolger, G. and Houslay, M. D. (1995). *Biochemical Journal* 310, 965-974.

158. Meacci, E., Taira, M., Moos, M. J., Smith, C. J., Movsesian, M. A., Degerman, E., Belfrage, P. and Manganiello, V. (1992). *Proceedings of the National Academy of Science USA* 89, 3721-3725.

159. Meinkoth, J. L., Ji, Y., Taylor, S. S. and Feramisco, J. R. (1990). *Proceedings of the National Academy of Science USA* 87, 9595-9599.

160. Michaeli, T., Bloom, T. J., Martins, T., Loughney, K., Ferguson, K. Riggs, M., Rodgers, L., Beavo, J. A. and Wigler, M. (1993). *Journal of Biological Chemistry* 268, 12925-12932.

161. Milatovich, A., Bolger, G., Michaeli, T and Francke, U. (1994). *Somatic Cell and MolecularGenetics* 20, 75-86.

162. Mizobe, T., Mervyn Maze, M., Lam, V., Suryanarayana, S., and Kobilka, B. (1996). *Journal of Biological Chemistry* 271, 2387-2389.

163. Monaco, L., Vicini, E. and Conti, M. (1994). *Journal of Biological Chemistry* 269, 347-357.

164. Mons, N., Harry, A., Dubourg, P., Premont, R. T., Iyengar, R. and Cooper, D. M. F. (1995). *Proceedings of the National Academy of Science USA* 92, 8473-8477.

165. Morris, A. and Scarlata, S. (1997). *Biochemical Pharmacology* 54, 429-435.

166. Muller, T., Engles, P. and Fozard J. R. (1996). *Trends in Pharmacological Sciences* 17 (8), 294-8.

167. Mumby, M. C., Prigent, A. F., Moueqqit, M., Fougier, S., Mascovischi, O. and Pacheco, H. (1985). *Biochemical Pharmacology* 34, 2997-3000.

168. Nemoz, G., Prigent, A. F., Moueqqit, M., Fougier, S., Mascovschi, O. and Pacheco, H. (1985). *Biochemical Pharmacology* 34, 2997-3000.

169. Nemoz, G., Zhang, R., Sette, C. and Conti, M. (1996). *FBES Letters* 384, 97-102.

170. Obernotle, R., Bhakta, S., Alvarez, R., Bach, C., Zuppan, P., Mulkins, M., Jarnagin, K., Shelton, E. R. (1993). *Gene* 129, 239-247.

171. O'Connell, J. C., McCallum, J. F., McPhee, I., Wakefield, J., Houslay, E. S., Wishart, W., Bolger, G., Frame, M. and Houslay, M. D. (1996). *Biochemical Journal* 318, 255-262.

172. Ovchinnikov, Y. A., Gubanov, V. V., Khramtsov, N. V., Ischenko, K. A., Zagranichny, V. E. (1987). *FEBS Letters* 223, 169-173.

173. Owens, R. J., Catterall, C., Batty, D., Jappy, J., Russell, A., Smith, B., O'Connell, J. and Perry, M. J. (1997). *Biochemical Journal* 326, 53-60.

174. Pan, X., Arauz, E., Krzanowski, J. J., Fitzpatrick, D. F. and Polson, J. B. (1994). *Biochemical Pharmacology* 48, 827-835.

175. Parma, J., Van Sande. J., Swillens, S., Tonacchera, M., Dumont, J. and Vassart. G. (1995). *Molecular Endocrinology* 9, 725-733.

176. Pawson, T. and Scott, J. D. (1997). *Science* 278, 2075-2080.

177. Pellegrino, S., Zhang, S., Garritsen, A. and Simonds, W. F. (1997). *Journal of Biological Chemistry* 272, 25360-25366.

178. Pieroni, J. P., Harry, A., Chen, J., Jacobwitz, O., Magnusson, R. P. and Iyengar, R. (1995). *Journal of Biological Chemistry* 270, 21368-21373.

179. Pillai, R., Kytle, A., Reyes, A. and Colicelli, J. (1993). *Proceedings of the National Academy of Science* 90, 11970-11974.

180. Pillai, R., Staub, S. F. and Colicelli, J. (1994). *Journal of Biological Chemistry* 269, 30676-30681.

181. Polson, J. B. and Strada, S. J. (1996). *Annual Review of Pharmacology and Toxicology* 36, 403-427.

182. Potter, R. L., Stafford, P. H. and Taylor, S. (1978). *Archives of Biochemistry and Biophysics* 190, 174-180.

183. Potter, R. L. and Taylor, S. S. (1979). *Journal of Biological Chemistry* 254, 2413-2418.

184. Probst, W. C., Snyder, L. A., Schuster, D. I., Brosius, J. and Sealfon, S. C. (1992).

DNA Cell Biology 11, 1-20.

185. Pyne, N. J., Anderson, N., Lavan, B. E., Milligan, G., Nimmo, H. G. and Houslay, M. D. (1987). *Biochemical Journal* 248, 897-901.

186. Qui, Y. and Davis, R. L. (1993). *Genes and Development* 7, 1447-1458.

187. Raine, C. S. (1995). *Nature Medicine* 1, 244-248.

188. Reeves, M. L., Leigh, B. K. and England, P. J. (1987). *Biochemical Journal* 241, 535-541.

189. Remy, J. J., Couture, L., Pantel, J., Haertle, T., Rabesona, H., Bozon, V., Pajot-Augy, E., Robert, P., Troalen, F., Salesse, R. and Bidart, J. M. (1996). *Molecular and Cellular Endocrinology* 125, 79-91.

190. Resh, M. (1996). *Cell Signal* 8, 403-412.

191. Romano, C., Yang, W. L. and O'Malley, K. L. (1996). *Journal of Biological Chemistry* 271, 28612-28616.

192. Rossi. P., Giorgi, M., Geremia, R. and Kincaid, R. L. (1988). *Journal of Biological Chemistry* 263, 15521-15527.

193. Rubin, C. S. (1994). *Biochimica et Biophysica Acta* 1224, 467-479.

194. Ryu, K., Lee, H., Kim, S., Beauchamp, J., Tung, C., Isaacs, N. W., Ji, I., and Ji, T. H. (1998). *Journal of Biological Chemistry* 273, 6285-6291.

195. Samama, P., Cotecchia, S., Costa, T. and Lefkovitz, R. J. (1993). *Journal of Biological Chemistry* 268, 4625-4636.

196. Sarkar, D., Erlichman, J. and Rubin, C. S. (1986). *Journal of Biological Chemistry* 259, 9840-9846.

197. Sass, P., Field, J., Nikawa, J., Toda, T. and Wigler, M. (1986). *Proceedings of the National Academy of Science USA* 83, 9303-9307.

198. Sawaya, M. R., Prasad, R., Wilson, S. H, Kraut, J. and Pelletier, H. (1997). *Biochemistry* 36, 11205-11215.

199. Schneider, T., Igelmund, P. and Herscheler, J. (1997). *Trends in Pharmacological Sciences* 18, 8-11.

200. Scotland, G. and Houslay, M. D. (1995). *Biochemical Journal* 308, 673-681.

201. Scott, A. I., Pierini, A. F., Shering, P. A. and Whalley, L. J. (1991). *European Journal of Pharmacology* 40, 127-129.

202. Scott, J. D., Stofko, R. E., McDonald, J. R., Comer, J. D., Vitalis, E. A. and Mangeli, J. (1990). *Journal of Biological Chemistry* 265, 21561-21566.

203. Scott, J. D. (1991). *Pharmacological Therapeutics* 50, 123-145.

204. Scott, J. D., Dell'Acqua, M. L., Fraser, I. D. C., Tavalin, S. J. and Lester, L. B. (2000). *Advances in Pharmacology* 175-207.

205. Sealfon, S., Weinstein, H. and Miller, R. (1997). *Endocrinology Review* 18, 180-205.

206. Sette, C. and Conti, M. (1996). *Journal of Biological Chemistry* 271, 16526-16534.

207. Sette, C. Iona, S. and Conti, M. (1994). *Journal of Biological Chemistry* 269, 9245-9252.

208. Sette, C., Vicini, E. and Conti, M. (1994). *Journal of Biological Chemistry* 269, 18271-18724.

209. Shabb, J. B. and Corbin, J. D. (1992). *Journal of Biological Chemistry* 267, 5723-5726.

210. Shakur, Y., Pryde, J. G. and Houslay, M. D. (1993). *Biochemical Journal* 292, 677-686.

211. Shakur, Y., Wilson, M., Pooley, L., Lobban, M., Griffiths, S. L., Campbell, A. M., Beattie, J., Daly, C. and Houslay, M. D. (1995). *Biochemical Journal* 306, 801-809.

212. Shaulsky, G., Escalante, R. and Loomis, W. F. (1996). *Proceedings of the National Academy of Science* 93, 15260-15265.

213. Shenolikar, S., Thompson, W. J. and Strada, S. J. (1985). *Biochemistry* 24, 672-678.

214. Skiba, N. P., Bae, H. and Hamm, H. E. (1996). *Journal of Biological Chenistry* 271, 413-424.

215. Smith, J. K., Scotland, G., Beattie, J., Trayer, I. P., and Houslay, M. D. (1996). *Journal of Biological Chemistry* 271, 16703-16711.

216. Soderling, S. H., Bayuga, S. J. and Beavo, J. (1998). *Journal of Biological*

Chemistry 273, 15553-15558.

217. Soderling, S. H., Bayagu, S. J. and Beavo, J. A. (1999). *Proceedings of the National Academy of Science USA* 96 (2), 7071-7076.

218. Sommer, N., Loschman, P.-A., Northoff, G. H., Weller, M., Steinbrecher, A., Steinbach, J. P., Lichtenfels, R., Meyermann, R., Reithmuller, A., Fontana, A., Dichgans, J. and Martin, R. (1995). *Nature Medicine* 1, 244-248.

219. Sondek, J., Bohm, A., Lambright, D., Hamm, H. and Sigler, P. (1996). *Nature* 379, 369-374.

220. Sparks, A. B., Rider, J. E., G., H. N., Fowlkes, D. M., Quilliam, L. A. and Kay, B. K. (1996). *Proceedings of the National Academy of Science* 93, 1540-1544.

221. Sprang, S. R. (1997). *Annual Review of Biochemistry* 66, 639-678.

222. Steitz, T. A. (1998). *Nature* 391, 231-232.

223. Strada, S. J., Martin, M. W. and Thompson, W. J. (1984). *Advances in Cyclic Nucleotide Research* 16, 13-29.

224. Stroop, S. D. and Beavo, J. A. (1991). *Journal of Biological Chemistry* 266,

23803-23809.

225. Stroop, S. D., Charbonneau, H. and Beavo, J. A. (1989). *Journal of Biological Chemistry* 264, 13718-13725.

226. Su, Y., Dostmann, W. R. G., Herberg, F. W., Durick. K., Xuong, N. H., Ten Eyck, L.,Taylor, S. S. and Varughese, K. I. (1995). *Science* 69, 807-813.

227. Su, Y., Taylor, S. S., Dostmann, W. R. G., Xuong, N. H. and Varughese, K. I. (1993). *Journal of Molecular Biology* 230, 1091-1093.

228. Sullivan, M., Egerton, M., Shakur, Y., Marquarsdon, A. and Houslay, M. D. (1994). *Cellular Siganlling* 6, 793-812.

229. Sullivan, M., Rena, G., Begg, F., Gordon, L., Olsen, A. S. and Houslay, M. D. (1998). *Journal of Biological Chemistry* 333, 693-703.

230. Sunahara, R. K., Dessauer, C. W. and Gilman, A. G. (1996). *Annual Review of Pharmacological Toxicology* 36, 461-480.

231. Sutherland, E. W. and Rall, T. W. (1957). *Journal of the American Chemistry Society* 79, 3608-3610.

232. Swinnen, J. V., Joseph, D. R. and Conti, M. (1989). *Proceedings of the National Academy of Sciences USA* 86, 5325-5329.

233. Szpirer, C., Szpirer, J., Riviere, M., Swinnen, J., Vicini, E. and Conti, M. (1995). *Cytogenetics and Cell Genetics.* 69, 11-14.

234. Taira, M., Hockman, S. C., Calvo, J. C., Belfrage, P. and Manganiello, V. C. (1993). *Journal of Biological Chemistry* 268, 18573-18579.

235. Takemoto, D. J., Hansen, J., Takemoto, L. J. and Houslay, M. D. (1982). *Journal of Biological Chemistry* 257, 14597-14599.

236. Takio, K., Wade, R. D., Smith, S. B., Krebs, E. G., Walsh, K. A. and Titani, K. (1984). *Biochemistry* 23, 4207-4218.

237. Tang, W. J. and Gilman, A. G. (1992). *Cell* 70, 869-872.

238. Tang, W. J. and Gilman, A. G. (1995). *Science* 268, 1769-1772.

239. Tang, W. J. and Hurley, J. H. (1998). *Molecular Pharmacology* 54, 231-240.

240. Tang, W. J., Stanzel, M. and Gilman, A. G. (1995). *Biochemistry* 34, 14563-14572.

241. Tang, X. and Downes, C. (1997). *Journal of Biological Chemistry* 272, 14193-14199.

242. Taussig, R. and Gilman, A. G. (1995). *Journal of Biological Chemistry* 270, 1-4.

243. Taylor, S. S., Buechler, J. A. and Yonemoto, Y. (1990). *Annual Review of Biochemistry* 59, 971-1005.

244. Tempel, B. L., Bonini, N., Dawson, D. R. and Quinn, W. G. (1983). *Proceedings of the National Academy of Science* 80, 1482-1486.

245. Tesmer, J. J. G., Sunahara, R. K., Gilman, A. G. and Sprang, S. R. (1997). *Science* 278, 1907-1916.

246. Thomas, M. K., Francis, S. H. and Corbin, J. D. (1990). *Journal of Biological Chemistry* 265, 14964-14970.

247. Thomas, M. K., Francis, S. H. and Corbin, J. D. (1990). *Journal of Biological Chemistry* 265, 14971-14978.

248. Thompson, W. J. and Appleman, M. M. (1971). *Biochemistry* 10, 311-316.

249. Thompson, W. J., Lavis, V. R., Whalin, M. E. and Strada, S. J. (1992). *Advances in Second Messenger Phosphoprotein Research* 25, 165-184.

250. Torphy, T. J., Barnette, M. S., Hay, D. W. P. and Underwood, D. C. (1994). *Environmental Health Perspectives* 102, 79-84.

251. Torphy, T. J., Dewolf, W., Green, D. W. and Livi, G. P. (1993). *Agents and Actions* 43, 51-71.

252. Torphy, T. J., Livi, G. P. and Christensen, S. B. (1993). *Drug News and Perspectives* 5,.

253. Torphy, T. J. and Undem, B. J. (1991). *Thorax* 149, 512-524.

254. Trong, H. L., Beier, N., Sonnenburg, W. K., Stroop, S. D., Walsh, K. A., Beavo, J. A. and Charbonneau, H. (1990). *Biochemistry* 29, 10280-10288.

255. Tucker, M. M., Robinson, J. B. J. and Stellwagen, J. (1981). *Journal of Biological Chemistry* 256, 9051-9058.

256. Unger, V., Hargrave, P., Baldwin, J. and Schertler, G. (1997). *Nature* 389, 203-206.

257. Vorherr, T., Knopfel, L., Hofmann, F., Mollner. S., Pfeuffer, T. and Carafoli, E. (1993). *Biochemistry* 32, 6081-6088.

258. Wachtel, H. (1983). *Neuropharmacology* 22, 267-272.

259. Walsh, D. A. and Van Patten, S. M. (1994). *The FASEB Journal* 8, 1227-1236.

260. Wang, Y., Scott, J. D., McKnight, G. S. and Krebs, E. G. (1991). *Proceedings of the National Academy of Science USA* 88, 2446-2450.

261. Wayman, G. A., Wei, J., Wong, S. and Storm, D. R. (1996). *Molecular Cell Biology* 16, 6075-6082.

262. Weber, I. T., Takio, K., Titani, K. and Steitz, T. A. (1982). *Proceedings of the National Academy of Science USA* 79, 7679-7683.

263. Wei, J., Wayman, G. and Storm, D. R. (1996). *Journal of Biological Chemistry* 271, 24231-24235.

264. Wells, J. A. (1996). *Proceedings of the National Academy of Science USA* 93, 1-6.

265. Wells, J. N. and Hardman, J. G. (1977). *Advances in Cyclic Nucleotide Research* 8, 119-143.

266. Wess, J. (1997). *The FASEB Journal* 11, 346-354.

267. Whisnaut, R. E., Gilman, A. G. and Dessauer, C. W. (1996). *Proceedings of the National Academy of Science USA* 93, 6621-6625.

268. Woodford, T. A., Correll, L. A., McKnight, G. S. and Corbin, J. D. (1989). *Journal of Biological Chemistry* 264, 13321-13328.

269. Wu, H. and Parsons, J. (1993). *Journal of Cell Biology* 120, 1417-1426.

270. Wu, Z., Wong, S. T, and Storm, D. R. (1993). *Journal of Biological Chemistry* 268, 23766-23768.

271. Wyatt, T. A., Naftilan, A. J., Francis, S. H. and Corbin, J. D. (1998). *American Journal of Physiology* 274, H448-H55.

272. Xia, Z. G. and Storm, D. R. (1997). *Current Opinions in Neurobiology* 7, 391-396.

273. Yan, C., Zhao, A. Z., Bentley, J. K. and Beavo, J. A. (1996). *The Journal of Biological Chemistry* 271 (41), 25699-25706.

274. Yan, C., Zhao, A. Z., Bentley, J. K., Loughney, K., Ferguson, K. and Beavo, J. A.

(1995). *Proceedings of the National Academy of Science USA* 92, 9677-9681.

275. Yan, S. Z., Hahn, D., Huang, Z. H. and Tang, W. J. (1996). *Journal of Biological Chemistry* 271, 10941-10945.

276. Yan, S. Z., Huang, Z. H., Andrews, R. K. and Tang, W. J. (1998). *Molecular Pharmacology* 53, 182-187.

277. Yan, S. Z., Huang, Z. H., Rao, V. D., Hurley, J. H. and Tang, W. J. (1997). *Journal of Biological Chemistry* 272, 18849-18854.

278. Yan, S. Z., Huang, Z. H, Shaw, R. S, and Tang, W. J. (1997). *Journal of Biological Chemistry* 272, 12342-12349.

279. Yang, Q., Paskind, M., Bolger, G., Thompson, W. J., Repaske, D. R., Cutler, L. S. and Epstein, P. M. (1994). *Biochemical and Biophysical Research Communications* 205, 3, 1850-1858.

280. Yasuda, H., Lindorfer, M., Woodfork, K., Fletcher, J. and Garrison, J. (1996). *Journal of Biological Chemistry* 271, 18588-18595.

281. Yoshimura, M. and Cooper, D. M. (1992). *Proceedings of the National Academy of Science USA* 89, 6716-6720.

282. Zhang, G., Liu, Y., Ruoho, A. E. and Hurley, J. H. (1997). *Nature* 386, 247-253.

283. Zimmermann, G., Zhou, D. and Taussig, R. (1998). *Journal of Biological Chemistry* 273, 19650-19655.

GLASGOW U .TY Library